Fabrication of novel poly (vinylidene fluoride) /MWCNT nanocomposite ultrafiltration membranes for natural organic matter removal

A thesis submitted in fulfillment of the requirements for the degree of Doctor of Philosophy

by

Banan Hudaib

Faculty of Engineering and IT
School of Chemical and Biomolecular Engineering

2017

DECLARATION

I hereby declare that this thesis, submitted in fulfilment of the requirements for the award of Doctor of Philosophy degree in chemical engineering in the School of Chemical and Biomolecular Engineering, University of Sydney, is entirely my own work unless otherwise referenced or acknowledged. The document has not been submitted for qualifications at any other academic institution.

Banan Ismail Hudaib

August, 2016

ACKNOWLEDGEMENT

First and foremost, praise and gratitude go to Allah S.W.T, the Almighty, for bestowing me with great strength, patience, and ability to completing this thesis.

I would like to thank the **University of Sydney Dean of Engineering & IT Ph.D. Scholarship for Jordan** for offering me and my country this unique opportunity to complete my tertiary studies through this scholarship and generous funding of my project.

I owe my deepest gratitude and appreciation to my supervisor Prof. Zongwen Liu. Thank you so much for giving me this amazing opportunity and standing with me in hard times and for your continuous support and guidance throughout this project. It has truly been a great pleasure working with you. I would also like to show my utmost appreciation to Prof. Vincent Gomes for all his help, support and for reading my work. Big thanks also go to Dr. Jeffrey Shi for helping me in the laboratory. I would like to thank warmly Prof. Dianne Wily, the head of the school for her time in reading the conference paper manuscript. I would also like to thanks, Dr. Tino Kausmann, Ms. Nancy Xie and Dr. Rachel for all technical help and good laughs. I am also grateful to Dr. Cuifeng Zhou at USyd for her technical help and support. I would like to thank Prof. Vicki Chen and Dr.Yun Ye at UNSW for permitting me doing my experiments and their great technical help and advice in the UNESCO center labs in UNSW.

I would like to express my deepest appreciation to my beloved husband, Baker. Thank you so much my “love forever” for your unconditional encouragement and support. It would have been impossible for me to complete my study without your love, patience, and help. Also, I want to extend my appreciation to my sweet heart kids; Omar and Mohammad, I wish you will be proud of your mother one day.

Finally, I would like to express my warmest gratitude and respect to my parents for their persistent blessings, never-ending love, and support. Pursuing a Ph.D. was always my mother's dream, and it would not have been achieved without her love and empathy. I would also like to extend my thankfulness to my sisters and brothers for their constant support.

PUBLICATIONS

Conference papers:

1. Banan Hudaib, Vincent Gomes, Jeffrey Shi, Zongwen Liu, (2016). Fabrication of Novel PVDF/MWCNT Nanocomposite Ultrafiltration Membrane, presented in ICONN2016.

2. Banan Hudaib, Vincent Gomes, Jeffrey Shi, Dianne Wiley, Zongwen Liu, (2016). Poly (vinylidene fluoride)/Polyaniline/MWCNT Nanocomposite Ultrafiltration Membrane for natural organic matter removal. Accepted for oral presentation at ANNIC2016

Journal paper under review:

1. Banan Hudaib, Vincent Gomes, Jeffrey Shi, Jiuen Lee, Zongwen Liu, (2016). Enhanced permeability and antifouling properties of Poly (vinylidene fluoride) ultrafiltration membranes using polyaniline as additives, submitted to Journal of water science and technology: water supply.

TABLE OF CONTENT

LIST OF FIGURES

LIST OF TABLES

NOMENCLATURE

APS	Ammonium peroxydisulfate
BSA	Bovine serum albumin
BET	Brunauer-Emmett-Teller method
CA	Contact angle
CF_2	Diflouromethylene
CNTs	Carbon nanotubes
D_{H0}	Hydraulic diameter
DBPs	Disinfection by-products
DMAc	N, N-Dimethylacetamide
DMF	N, N-Dimethylformamide
DMSO	DIMETHYLSIFOXIDE
F	Water flux (m3/m2.h)
FE-SEM	Field Emission Scanning electron microscopy
F_{RW}	Flux recovery
FTIR	Fourier-transform infrared spectroscopy
GO	Graphene oxide
HA	Humic acid
HPAE	Hyper branched poly (amine-ester)
H_2O_2	Hydrogen Peroxide
LMH/bar	Liters/m^2.hour.bar
MD	Membrane distillation
MWCNT	Multi-walled carbon nanotubes
MWCOs	Molecular weight cut-offs

NMP	N-Methyl-2-pyrrolidone
NOM	Natural organic material
PAN	Poly (acrylonitrile)
PANI	Polyaniline
PDA	Polydopamine
PVDF	Poly (vinylidene fluoride)
PVP	Poly (vinyl pyrrolidone)
RO	Reverse osmosis
R_t	Total fouling ratio
SWCNTS	Single wall carbon nanotubes
TMP	Trimethyl phosphate
UF	Ultrafiltration
UV	Ultraviolet

SYMBOLS

ε	Porosity of the membrane
δ	Effective thickness
ρ_p	the polymer density
ρ_{water}	Water density (0.998 g·cm−3)
η	Water viscosity (8.9×10^{-4}Pa s)
Δ P	Membrane pressure

ABSTRACT

Membrane technology has been receiving substantial attention in advanced water treatment as a response to the global demand for purifying drinking water. Poly (vinylidene) fluoride (PVDF) has advantages as a membrane material compared to other commercialized polymeric materials as it is easily dissolved in common organic solvents and its proper asymmetric structure for separation. However, its hydrophobic characteristics lead to low water flux and makes PVDF membrane easily fouled while treating solutions containing natural organic matters. The drawback mentioned above of PVDF-UF membranes must be overcome to facilitate wide applications. Blending which is the addition of polymer in the membrane casting solution is one of the methods to improve membrane morphology, increase the hydrophilicity, porosity and enhance the membrane performance such as water flux and antifouling. The aim of this research is to enhance the performance of PVDF ultrafiltration membrane by using different additives.

In the first part (MWCNT)/ polydopamine (PDA) was used as additives with different MWCNT concentrations. These were prepared by in-situ polymerization of dopamine over the MWCNT and then used as an additive for the blended PVDF membrane. Flux and rejection studies included measurement of contact angle, porosity measurement, zeta potential, tensile strength, and characterization by scanning electron microscopy (SEM) were performed. The PVDF membrane blended with a mixture of 2% dopamine/ 1% MWCNT showed 20 fold improvements in permeability in comparison to pristine PVDF ultrafiltration membrane. Furthermore, it demonstrated about 81% rejection for Suwannee River Humic acid (HA) filtration test. Water contact angle measurements show improvement of the hydrophilicity of the resultant membrane compared to the pristine PVDF membrane.

In the second part, (PANI) was used as an additive for application in natural organic matter (NOM) removal from water. In this study, PANI was synthesized by aniline polymerization

using ammonium persulfate as oxidant and DMF as a solvent. Two blending methods of aniline were applied, and the synthesized PANI was used as an additive to produce PANI/PVDF modified membranes. Flux and rejection studies, hydrophilicity, porosity, zeta potential, mechanical properties and morphological assessment by scanning electron microscopy (SEM) were performed. Results show that the water permeability and antifouling properties of the modified PVDF membranes were both improved. Water permeability of PANI/PVDF modified membranes were 7-16 times greater than pristine PVDF. Water contact angle measurements show improvement of the hydrophilicity of the resultant membrane compared to the pristine PVDF membrane.

Finally, Multi-wall Carbon Nanotubes (MWCNT)/ polyaniline (PANI)/ poly (vinylidene fluoride) (PVDF) ultrafiltration membrane was prepared by phase inversion technique through in situ polymerization method of aniline for removal of natural organic matter (NOM) in water. Aniline was polymerized in situ with different dosages of MWCNT ranging from 0.25 wt. % to 2 wt. % in PVDF casting solutions. Permeability, rejection studies, contact angle, porosity measurement, tensile strength, zeta potential and characterization by scanning electron microscopy (SEM) were performed. The resultant membrane of (PANI/ 1.5 % MWCNT) showed the highest permeability results (1320 LMH/bar) among membranes we tested, with 40 fold permeability improvement in comparison to pristine PVDF ultrafiltration membrane. Furthermore, it showed about 79% rejection of Suwannee River Humic acid (HA) filtration test. This significant enhancement of the fabricated membrane is attributed to the high hydrophilicity, porosity, larger pore sizes and positive membrane charge resulting from modification with MWCNT/PANI complex.

CHAPTER 1. Introduction

1. 1 Background

Clean water is vital for life, and as its supply becomes limited, we need to look into special water treatment technologies like membrane filtration to meet the progressively stringent water quality standards and the unceasing water supply needs. Membrane technologies provide an acceptable permeate using much smaller footprint than conventional water treatment processes. Thus, the membrane industry is growing rapidly, supplying modifier systems for drinking, wastewater and industrial water treatment, as well as desalination.

1.2 Overview of membrane technology

A membrane is fundamentally defined as a thin barrier that separates two phases and is capable of restricting the transfer of diverse components in a selective manner [1]. Different membrane processes have been used for water treatment, like microfiltration (MF), ultrafiltration (UF), nanofiltration (NF) and reverse osmosis (RO) [1]. These are pressure-driven membrane separation processes. Since 1960, membrane technology has been converted from laboratory development to industrial applications. More than 95% of the applications are for liquid separations. Nowadays membranes are being used for desalination of seawater and brackish water, potable water production and for treating industrial effluents, and water reclamation and reuse. Moreover, Membranes are used in medical devices such as hemodialysis units, blood oxygenators, and controlled drug delivery systems. Membrane separation processes are being increasingly integrated with conventional technologies as

hybrid membrane systems to decrease energy consumption and reduce environmental impact [2].

Membranes play a leading role in water treatment processes; they affect the technological and economic efficiency of the technologies mentioned above. A well-designed membrane, with high porosity and permeability, can intrinsically provide better flux and improved economics [3, 4].

The choice of membrane material and its pore size depend on the separation process for which it would be used [3]. **Fig. 1.1** represents the average pore size limits for membranes in different water treatment processes.

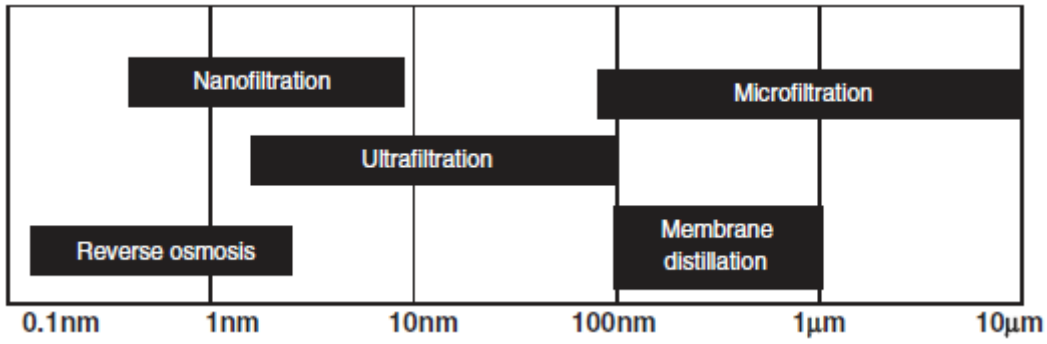

Fig.1.1. The average pore size of membranes used in various water treatment processes [4].

To be beneficial for industrial separation process, a membrane must show high flux, high selectivity (rejection), mechanical stability, tolerance to all feed stream components (fouling resistance), ability to tolerate temperature variations, manufacturing reproducibility, low manufacturing expenses and the ability to be packaged into high surface area modules [5]. During the last twenty years, significant advances have been made in the development of preparation of polymers with higher selectivity and permeability than the usually available commercial membrane materials [6].

1.3 Ultrafiltration membrane technology

Ultrafiltration (UF) has been widely used in water treatment [7], UF membrane is defined as a low-pressure membrane with pore diameter ranging from 2 to 100 nm and an operating pressure of approximately 200-700 kPa. Most UF membranes have an asymmetric porous structure; it can reject colloids, proteins, viruses and natural organic material (NOM) with constraints related to low flux and fouling [1]. The natural organic material is a complex matrix of organic compounds existing in natural surface water sources. Not only does it affect the smell, color, and taste of water, but it also forms complexes with heavy metals and pesticides, and reacts with chlorine, the most widely used oxidant for water disinfection to form chlorinated disinfection by-products (DBPs) which have been identified as human carcinogens [8]. A considerable portion of dissolved natural organic material in aquatic environments is contributed by humic substances [9].

In general, UF membrane eliminates low concentrations of NOM which are considered to be a critical issue in drinking water treatment. UF membrane can only reject 20-50 % of NOM [10]. A hybrid membrane system with chemical/physical processes is one of the solutions proposed in the literature [11]. Combining coagulation process with UF system is capable of eliminating up to 80% of NOM [12]. Fouling is considered a challenging problem in UF membrane technology application for NOM removal as flux reduction due to the adsorption and deposition of foulants is usually encountered [13].

Membrane fouling is the deposition of material on or within the structure of the membrane. Fouling can be classified according to the strength of particle attachment to the membrane surface to reversible or irreversible. Reversible fouling, caused by solids aggregation on the membrane surface and is typically treated physically by intermittent hydraulic backwashes. Irreversible fouling occurs with the strong attachment of solid particles to the membrane surface, and these cannot be removed by physical cleaning.

Irreversible fouling demands chemical cleaning of the membrane which limits the viability of UF as a water treatment process that is not readily reversed by simple pressure release or backwashing [13]. A sequel to membrane fouling is decreased membrane permeability (flux declines at constant pressure or pressure rises at constant flux), and alteration of solute retention [14]. Progress in fouling resistant materials production can improve energy efficiency in seawater desalination plants [15].

Specially engineered plastics like poly (ether sulfone) (PES), polysulfone (PS), poly (vinylidene fluoride) (PVDF), and poly(acrylonitrile) (PAN) have become important UF membranes are desirable due to their good performance and characteristics such as high mechanical properties, excellent heat aging resistance, and chemical stability [16]. However, UF membranes made from the previously mentioned materials have surfaces with reduced wettability, which results in serious membrane fouling in many processes because of the solute–membrane hydrophobic interactions [17]. Several researchers investigated the effect of membrane hydrophilicity and organic compound polarity on fouling and stated that hydrophobic compounds appeared to be the principal foulant materials [8, 14, 18]. Accordingly, researchers have carried out hydrophilic modifications of membrane surface with different methods like physical adsorption [19] polymer blend [20], and plasma modification [21]. The hydrophilic surface modifications could produce membranes with low fouling behavior and high flux. However, some surface modifications might damage membrane structure and cause the decline in rejection and mechanical properties [8].

The use of nanotechnology in membrane modification is a new promising membrane technology; researchers are trying to enhance UF membrane performance through the addition of nanomaterials [8]. Nanocomposites can exhibit properties that are considerably differing from those of the bare polymer [22].

Nanocomposite membranes can be developed by assembling engineered nanoparticles into porous membranes [23] or by blending them with polymeric or inorganic membranes [24, 25]. Many membranes were fabricated and modified by nanoparticles like silica, zeolite,

graphite, metal oxide or carbon nanotubes to increase the novelty of membrane materials, permeability, and fouling resistance [26, 27, 28]. Among various nanoparticles, carbon nanotubes (CNTs) have attracted great interest since their discovery in 1991 by Iijima [29] as CNTs have high water treatment capabilities which were proven to work effectively against both chemical and biological contaminants with high adsorbent properties due to its large specific surface area [30].

1.4 Research scope and objectives

The scope of this research is focused mainly on the improvement of ultrafiltration (PVDF) membranes for NOM removal by modification with MWCNT. The principal aim is enhancing the flux and rejection properties of a newly synthesized novel membranes based on (PVDF/PDA/MWCNT) and (PVDF/PANI/MWCNT) compared to pristine PVDF UF membrane. The specific research objectives are listed as follows:

- Fabrication of novel PVDF/PDA/MWCNT ultrafiltration membranes to allow enhanced rejection efficiency, flux recovery and high flux for effective NOM removal.
- Fabrication of novel PVDF/PANI/MWCNT membranes with potential higher flux and good flux recovery for effective NOM removal.
- Studying different fabrication techniques to optimize the performance of PVDF/PANI and PVDF/PDA ultrafiltration membranes.
- Studying the effects of modification of PVDF-based ultrafiltration membranes by carbon nanotube (CNT) addition to improving hydrophilicity and anti-fouling properties.
- Characterization of fabricated membranes for physical and chemical properties e.g. porosity, composition (FTIR), tensile strength, hydrophilicity and zeta potential as well as studying the structural morphology by SEM.

- Studying the key factors influencing the new fabricated membranes performance; including the effect of PDA or PANI and MWCNT concentrations and blending method.

1.5 Dissertation structure

This dissertation has been written in an integrated article format and divided into seven chapters.

Chapter 1 includes the introduction, study background, and established objectives.

Chapter 2 includes general overview of membranes types, material and production methods, First, the properties of the base polymer (PVDF) as it is regarded to be one of the most promising membrane materials for industrial applications concerning its outstanding properties. Then the fabrication process of PVDF by phase inversion technique and the factors affecting the fabrication process including the solvent type, PVDF concentration, non-solvent additives, coagulation bath medium and temperature. Several additives used to improve the characteristics of PVDF ultrafiltration membranes were discussed. Moreover, the most recent advances in the modification of PVDF ultrafiltration membranes through nanotechnology by adding carbon nanotubes to improve the hydrophilicity and decrease fouling of PVDF membranes were reviewed. Finally, membrane fouling and the antifouling mechanism by natural organic material and the cleaning methods used were discussed.

Chapter 3 introduces the experiment methodology including the material used and the experimental procedure of membrane fabrication, as well as the characterization methods used to evaluate the modified membranes performance.

Chapter 4 presents the performance, and characterization results of MWCNT/PDA/PVDF modified membranes for natural organic matter removal (NOM). The aim of this work is to enhance the permeability and antifouling properties of PVDF ultrafiltration membrane by

using MWCNT/PDA as an additive for application in NOM removal from water. This chapter was presented as a conference paper in ICONN2016.

Chapter 5 presents the effect of fabrication method on the performance and characterization results of PANI/PVDF modified membranes. The aim of this work is to enhance the permeability and antifouling properties of PVDF ultrafiltration membrane by using PANI as an additive for application in NOM removal from water. Two blending methods of aniline were applied, and the synthesized PANI was used as additive to produce PANI/PVDF modified membranes.

Chapter 6 presents the performance and characterization results of MWCNT/ PANI/ PVDF ultrafiltration membrane prepared by phase inversion technique through in situ polymerization method of aniline for removal of NOM in water. The aim of this work is to enhance the results of the fabricated membrane in chapter 5 by adding MWCNT. This chapter was accepted as a conference paper and will be presented in ANNIC2016.

Chapter 7 summarizes the results and conclusions of the research presented in this thesis and provides future work suggestions.

References

[1] Lawrence K. et al., (2011). Membrane and Desalination Technologies, Volume 10, Springer Science, Business Media, London. ISBN: 978-1-58829-940-6.

[2] Singh R., (2015). Membrane Technology and Engineering for Water Purification, Application, Systems Design and Operation. Elsevier Ltd publication. ISBN: 978-0-444-63362-0.

[3] Tarleton S., Wakeman R., (2011). Solid/Liquid Separation: Scale-up of Industrial Equipment, Elsevier, Technology & Engineering, ISBN-10 1856174204.

[4] Pinnau I., Freeman B.D., (2000). Formation and Modification of Polymeric Membranes : Overview. Academic press.

[5] Lalia B.S. et al., (2013). A review on membrane fabrication: Structure, properties and performance relationship. Desalination, 326, pp.77–95.

[6] Baker, R.W. et al., (1991). Membrane Separation Systems-Recent Developments and Future Directions, Noyes Data Corporation, Park Ridge, NJ.

[7] Fan Z. et al., (2008). Preparation and characterization of poly (aniline)/poly (sulfone) nanocomposite ultrafiltration membrane. Journal of Membrane Science, 310(1-2), pp. 402–408.

[8] Crozes G., White P., Marshall M., (1995). Enhanced coagulation: its effect on NOM removal and chemical cost. Journal AWWA, 87, pp. 78-89.

[9] Mallevialle J., Anselme C., Marsigny O., (1989). Effects of humic substances on membrane processes, in I.H. Suffet, P. MacCarthy (Ed.), Aquatic Humic Substances: Influence on Fate and Treatment of Pollutants, ACS, Washington, pp. 749-767.

[10] Zularisam A.W. et al., (2011). Role of natural organic matter (NOM), colloidal particles, and solution chemistry on ultrafiltration performance. Separation and purification Technology, 78(2), pp.189-200.

[11] Kabsch-Korbutowicz M., (2005). Application of ultrafiltration integrated with coagulation for improved NOM removal. Desalination.174 (1), pp. 13-22.

[12] Mao R.R., et al., (2013). Impact of various coagulation technologies on membrane fouling in coagulation/ultrafiltration process. Chemical Engineering Journal, 225, pp. 387-393.

[13] Hyeok Choi et al., (2005). Effect of permeate flux and tangential flow on membrane fouling for wastewater treatment, Separation and Purification Technology 45, pp. 68–78.

[14] Aoustin E., (2001). Ultrafiltration of natural organic matter. Separation and Purification Technology, 22-23(1-2), pp. 63–78.

[15] Elimelech M. and Phillip W.A., (2011). The future of sea water desalination: Energy, Technology, and the Environment Science, 333(6043), pp.712-717.

[16] Mulder, M. (1996). Basic Principles of Membrane Technology, Kluwer Academic Publishers, Netherlands, 1996, pp. 56–58, 420.

[17] Marshall, A.D., Munro, P.A., Tragardh, G. (1993). The effect of protein fouling in microfiltration and ultrafiltration on permeate flux, protein retention and selectivity: a literature review, Desalination 91, pp. 65–108.

[18] Liu Charles et al., (2001). Membrane Chemical Cleaning : From Art to Science. American Water Works Association, 25, pp.1-25.

[19] Kavitskaya A.A., (2005). Separation characteristics of charged ultrafiltration membranes modified with the anionic surfactant, Desalination 184, pp. 409–414.

[20] Hester J.F., Mayes A.M., (2002). Design and performance of foul-resistant poly (vinylidene fluoride) membranes prepared in a single-step by surface segregation, J. Membrane. Sci. 202, pp.119–135.

[21] Kull K.R., Steen, M.L. Fisher, E.R., (2005). Surface modification with nitrogen-containing plasmas to produce hydrophilic, low-fouling membranes, J. Membrane. Sci. 246, pp. 203–215.

[22] Vatanpour V. et al., (2011). Fabrication and characterization of novel antifouling nanofiltration membrane prepared from oxidized multiwalled carbon

nanotube/polyethersulfone nanocomposite. Journal of Membrane Science, 375(1-2), pp. 284–294.

[23] Taurozzi, J.S. et al., (2008). Effect of filler incorporation route on the properties of polysulfone- silver nanocomposite membranes of different porosities, J. Membr. Sci. 325 (1), pp. 58-68.

[24] Celik E., Liu L., Choi H. (2011). Protein fouling behavior of carbon nanotube/polyethersulfone composite membranes during water filtration. Water Research, 45(16), pp. 5287–5294

[25] Bottino, A. Capannelli, G., Comite. A. (2002). Preparation and characterization of novel porous PVDF-ZrO2 composite membranes, Desalination 146 35.

[26] Peng, F. et al., (2007). Novel nanocomposite pervaporation membranes composed of poly (vinyl alcohol) and chitosan-wrapped carbon nanotube, J. Membrane. Sci. 300(1-2), pp.13-19.

[27] Lu, L.Y. et al., (2006). Novel graphite-filled PVA/CS hybrid membrane for pervaporation of benzene/cyclohexane mixtures, J. Membr. Sci. 281, pp. 245-252.

[28] Majeed S. et al., (2012). Multi-walled carbon nanotubes (MWCNTs) mixed polyacrylonitrile (PAN) ultrafiltration membranes. Journal of Membrane Science, 403-404, pp.101–109.

[29] Iijima, S. (1991). Helical microtubules of graphitic carbon. Nature, 354, pp. 56–58.

[30] Upadhyayula V. K. K. et al., (2009). Application of carbon nanotube technology for removal of contaminants in drinking water: A review. Science of the Total Environment, 408(1), pp. 1–13.

CHAPTER 2. Literature review

2.1 Types of membranes

There are several methods to classify synthetic membranes. They can be classified according to the nature of the membrane material, membrane morphology, geometrical configuration, fabrication methods, separation process, etc. For example, synthetic membranes can be divided to organic (polymeric) or inorganic (ceramic/metal), either solid or liquid; they can be homogeneous or heterogeneous, symmetric or asymmetric in structure. Depending on the geometric shape, synthetic membranes can be grouped into flat, tubular or hollow fiber membranes [1].

2.1.1 Symmetric (Isotropic) membranes

Isotropic membranes have a uniform structure throughout whole membrane thickness. The separation properties of symmetric membranes are decided by their entire structure [13]. Symmetric membranes are classified according to the separation regime into porous and nonporous membranes. Porous (microporous) membranes are analogous in structure and function to a conventional filter. The separation of solute by microporous membranes is mostly related to the molecular size and pore size distribution. A microporous membrane is a highly voided structure with randomly distributed interconnected pores. These pores are extremely small, and their diameters range between 0.01- l0 um. Thus, all particles larger than the largest pores in the membrane will be rejected, and particles smaller than the largest pores while larger than the smallest pores; part of it are rejected. For the pore size distribution

of the membrane; particles that are much smaller than the smallest pores would pass through the membrane pores.

In general, only molecules that vary substantially in size can be separated effectively by microporous membranes such as ultrafiltration and microfiltration membranes (filtration is a function of molecular size and pore size distribution) [13]. Nonporous dense membranes composed of a dense film through which permeates are transported by diffusion under the driving force of pressure, concentration or electrical potential gradient. Thus, this type of membranes can separate permeates of similar sizes if their concentration in the membrane material (i.e. their solubility) varies significantly. Most gas separation, pervaporation, and reverse osmosis processes use dense membranes for separation. These membranes have an anisotropic structure to enhance flux. The separation of different constituents of a mixture using a dense, nonporous membrane is related to their transport rate within the membrane, which depends mostly on their diffusivity and solubility in the membrane material. See **Fig.2.1**.

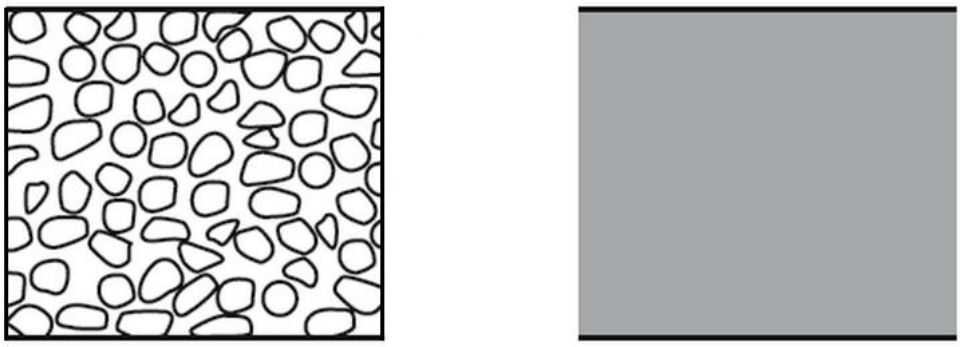

Fig.2.1. Symmetrical Isotropic microporous and Nonporous dense membranes [13].

2.1.2 Asymmetric (Anisotropic) membranes

Asymmetric membranes have relatively dense, exceedingly thin surface layer (i.e. the "skin", also called the perm-selective layer) supported on an open, much thicker porous substructure. The fabrication of the surface layer and its substructure is done in a single operation or separately. Separation properties and permeation rates of this membrane are determined

entirely by the surface layer while the substructure functions as a mechanical support [13, 14]. The transport rate of a material through a membrane is reciprocally proportional to the membrane thickness. The benefits of the higher fluxes provided by anisotropic membranes are so considerable that almost all commercial processes use such membranes.

Asymmetric membranes are classified into two basic categories; when the same material used for the top layer and porous sub-layer, the membrane is referred to as integrally skinned asymmetric membrane; on the contrary, if the material of the top skin layer is different from that of the porous sub-layer, the membrane is called composite membrane [15] (as demonstrated in **Fig. 2.2).**

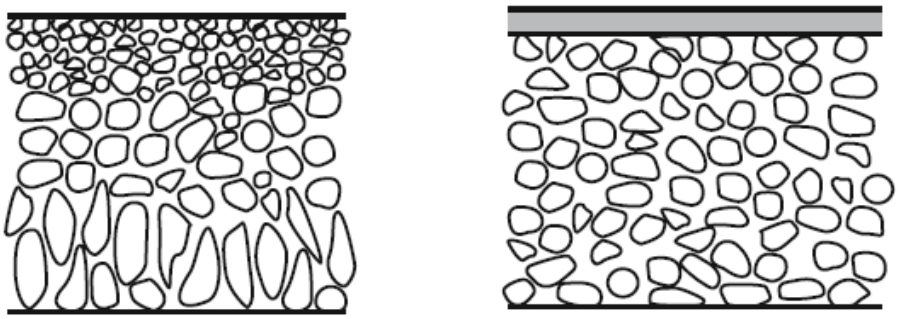

Fig.2.2. Integrally asymmetric skinned membrane and composite membrane [13].

There are different methods for the preparation of asymmetric membranes; these are described in the following sections.

2.2. Membrane Materials and Production

Membranes can be fabricated from a wide range of different materials. Synthetic membranes can be divided into organic (e.g. polymers) or inorganic types (e.g. metal oxides, zeolites, carbons…etc.) [16]. Nowadays, the majority of commercial membranes is made from polymers. Some commonly used polymers in membrane fabrication are listed in **Table 2.1**.

Table 2.1. Common polymers used for the production of commercial membranes [16].

Membrane Material	Membrane Process*(a)
Cellulose acetate	GS, RO, D, UF, MF
Poly(amide)	RO, NF, D, UF, MF
Poly(sulfone)	GS, UF, MF
Poly (ether sulfone)	UF, MF
Poly(carbonate)	GS, D, UF, MF
Poly(vinylidene fluoride)	UF,MF,MD
Poly(propylene)	MF
Poly(acrylonitrile)	D, UF, MF

(a) GS: gas separation, UF: ultrafiltration, MF: microfiltration, D: dialysis, PV: pervaporation, RO: reverse osmosis, MD: membrane distillation.

The selection of the membrane material has a tremendous influence on the membrane performance [17], as the material functions a critical role in interacting with feed solution. The material determines several membrane properties, such as hydrophilicity, surface charge, chlorine tolerance limit and allowable pH range. Regarding hydrophilicity, cellulosic materials such as cellulose acetate show a high degree of hydrophilicity while Poly (propylene) is highly hydrophobic in nature.

Different polymers show intermediate hydrophilicity, such as poly (sulfone) (PS), poly (ether sulfone) (PES) family, poly (acrylonitrile) (PAN) and poly (vinylidene fluoride) (PVDF) are also used as a selective layer for the membranes [18].

2.3. Preparation of asymmetric synthetic membrane

Loeb and Sourirajan described the first membrane material in the late 1950s. Since then, numerous materials have been developed aiming to ameliorate the capacity and performances of the existing membrane technology. Different techniques are available to prepare synthetic membranes which can be fabricated from various types of materials whereby polymers and ceramics are the most valuable [13, 14].

The selection of fabrication method for polymeric membrane depended on the polymer type and desired structure of the membrane [19]. Techniques commonly used for polymeric membranes fabrication are phase inversion, interfacial polymerization, stretching, track-etching and electrospinning [19]. Most commercially available membranes are manufactured by phase inversion technique which enables the production of various membrane morphologies [14, 20]. In the next section phase, inversion technique will be discussed in details.

2.3.1 Phase inversion technique

Phase inversion technique is described as a demixing process whereby the originally homogeneous polymer solution converted in a controlled method from a liquid to a solid state [2]. This transformation can be achieved by several processes [20] include:

1. Thermal gelation: a process where polymer solution is cast hot, polymer precipitation stimulated by lowering the temperature of the cast film. As it cools, the polymer precipitates and the solution separates into a polymer matrix phase containing dispersed pores clogged with solvent. After the polymer solution is cast, the volatile solvent evaporates, and the cast film is enriched in a nonvolatile solvent, thus encouraging the polymer precipitation to form the membrane structure.

2. Solvent evaporation: A mixture of solvents, with one of them being volatile, is used to form the casting solution. After casting, the volatile solvent evaporates, thus changing the polymer-film–solution composition, which induces precipitation.

3. Water vapor adsorption: The cast film is placed under a moist atmosphere. As water is typically a strong non-solvent, water adsorption into the cast film causes polymer precipitation. In its most rigorous form, this process is the reverse of the solvent evaporation. Instead of inducing precipitation by evaporating a volatile solvent, the polymer film is exposed to a humid environment permitting water vapor adsorption onto the cast film.

4. Immersion Precipitation: The polymer solution is immersed in a non-solvent coagulation bath (typically water). Demixing and precipitation take place due to the exchange of solvent (from polymer solution) and non-solvent (from coagulation bath), that is, the solvent and non-solvent must be miscible [19].

A combination of the above- mentioned methods is usually applied. Amongst the four types of phase inversion processes, noticeably immersion precipitation remains the most important membrane preparation technique.

2.3.1.1 Immersion precipitation technique

Immersion precipitation is a procedure where a polymer solution cast on an appropriate support, then immersed in a coagulation bath which contains a non-solvent, where an exchange of solvent and non-solvent happens and a membrane is formed [21]. Many factors participate in the successful fabrication of high-performance membrane module. Extensive research works discussed the optimization of the factors influencing porous membrane production by selection of the polymer, the solvent, non-solvent additive types, precipitation time, the constitution of coagulation bath, its temperature and other parameters during immersion precipitation [20, 22, 23].

2.4. Mechanisms of membrane formation by immersion precipitation

Membrane formation mechanisms can be clarified by a three-component phase diagram which is used to demonstrate the components used in membrane preparation (polymer, solvent, non-solvent) by immersion precipitation in an isothermal process. as shown in **Fig. 2.3** (a)). The cast film composition begins from the original casting solution region (A). As the solvent and non-solvent are miscible the casting solution shifts to the two-phase unstable region by losing solvent and gaining non-solvent, thus crossing the binodal boundary. This brings the casting solution into the metastable two-phase region, where it starts to demix. Polymer solution constituents in this region are thermodynamically unstable, but will not precipitate unless well-nucleated. At point (C), as more solvent and non-solvent exchange, the composition crosses into another region of the phase diagram in which the solution is always thermodynamically unstable. At (D), the final membrane composition is solidified, and the matrix of the final formed membrane is represented by point (S).

Thus, a solid (polymer-rich) phase and a liquid (polymer-poor) phase are formed; the precipitant filled membrane pores are represented by point L. The place of point D on the line S-L a ccount for the total porosity of the membrane [14, 20].

The rate of solvent and non-solvent exchange relies on the miscibility of the two, and the affinity of the non-solvent for the polymer.

Two distinct demixing processes creating two recognized types of membrane morphology are present; membranes formed by immediate demixing which result in the production of the porous top layer and open-cell macrovoid-like membranes while delayed demixing is forming membranes with a relatively dense top layer [14, 20, 23].

The types of demixing are illustrated in **Fig. 2.3** (b). In immediate demixing the casting film underneath the top layer has crossed the bimodal region, suggesting that liquid-liquid demixing begins immediately after immersion. While when the demixing delayed all compositions directly underneath the top layer remain in the one phase region and are still

miscible, this indicates the lack of immediate demixing after immersion; it takes place sometimes before it crosses the bimodal region and liquid-liquid demixing will start [14, 20].

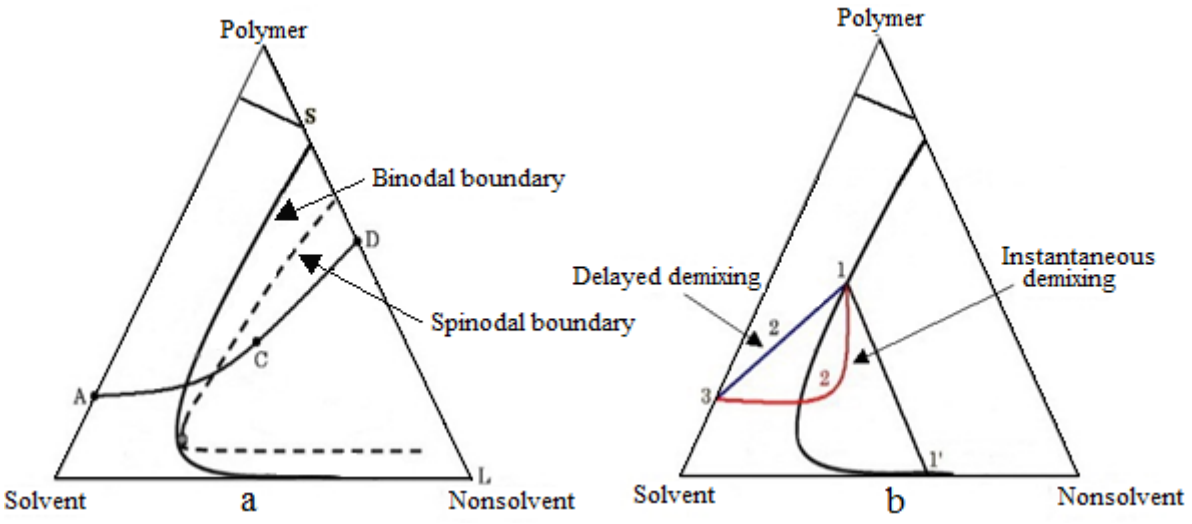

Fig. 2.3 (a): Three-component phase diagram from the initial casting solution (A) to the final membrane (D), (b): Instantaneous and delayed liquid-liquid demixing (composition present at the top, middle, and bottom of the film indicated by 1, 2, and 3, respectively).

2.5. PVDF as a membrane material

Poly (vinylidene) fluoride (PVDF) has encountered a great concern as a membrane material since the 1980s [24, 25] in comparison to other commercialized polymeric substances such as poly (sulfone) (PS), poly (ether sulfone) (PES) and polyimide (PI) [26]. PVDF dissolves readily in common organic solvents; it has been used widely in MF, UF, MD, and PV membranes due to its convenient asymmetric structure for separation [27, 28]. However, it has hydrophobic characteristics, and this hydrophobic nature leads to its low water flux and makes PVDF membrane easily fouled while processing aqueous solutions containing natural organic materials [29].

For wide-range applications, the previously mentioned drawbacks of PVDF-UF membranes must be overcome [30]. Therefore, many efforts have been performed to improve the

hydrophilicity of PVDF by dip coating, physical blending [31-33], chemical/radiochemical grafting or surface modification [34-39]. Among these methods physical blending with organic and inorganic materials has gain much interest due to easy preparation procedure and good performance results [40].

2.5.1 Crystalline properties of PVDF

PVDF is a fluoropolymer with alternating –CH2 and –CF2 groups over the polymer chains that generate a polarity permitting the polymer to dissolve in certain solvents. Homopolymers of PVDF are semicrystalline, with crystallinity typically around 35%–70%, with long chain macromolecules, which contain 59.4 wt% fluorine and 3 wt% hydrogen [41]. The spatial arrangement of CH2 and CF2 groups along the polymer chains participates in the distinctive properties of PVDF generated from its crystalline structure.

In general, polymer crystallinity and the resultant membrane morphology are among significant factors in determining the mechanical strength properties, as well as the impact resistance of the membranes [23]. Increased level of crystallinity yields PVDF stiffness, toughness, and creep resistance [20]. PVDF chains can crystallize into three separate forms: α, β, and γ with density of 1.68, 1.92, 1.97 respectively [23, 42]. The most common polymorph of PVDF is α phase. On account of its excellent combination of properties and processability, PVDF is available in a wide range of melt viscosities as powders and pellets to satisfy typical fabrication requirements. The chemical structure of PVDF homo polymer is shown in **Fig. 2.4**.

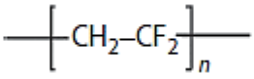

Fig. 2.4. PVDF homopolymer.

2.6. PVDF membrane fabrication

The preparation of PVDF membranes had begun from the early 1980s [24-25]. Various methods are employed in the fabrication of PVDF membrane like sintering, track etching [43, 44], and phase inversion. Most commercial membranes are produced by phase inversion method as it is one of the most versatile, economical and flexible processes used to generate both dense and porous membranes. Immersion precipitation remains the most used technique among the types of phase inversion processes used to prepare PVDF membrane [20].

2.7. Factors affect PVDF membrane Fabrication

This section discusses the different factors influence the PVDF flat sheet membrane development using immersion precipitation, in particular for UF membrane. Fabrication process parameters are the crucial factors that affect the UF membrane performance. It is well known that fabrication parameters have a tremendous effect on the final membrane morphology and performance. An ideal porous membrane must have high permeability, good hydrophilicity, and excellent chemical resistance to the feed stream [20, 40]. High membrane permeability is achieved if the membrane surface porosity and pore structure are good. Different parameters affecting PVDF membrane production include polymer concentration, solvent type, non-solvent additives, precipitation time, coagulation bath composition and temperature will be reviewed.

2.7.1 Effect of solvent type

Solvent plays a principal role in determining the eventual membrane properties and performance. The most important criterion for solvent selection is its ability to dissolve the polymer completely [20]. The low miscibility of a polymer in the solvent leads to fabrication of a non-porous membrane, while more porous membranes are obtained when the miscibility is high; as with increased miscibility, more solvent is required in the non-solvent bath to

affect demixing [14, 23]. The commonly used organic solvents to prepare PVDF membrane through immersion precipitation are listed in **Table 2.2**.

Table 2.2 Solubility parameters of common solvents for PVDF [45].

Solvent	Dispersion parameter $\delta_{d,P}$ (MPa1/2)	Polar parameter $\delta_{p,P}$ (MPa1/2)	Hydrogen bonding parameter $\delta_{h,P}$ (MPa1/2)	Total solubility parameter $\delta_{t,P}$ (MPa1/2)
N,N-Dimethylacetamide (DMAc)	16.8	11.5	10.2	22.7
N,N-Dimethylformamide (DMF)	17.4	13.7	11.3	24.8
Dimethylsulfoxide (DMSO)	18.4	16.4	10.2	26.7
Hexamethyl phosphoramide (HMPA)	18.4	8.6	11.3	23.2
N-Methyl-2-pyrrolidone (NMP)	18	12.3	7.2	22.9
Tetramethylurea (TMU)	16.8	8.2	11.1	21.7
Triethyl phosphate (TEP)	16.8	11.5	9.2	22.3
Trimethyl phosphate (TMP)	16.8	16	10.2	22.3

Bottino et al. investigate (PVDF) membranes prepared by casting and coagulating solutions of the polymer in eight different solvents to identify the suitable solvent for PVDF polymer. Depending on Bottino's study the solubility parameters of solvent for PVDF are tabulated in **Table 2.2.** Their experimental results indicate that thermodynamic did not affect the performance of the final PVDF membrane, whereas a good correlation was found between solvent- non-solvent mutual diffusivity, thus the membrane performance can be correlated to the mutual diffusivity [45].

Shih et al. reported a rise in the mean pore size and effective porosity with increasing glycerol as non-solvent additives to PVDF membrane with TEP solvent system, while they noticed reduced effective porosity when using DMSO as a solvent. The authors suggested the results are due to the different affinity of the solvent to the water coagulation bath [46].

2.7.2 Effect of PVDF concentration

Increasing PVDF concentration in the casting solution augments the solution viscosity and hence the polymer concentration increased at the interface, this implies that the volume fraction of polymer increased, and it will lower the porosity and contact angle of the membrane [14, 47]. The viscosity and concentration of the polymer solution are principal factors that rule the morphological structure of the produced membrane. The polymer chains tend to align more tightly as a result of the formation of a denser skin. This closer structure of the membrane with high polymer concentration increases the thickness of the top layer. It also reduces both number and size of macrovoids/cavities [47]. A similar result was deduced by Tomaszewska, who investigated the relation between PVDF polymer concentration and the porosity, the resultant relation is presented in **Fig. 2.5** [48].

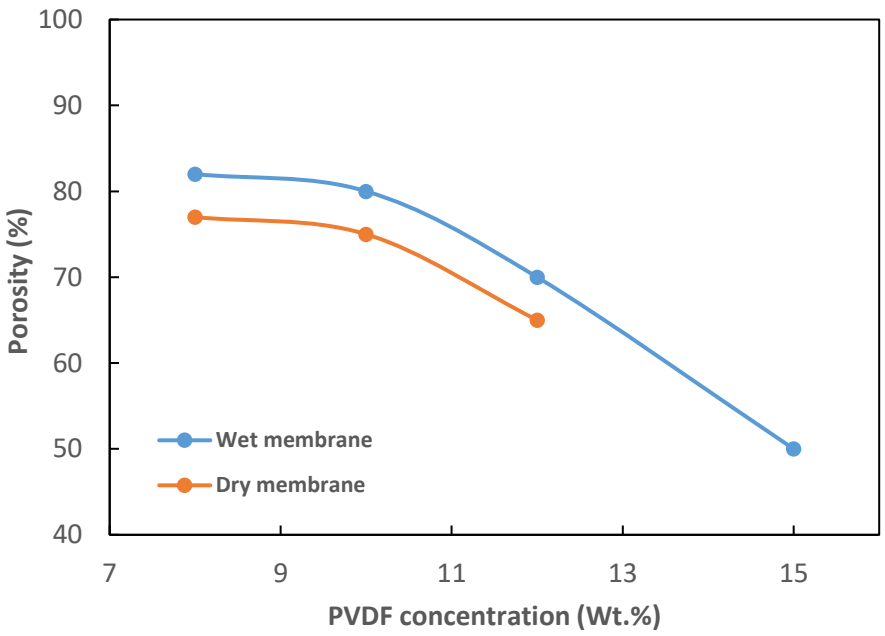

Fig. 2.5. Effect of PVDF concentration in casting solutions on the porosity of the resultant membrane: (a) wet, (b) dry [48].

Buonomenna et al. studied the influence of PVDF concentration on membrane morphology and porosity by phase inversion process for PVDF cast in DMA solvent, he suggested that the

effect of polymer concentration on morphology is comparatively small as can be seen in **Fig. 2.6**; in the three membranes with various PVDF concentrations the same distinct regions can be identified. The skin layer is gradually tighter and nonporous. He concluded that the main effect of increasing polymer concentration is a decline in pore dimensions and overall porosity [49].

Song et al. studied the effect of PVDF concentration on a modified PVDF membranes fabricated by the addition of different concentrations of PEG and TiO_2 particles. He found that the membrane flux decreased progressively with increasing PVDF content, while the rejection of pepsin increased gradually with the increase of PVDF content. Also, he observed that the casting solution became too viscous to produce a membrane when the PVDF content transcended 18 wt. %, but when PVDF content was 12 wt. %, the membrane had a good combination of membrane flux and rejection [50].

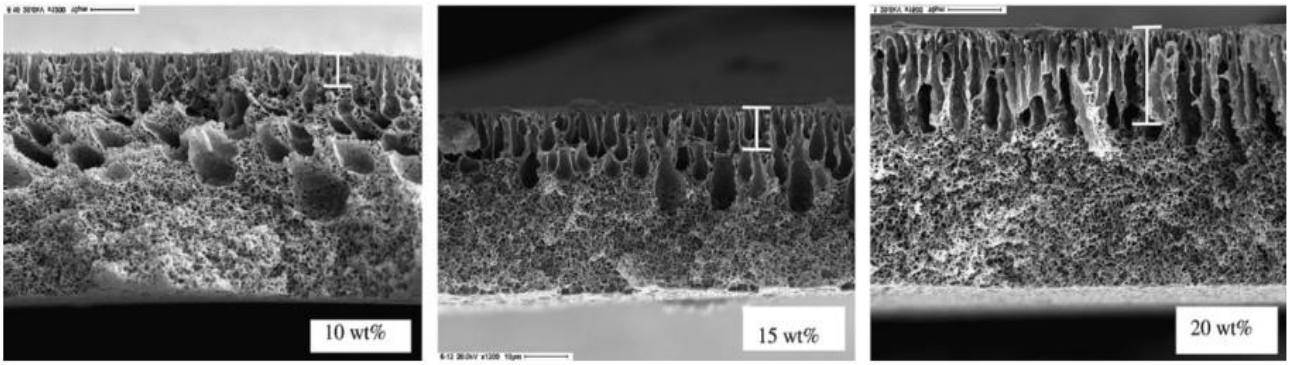

Fig. 2.6. SEM images of cross-sections of PVDF membranes prepared at different polymer concentration with porosity 65, 55, 41 respectively [50].

2.7.3 Effect of coagulation bath medium and temperature

The coagulation medium is one of the fundamental factors determining the sequence of phase separation in the immersion precipitation process [20]. The interaction between the solvent and the non-solvent remarkably affects the demixing process and the solvent exchange rate [51]. Systems with a rapid phase inversion rate tend to form macrovoids with finger-like

structure, whereas systems with a slow phase inversion rate result in the formation of sponge-like structure [52].

It is well known that water acts as a powerful non-solvent. Thus, the presence of water in the coagulation medium during immersion precipitation often leads to a rapid liquid–liquid demixing process and accordingly the formation of a PVDF membranes with asymmetric structure and finger-like voids [20, 23].

Other weaker non-solvents can be used; they lead to the formation of a denser membrane [53]; Cheng et al. suggested that membrane structure is specified by the relative diffusion rate of solvent and non-solvent and the driving force between solvent and non-solvent. When the out-diffusion rate of the solvent is much faster than the in-diffusion rate of non-solvent, the top layer is very dense, thus lowering the diffusion rate for non-solvent into the sublayer, this results in fewer nuclei in the sublayer in the initial period. It is, therefore, feasible to compose a finger-like structure if the driving force between solvent and non-solvent is strong enough. On the other hand, the affinity between solvent-non-solvent is low, the membrane formed will have a sponge-like structure [53].

Sukitpaneenit and Chung investigated the thermodynamics of the phase inversion process of PVDF membranes through phase diagrams [54]. The triple phase diagrams of PVDF/NMP/non-solvent systems of different non-solvents at 25°C were formulated depending upon the cloud-point measurements, as shown in **Fig. 2.7**. It can be noticed that the gelation boundary for the PVDF/NMP/water system is nearer to the polymer–solvent axis as compared to the other PVDF/NMP/non-solvent systems; he indicated that the strength of non-solvent systems follows the sequence of water > methanol > ethanol > isopropanol. [54].

Lin et al. used pure water as coagulation bath for PVDF/ PMMA composite membrane, the formed membrane showed porous morphology with predominantly macrovoids and cellular pores. However with the addition of solvent (70% DMSO) to the coagulation bath, liquid–liquid demixing was sufficiently inhibited with the formation of sponge-like structure

membrane, as the presence of a solvent in the coagulation bath restricts the outflow diffusion of solvent in the cast film [55].

Wu et al. demonstrated a new approach to fabricating a porous asymmetric hydrophilic PVDF membranes by phase inversion method using a graphene oxide (GO) aqueous solution as a coagulation bath. An increment in pore size and surface roughness was noticed with increased water flux by 140%; authors attributed this to the improvement of hydrophilicity and increase in the surface roughness which caused by the deposition of hydrophilic GO layers on the membrane surface [56].

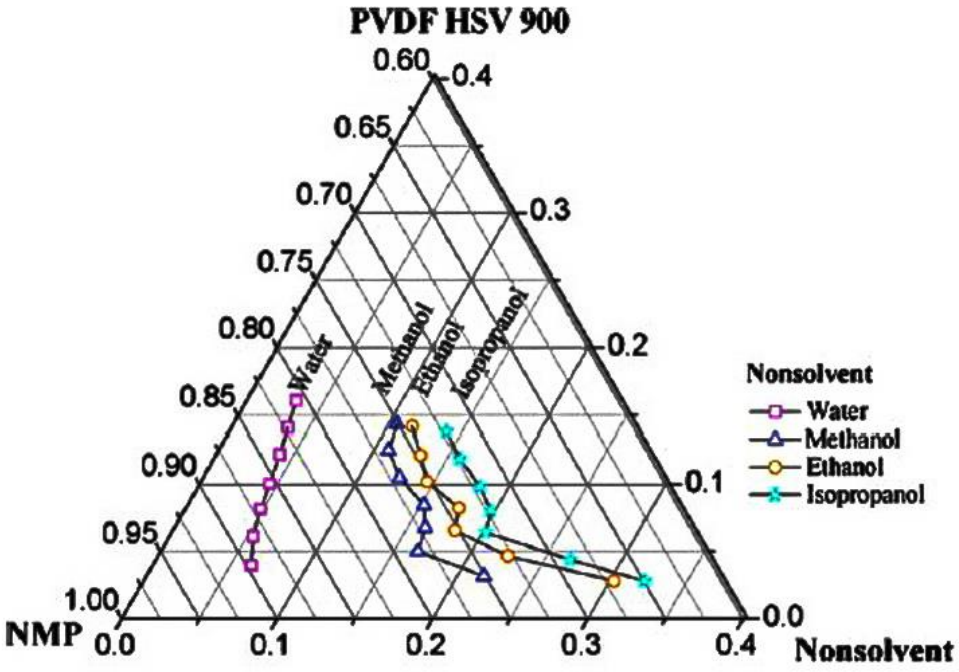

Fig. 2.7. Phase diagram of PVDF/NMP/non-solvent systems at 25^0C [54].

The effects of non-solvent and precipitation temperature on the morphology and crystalline structure of 1-octanol/DMF/PVDF and water/DMF/PVDF systems prepared by phase inversion process were studied by Cheng [57]. He found that casting membranes from PVDF-DMF system with rapid phase inversion rate using water (strong non-solvent) as a coagulation bath. This rapid phase inversion leads to formation of asymmetric structure membrane consisted of dense skin layer. While in system with slow phase inversion rate

using 1-octanol (weak non-solvent) as a coagulation bath, mass transfer became slow and liquid–liquid demixing was inhibited. The resultant PVDF membrane showed symmetric structure with a uniform cross section and almost similar spherical particles, as demonstrated in **Fig. 2.8**.

Cheng also examined different coagulation bath temperature ranges (25-85 ^{0}C) and suggested that at low temperatures, the membrane formed has a uniform particulate structure dominated by the crystallization mechanism. However, at high temperature the gelation region shrinks significantly more than the liquid-liquid demixing region. And so provided a preferred condition for liquid-liquid demixing to occur earlier than crystallization. As a result, asymmetric cellular morphologies with a dense skin layer were produced [57].

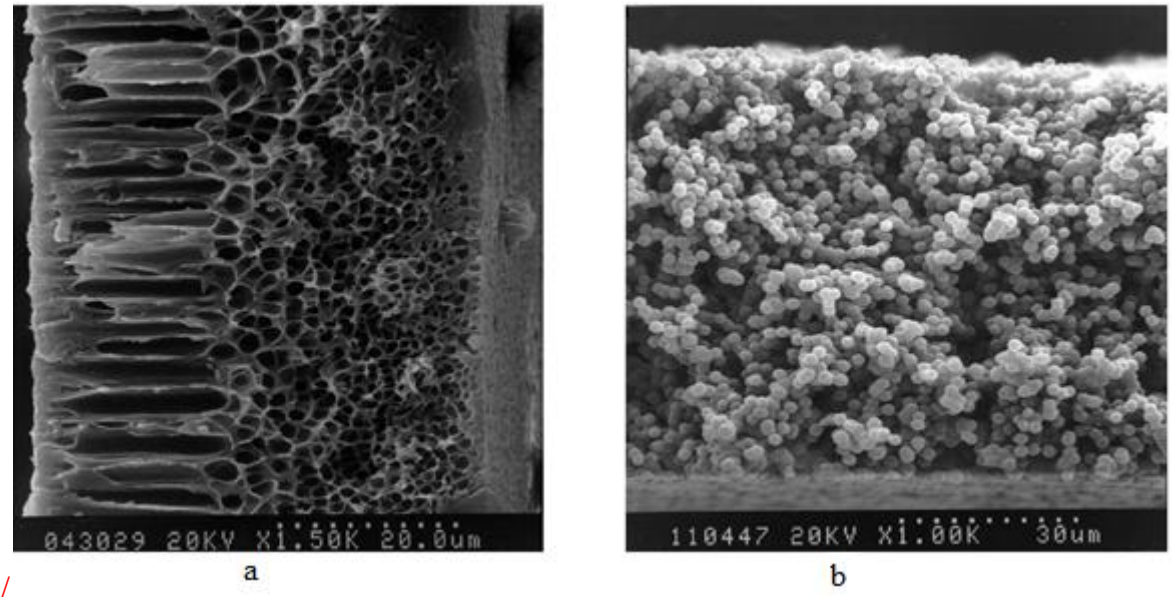

Fig. 2.8. Cross- section images of PVDF membrane with (a) water and (b) 1-octanol as coagulation bath respectively [57].

2.7.4 Effect of non-solvent additives

The incorporation of non-solvent in the membrane casting solution is one of the techniques to improve membrane morphology, increase the hydrophilicity, improve porosity and enhance the membrane performance parameters such as water flux and rejection [23]. Non-solvents conduct as pore former, increase solution viscosity or hasten the phase inversion process [23].

Additives used in PVDF membranes modification can be broadly classified into four groups: (a) low molecular weight inorganic additives like LiCl (b) polymeric additives such as Poly (vinyl pyrrolidone) (PVP) and Poly (ethylene glycol) PEG (b) weak non-solvent and co-solvent such as glycerol, ethanol and acetone [46] and (c) inorganic nanoparticles such as zeolite, silica and carbon nanotubes materials.

Fontananova et al. studied the effect of the addition of LiCl and PVP to PVDF membrane during phase inversion process; both additives were soluble in DMAC and H_2O. In the case of PVP addition, the membrane macrovoids became more emphasized and extended over the whole cross-section. While for low concentration of LiCl in the casting solution results showed bigger macrovoids and increase permeate flux. For high concentration of LiCl the macrovoids formation reduced, as the LiCl additives increased the solution viscosity increased and delayed the mutual diffusion between solvent in the coagulation bath and the cast film. Therefore, they delayed the phase separation [58]. Authors concluded that PVP is a better additive for the preparation of membranes with a higher permeate flux, whereas LiCl can be used to decrease macrovoids formation.

PEG has been reported to enhance water flux of membranes at the expense of lowering rejection rates [59]. However, Song et al. have documented different results using PVDF-PEG-TiO_2, they noticed an increase in humic acid (HA) rejection with flux decline; authors attributed these results to smaller membrane pores, and more hydrophilic membrane on the surface [50].

2.7.4.1 Dopamine as a membrane additive (Bio-glue)

Dopamine is newly discovered as a promising novel bio-inspired polymer used for membrane modifications, it has properties similar to adhesive secretions of mussels and is capable of adhering on the surface of most substrates such as poly (tetrafluoroethylene) (PTFE) and PVDF via polymerization of dopamine [60-62]. Also, it has been proved that polydopamine

(PDA) has an excellent environmental stability, good biocompatibility, and a particularly outstanding dispersibility in water [63].

PDA coating with inorganic nanomaterials such as metals and metal oxides is feasible [60-64]. Furthermore, when PDA is applied to a substance its surface properties dominate over those of the surface substrate which facilitates the compatibilization of other organic fibers or carbon nanotubes to the surface [65]. Recently, Zhen et al. have utilized PDA produced by self-polymerization to alter the surface of various porous membranes like PS, PE, PTFE, and PVDF; the results are denoting that the membrane hydrophilicity was markedly improved.

Due to distinguished adhesion features of dopamine, nanoparticles such as TiO_2 nanoparticles, as shown in **Fig. 2.9** [62], and clay [66] have been surface modified with PDA coating to enhance interfacial interactions between nanomaterials and polymer matrices. Authors reported that both water flux and rejection of BSA were simultaneously improved, the research results suggested that the interfacial PDA layers not only alleviate the dispersion of these nanomaterials in the polymer matrices due to the remarkably increased interfacial interactions (a combination of covalent and noncovalent interactions) but also supply the nanocomposite with a new functionalities and strong binding forces for further modification [60, 67].

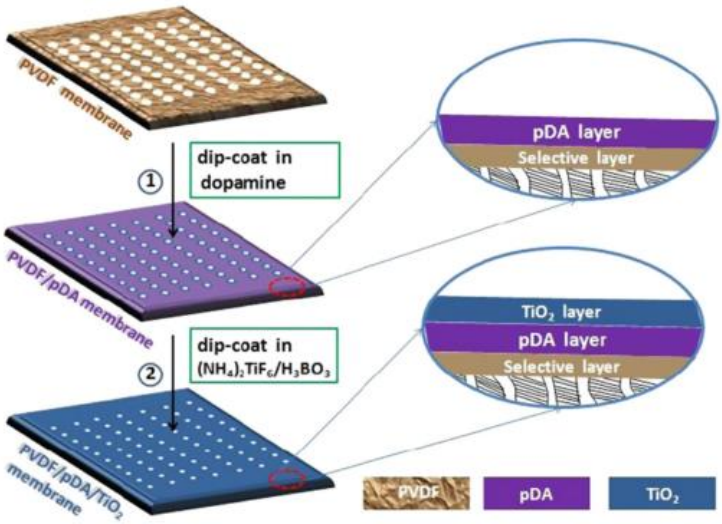

Fig. 2.9. A modified membrane surface via self-polymerized polydopamine with binding TiO_2 films [62].

Jiang et al. studied the preparation of PVDF/PDA nanoparticles blends membranes under different polymerization conditions. The resultant membrane prepared by in situ polymerization of PDA on PVDF found to be beneficial to form uniform surface pores and inner connected pores. As unpolymerized dopamine and a few of PDA, nanoparticles are released from developing films into a water bath, leaving pores in the resultant PVDF/PDA blend membranes, which lead to high permeate flux and tensile strength. Authors suggested that PDA performed as both pore-forming agent and hydrophilic modifier. The resultant membrane also showed permeability up to 100 LMH/bar with 15% rejection [67].

2.7.4.2 Aniline as a membrane additive

Polyaniline (PANI) is one of the most important conducting polymers that has many applications for membrane separation processes [68]. It is used in ultrafiltration membranes [69, 70], gas separation membranes [71], pervaporation membranes [72] and semi-conducting membrane [73] for its stability and relatively cheap cost [74, 75]. The interest in polyaniline as a membrane modification material came from its easy preparation by the polymerization reaction, and the chemically flexible NH group, which is responsible for an interesting doping/developing chemistry that can potentially improve its characteristics for specific separation applications [68, 76].

Zhao et al. [68] suggested PANI addition as a filler to (PSF) membrane by in-situ blending method, results showed that PANI played as a pore former, which led in increased hydrophilicity and porosity of the membrane, with a results in 2-4 more permeable than pristine PSF membrane and 96% BSA rejection. A comparative study between PANI and PVP addition to PSF membrane was done by Zhao et al. [77] results showed that at the same additive concentration, PSF/PANI nanocomposite membranes had higher protein rejections, higher FRR values, and larger breaking strength than PSF/PVP membranes.

2.7.4.3 Inorganic nanoparticles as a membrane additives

Application of inorganic nanoparticles in membrane fabrication is a new promising membrane technology. Recently, extensive studies on membrane modifications with the blending of inorganic nanomaterials with casting solution have been done. Performance results of several inorganic nanoparticles that have been blended with PVDF are summarized in **Table 2.3**.

Table 2.3 Results of modified PVDF membranes with different inorganic nanoparticles [78].

Inorganic filler	Inorganic fillers dimensionality	Optimum dosage of inorganic material (PVDF, g,g)	Decreased in contact angle (º)	Rate of change in water flux (%)	Rate of change in rejection (%)	Rate of change in tensile strength (%)	References
ZnO	3D	6.70%	13	75	-	7.8	[79]
SiO2	3D	5%	-	140	-	109	[80]
	3D	3%	29.5	275	-8	-	[81]
Al2O3	3D	2%	26.2	400	1	50	[82]
ZrO2	3D	150%	-	500		-	[83]
Fe3O4	3D	70%	-	270	18	8.6	[84]
TiO2	3D	2%	4	19	3	-	[85]
	1D	5%	48.3	66	7	33	[86]

It is clear that the introduction of inorganic nanoparticles enhances the morphology, permeability and improves the anti-fouling performance of membranes, likely due to the high specific surface area, and chemical stability [56].

Among these nanoparticles, the implementation of graphitic carbon materials in ultrafiltration membranes fabrication has attracted substantial attention, and the use of carbon nanotubes (CNTs) which have distinctive features is a new research field in membrane fabrication techniques.

2.7.4.4 Carbon nanotubes in membrane fabrication

Carbon nanotubes have gained considerable interest since their discovery in 1991 by Iijima [87]. CNTs are defined as minute cylinders of graphite which are closed at the ends by half C60. CNTs ordinarily have a diameter less than 10 nm [88]. Carbon nanotubes are classified to single-walled nanotubes (SWNTs) and multi-walled nanotubes (MWNTs). SWCNTs, are a cylinder of a single graphene sheet, consist of an array of benzene molecules with hexagonal rings with double and single carbon-carbon bonding. The MWCNT is multi-layers of rolled graphene sheets [88], as shown in **Fig. 2.10**).

CNTs are considered to have important physical properties, such as unique mechanical properties (stiffness and flexibility), high electrical and thermal conductivities, and due to the presence of delocalized π- an electron in the z-axis [89]. Additionally, CNTs have extraordinary water treatment capabilities which were proven to perform effectively against both chemical and biological contaminants [90].

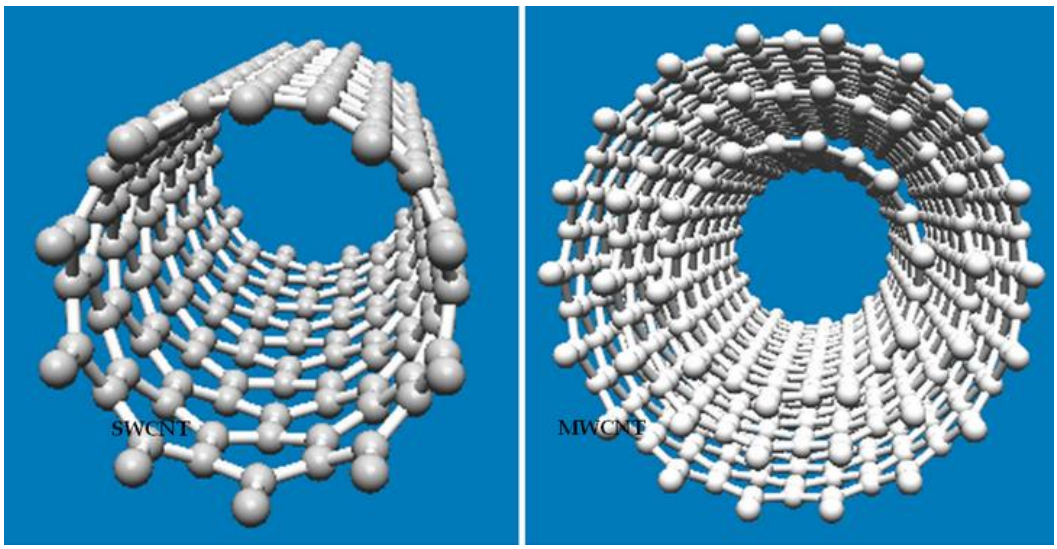

Fig. 2.10. The structure of SWCNT and MWCNT [91].

CNTs also used as an adsorbent media which is capable of removing various contaminants such as heavy metals, metalloids, organics and a range of biological contaminants including NOM [92-94].

The excellent adsorption features are attributed to the large specific surface area [95], the mesoporous structure and the less negative surface charge on the CNTs, also the effective π - π stacking interaction between carbon nanotube and aromatic compounds [96,97]. Their distinctive properties make them attractive candidates for polymer composites. However due to the strong van der Waals binding energies, CNTs are tightly bundled by calculated interaction energy of ca. 500 eV/μm of tube–tube contact and as a result it is insoluble in most organic solvents [98], making efficient dispersion in bulk solution hard to achieve. Moreover, the inert surface of CNTs results in intrinsically weak interactions and poor interfacial adhesion between CNTs and membrane materials

2.7.5 MWCNT/polymer composite in membrane fabrication

MWCNT/polymer composite membrane initially designed to improve the separation performance of polymeric membranes. The incorporation of MWCNT as inorganic fillers to polymeric membranes was introduced to enhance the chemical and physical properties of membranes [99]. However, there are significant obstacles in the preparation of CNT/polymer composites, particularly concerning the need to ensure sufficient adhesion between the CNTs and the polymer to ensure uniform distribution of CNTs in the composite and avoid agglomeration. As it is reported that agglomeration causes voids which may decrease the mechanical properties, and also may minimize the effect of nanomaterial for the large surface area and reduce the membrane performance [100].

There are many studies on CNT dispersion in polymers and solvents; two main methods for dispersing carbon nanotubes are suggested [101]: the mechanical methods and the chemical methods which designed to modify the surface energy of MWCNT, either physically (non-covalent treatment) or chemically (covalent treatment).

Mechanical dispersion methods, such as ultrasonication (either by ultrasonication tip or bath), detaches nanotubes from each other by applying high local shear forces, particularly to the nanotube bundle to overcome van der Waals binding energy, but adversely this method can lead to fragmentation of nanotubes which affect its performance [102].

Chemical methods use surface functionalization of CNT to enhance their chemical compatibility with the solvent or polymer by breaking sp^2 hybrid carbon bonds on the sidewalls and binding with carboxyl/hydroxyl groups; this method can improve adhesion characteristics of CNTs and reduce their agglomeration. However, attention should be taken in the aggressive chemical method used in CNT dispersion, which might lead to defects in CNT and hence low-grade properties [103, 104]. Functionalized carbon nanotubes enhance membrane properties by increasing hydrophilicity and surface charge of top membrane layer [105].

The potential application of carbon nanotubes (CNTs) in membrane materials has gain more attention recently; it has been studied with many types of base polymers like PES, PS, PANI [106-112] and PVDF. Few studies examined the effect of CNT addition to PVDF-based membranes used for ultrafiltration process.

Zhao et al. used functionalized MWCNTs with hyper branched poly (amine-ester) (HPAE) based on Zhang's technique [113] and applied them as an additive to prepare PVDF nanocomposite membranes. $MWNT_{HPAE}$ was dispersed in DMF via sonication. The results of the prepared PVDF/ $MWNT_{HPAE}$ nanocomposite membrane showed lower water contact angle (higher hydrophilicity) and enhanced antifouling properties as the surface coverage of hydrophilic hyper branched poly (amine-ester) groups, which could induce denser and more stable hydration layer. Consequently, protein adsorption was significantly suppressed due to hydrogen bonding interactions between hydrophilic groups and water molecules. Different $MWNT_{HPAE}$ percentages were used. The flux recovery increased from around 82% for PVDF to 95.7% for PVDF/$MWNT_{HPAE\ (2\%)}$ [114].

A comparative study of PVDF/graphite oxide (GO) and PVDF/ (MWCNTs) ultrafiltration membranes was carried out by Zhao et al. using the phase inversion method to fabricate PVDF/carbon materials/ dimethylacetamide (DMAc). It was reported that the modified membranes exhibited better pore structure and higher surface roughness than the pristine ones, and PVDF/GO blended membranes demonstrate bigger pores but lower surface roughness than PVDF/MWCNTs blended membranes. For PVDF/MWCNTs and PVDF/GO blend membranes, 114% and 74% improvement of pure water permeation flux was achieved, respectively. The hydrophilicity was improved significantly, and the bovine serum albumin rejection of PVDF/MWCNTs and PVDF/GO blended membranes was enhanced about 31.8% and 28.7% respectively, compared to those of the pristine PVDF membranes [40].

To investigate the influence of the oxygen-containing groups of inorganic modifiers on PVDF membrane performance, Ma et al. [78] fabricated a PVDF/multi-walled carbon nanotube (MWCNT) hybrid ultrafiltration membranes via phase inversion by dispersing pristine and different concentrations of oxidized MWCNTs ranging from 0.2 wt.% to 2 wt.% in PVDF casting solutions. The prepared membrane of oxidized MWCNT at an optimum dosage of 1wt %, show 11 times increase in water flux compared with pure PVDF membrane and 22.2% increase in BSA rejection, authors explained the good results of separation and permeability by the presence of hydrophilic oxygen-containing groups on the surface of MWCNTs.

Sianipar et al. [115] investigated the use of PDA coated MWCNT as a filler in polysulfone (PSF) ultrafiltration membrane to improve the dispersion of MWCNT and the hydrophilicity. Results demonstrated the role of PDA in increasing the hydrophilicity and antifouling property of the resultant membranes with high rejection up to 99.8, however, permeability reached 81 LMH/bar.

2.8 Membrane fouling

With the recent advances in the membrane technology, novel fabricated membranes increasingly show high permeability and better efficient selectivity than membranes available 30 years ago. However, membrane fouling is still considered to be the main determining factor in the system performance. Fouling is a gradual drop in permeability during filtration process with time due to deposition of material on or within the structure of the membrane and accumulates with time making foulant layer on the membrane surface [116].

Understanding of fouling mechanisms is vital to decrease the membrane fouling phenomena and so reduce the cost of membrane recovery. Membrane fouling can occur due to [116]: (a) Solute adsorption/deposition on the surface of the membrane. (b) Solute adsorption/deposition within the membranes pores. (c) Irreversible changes to the solute fouling layer like cake consolidation.

Fouling Mechanisms of the membrane were described in detail in the literature [117, 118, 119]. There are four different physical-based types of fouling: complete blocking (pore blocking), intermediate blocking (long-term adsorption), standard blocking (direct adsorption), and cake filtration or boundary layer resistance (**Fig. 2.10**). Complete blocking occurs when each particle arriving at the membrane engage in blocks of one or more pores with no superposition of particles. Intermediate blocking takes place as each particle settles on other previously-arrived particles already blocking some pores or even directly blocking some membrane areas.

When each particle arriving at the membrane is deposited into the internal pore walls, leading to a decrease in the pore volume, it is called standard blocking. While in cake filtration, each new foulant particle rests on one or more previously arrived foulant particles that are already blocking some pores. So in cake filtration, there is no direct contact between the newly arrived foulant particles and the membrane surface.

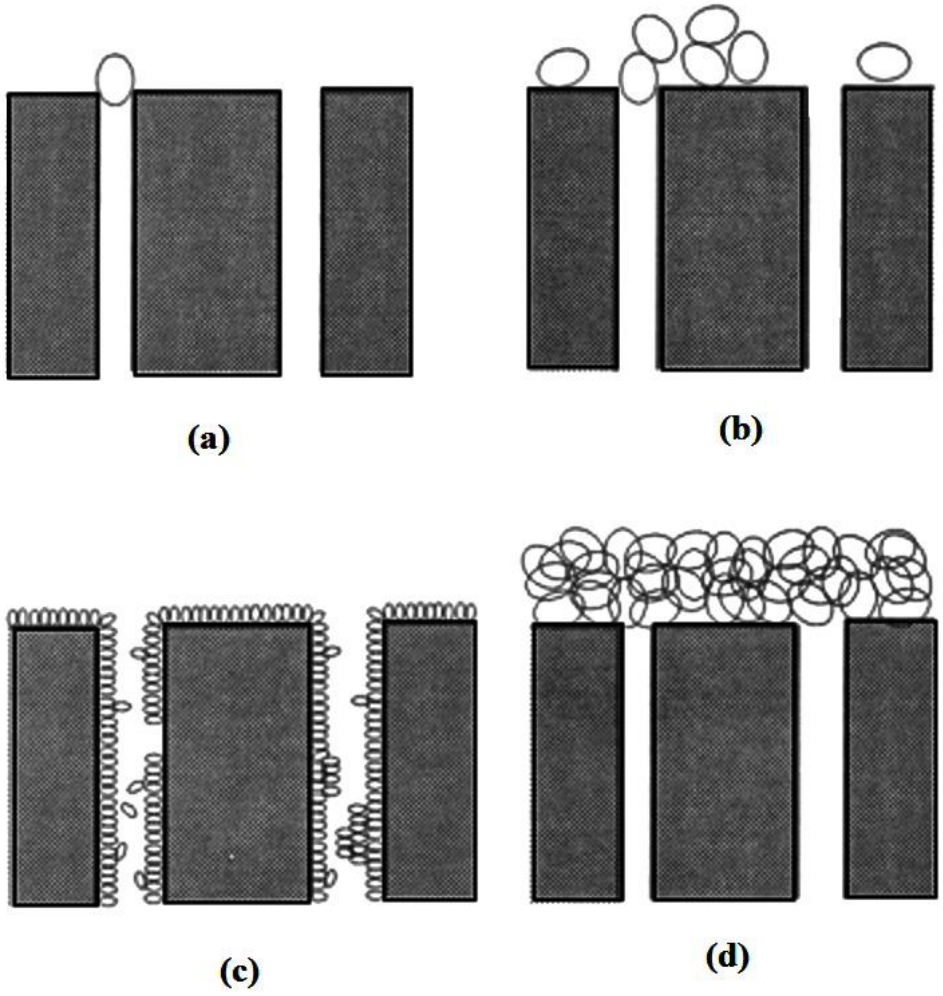

Fig. 2.11. Fouling mechanisms: (a) complete blocking, (b) intermediate blocking,(c) standard blocking, (d) cake filtration [119].

It is noticed that all the above mechanisms can dominate at different times for a filtration cycle. For standard blocking (**Fig. 2.11** (c)) solute molecules are smaller than membrane pores, hence solute particles deposit along the pore walls. While for other fouling mechanisms **(Fig. 2.11** (a, b, d)); the solute molecules are bigger or equal to the membrane average pore sizes. Thus, fouling occurs outside the pore walls.

Several mathematical methods were proposed to calculate the filtration volume (V) of each model. Hermia [118] developed different models for dead-end filtration as summarized in **Table 2.4**.

Table 2.4. Fouling models [117, 118, 120]

Model	Equation	Description
Complete blocking	$V = \frac{J_0}{k_{CB}}(1 - e^{-k_{CB}t})$	$d_{particle} \cong d_{pore}$
Intermediate blocking	$V = \frac{J_0}{k_{IB}} ln(1 + k_{IB}t)$	$d_{particle} \cong d_{pore}$
Standard blocking	$\frac{t}{V} = \frac{1}{J_0} + \frac{k_{SB}}{J_0}t$	$d_{particle} \ll d_{pore}$
Cake filtration	$\frac{t}{V} = \frac{k_{CF}}{4J_0^2}V + \frac{1}{J_0}$	$d_{particle} > d_{pore}$

Where: J_0 is initial feed flux, k_{CB} is complete blocking filtration constant, k_{IB} is intermediate blocking filtration constant, k_{SB} is standard blocking filtration constant, t is time, $d_{particle}$ is the diameter of the solute particles, d_{pore} is the diameter of membrane pore.

These models assume that a single type of fouling controls the filtration behavior. However, membrane fouling is sometimes more sophisticated and can be caused by a combination of all these mechanisms.

Fouling can be divided into reversible and irreversible depending on the type of foulant and the degree of attachment strength of foulants to the membrane surface. In reversible fouling foulants are loosely attached and can be removed easily by a physical cleaning like strong shear force or backwashing. However, for irreversible fouling foulants are a strong attachment to the membrane surface or into the membrane pores wall and causing pore blocking, and cake layer, so it is difficult to be removed by such physical methods, therefore, it needs chemical methods [121,122], as will be discussed in section 2.11.

2.9. Types of foulants

Membrane fouling occurred by combined physical and chemical interactions between the different foulants present in the feed and the membrane surface [123].

Foulants can be classified into four types:

1. Particulates (colloidal): inorganic or organic particles/colloids act as foulants which deposited on the membrane surface blocking the pores, and developing a cake layer.
2. Inorganic salts: dissolved components (e.g. iron, manganese, and silica) that interact with the membrane directly and precipitate on or within the porous structure of the membrane due to oxidation such as the formation of an iron and manganese oxide cake on the membrane.
3. Micro-biological organisms: the microbiological type contains vegetative matter like algae and microorganisms like bacteria which can adhere to the membrane and cause biofouling (biofilm formation).
4. Organic: dissolved components and colloids (e.g. humic and fulvic acids, hydrophilic and hydrophobic materials and proteins) which connected to the membrane by adsorption.

2.9.1 Organic foulants (NOM)

NOM and proteins are the two principal types of organic foulants studied in the literature. NOM are a group of organic compounds formed by the association of high-molecular-mass substances from microbiological, vegetative and animal origin [124]. They consist of a range of different compounds, from largely aliphatic to highly colored aromatics. Part of this organic matter is negatively charged, composed of a wide variety of chemical compositions and molecular sizes [125].

The presence of NOM in the water was reported to decrease the permeability and water sensitivity to pH thus reduces the permeability at all pH values due to the adsorption of foulants on the membrane surface [126]. Humic substance accounts for a large fraction of the organic matter in water. They are amorphous, brown or black, hydrophilic, acidic, polydisperse substances of molecular weights ranging from hundreds to tens of thousands [127]. NOM is composed of humic and non-humic substances according to the hydrophobic and hydrophilic components. In surface water, the hydrophobic acids which are rich in aromatic carbon, are described as humic substances and constitute the major NOM fraction, more than half of the dissolved organic carbon (DOC) in water [128, 125].

Hydrophilic matter contains less refractory molecules such as carbohydrates, proteins, sugars and amino acids [129, 130]. Based on their solubility, humic substance can be divided into three main types [124]: (i) humic acids as shown in**Fig. 2.12**), which are soluble in pH >2; (ii) fulvic acids, which are soluble in wide pH range, and (iii) the humin fraction which is not soluble at all. It is found that the three humic fractions are similar in structure, but their molecular weight is different. In addition to their effect on membrane fouling, the NOM has been shown to play a key role in the cohesion of colloids deposited on membranes surface. Analysis of the organic foulants in natural waters and their relative concentration in the cake formation suggests that polyphenolic compounds, proteins, and polysaccharides bind together with colloids and may cement the cake to the membrane surface [126, 130, and 131].

The degree of NOM-membrane interactions can be affected by NOM properties (NOM concentration, humic/non-humic fraction, molecular weight distribution, charge), membrane properties (physical structure, surface/pore charge, hydrophobicity), ion competitions and operating conditions [132].

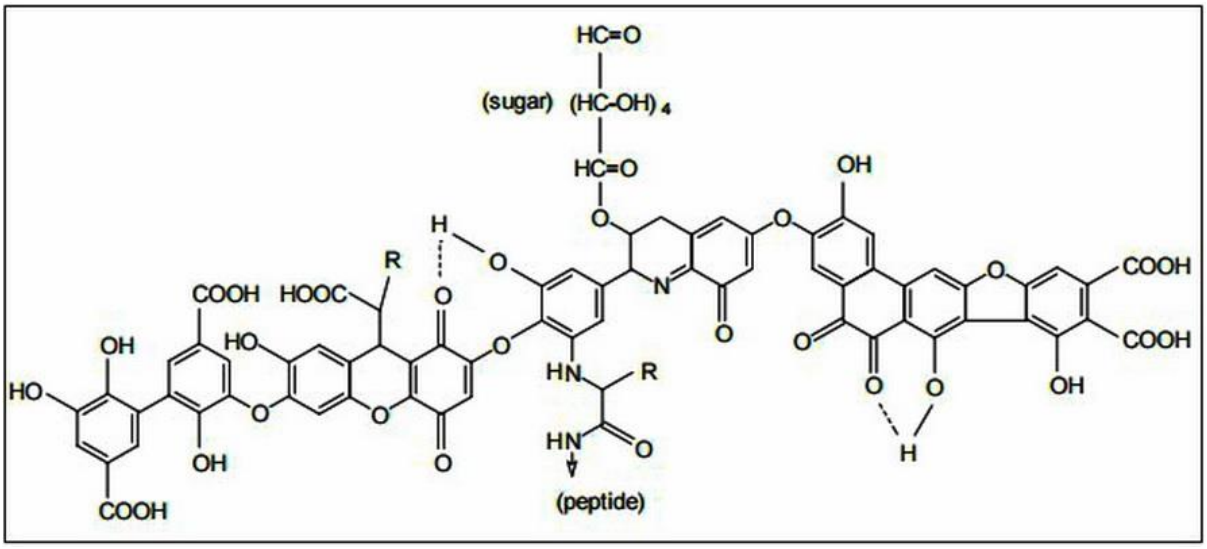

Fig. 2.12. Model structure of humic acid according to Stevenson; R can be alkyl, aryl or aralkyl [133].

2.10. How fouling affects membrane flux

The effect of membrane fouling on flux can be demonstrated by simplified theoretical model of Hagen-Poiseuille equation (2.1):

$$J = \frac{\varepsilon d^2 \Delta P}{32 \delta \mu} \qquad (2.1)$$

where: J is the flux, ε is the porosity of the membrane, d is the diameter of the membrane, ΔP is membrane pressure, δ is the effective thickness, μ is viscosity of the fluid (water).

As Hagen-Poiseuille equation is a special form of Darcy equation with the assumption that flows regime within the membrane is laminar, and the pores are rounded in shape. However, for non-rounded shape d should be corrected with hydraulic diameter D_H (the ratio of section area of flow to the wetted perimeter).

According to the previous equation (2.1) for a certain membrane pressure and viscosity, the flux of the membrane depends on (1) porosity of the membrane, ε, (2) diameter of the membrane pores d, and (3) the effective thickness of the membrane, δ.

When a membrane is fouled, porosity decreases, consequently, pores diameter decreases and the effective thickness increases. If J_0, ε_0, D_{H0}, and d_0 represent flux, porosity, hydraulic diameter, and effective thickness of a clean membrane, respectively. The influence of membrane fouling on flux can be explained by the flux ratio of the fouled membrane and the clean membrane, J/J_0 as equation (2.2):

$$\frac{J}{J_0} = \frac{(\frac{\varepsilon}{\varepsilon_0})(\frac{D_H}{D_{H0}})^2}{(\delta/\delta_0)} = (\frac{\varepsilon}{\varepsilon_0})(\frac{D_H}{D_{H0}})^2(\frac{\delta}{\delta_0})^{-1} \quad (2.2)$$

The three terms on the right-hand side of the above equation (2.2) represents the three fouling mechanisms: pore blocking, and, internal pore plugging (slandered blocking), and cake filtration, respectively [134]. Liu et al. [135], graphically showed the impacts of internal pore plugging and cake filtration on flux reduction considering NOM fouling, as shown in **Fig. 2.13;** It demonstrates the steep decline of flux along the pore diameter axis D_H/D_{H0} indicating that the internal pore plugging makes more resistance and flux decline compared to cake formation on the membrane surface.

As most of the natural organic matters have sizes less than pore diameters of UF membranes used in water filtration; adsorption of natural organic matters on the membrane is the main mechanism. Jucker and Clark reported that pores wall are a preferable site for NOM adsorption, this may elucidate the reason why NOM causes severe flux decline compared to colloidal particles.

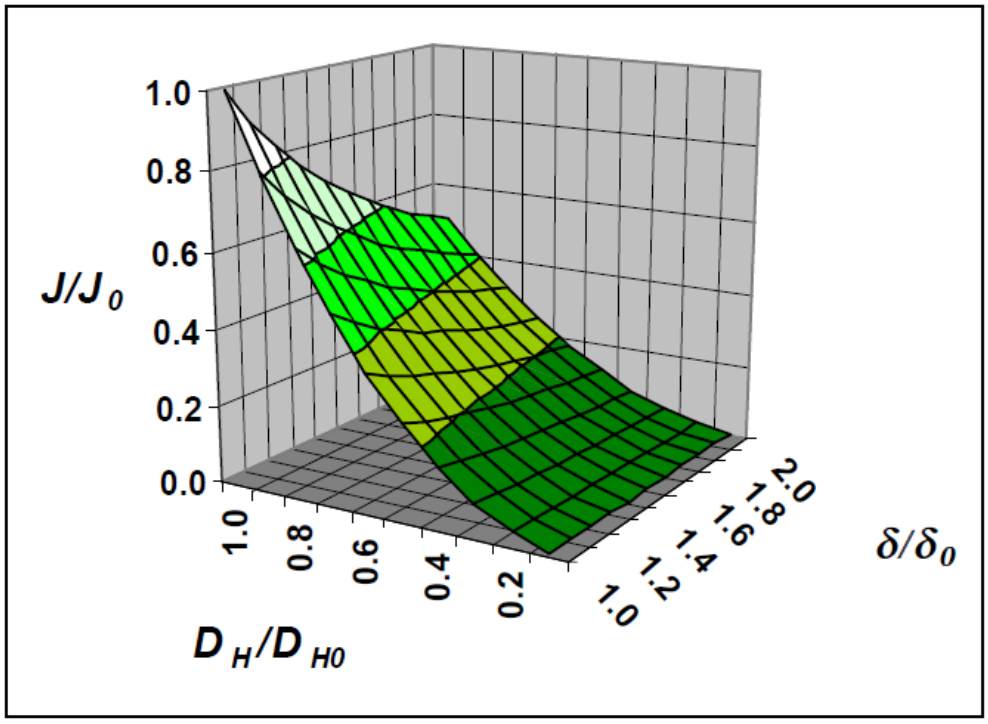

Fig. 2.13. Steep decline of flux along the pore diameter axis D_H/D_{H0} [135].

2.11. Membrane cleaning

Membrane cleaning is a procedure applied to the membrane material to remove all the foulant that deposited on the membrane surface either by physical or chemical methods [134, 136].

Since fouling is integral procedure during the filtration operation test to restore membrane flux and performance, there are different ways to clean membrane depending on the types of foulant [136, 137]. The fouled membrane could be physically cleaned by backwashing, pure water flushing, air flushing, gas-liquid flushing, reverse flow, hot water treatment or a combination of two or more of these methods [138]. Physical cleaning method can be used to remove the cake layer that has been deposited on the surface layer (reversible fouling). However, it is ineffective in the case of irreversible fouling where foulants adsorbed into the membrane layer induced by a chemical reaction between the foulants and membrane surface causing pore narrowing. Consequently, chemical cleaning is the proper approach to remove irreversible foulants to regain optimum flux recovery [138, 139].

Chemical cleaning of membrane surface can be carried out in different ways [140]: (1) Directly immersing the fouled membranes in the chemicals in the same place (2) Immersing in a separate tank with higher concentration cleaning agents (3) Adding chemicals in the feed stream (chemical wash), and (4) Chemical cleaning combined with physical cleaning (chemical enhanced backwash).

Chemical cleaning methods use a various chemical agent such as alkalis, acids, surface-active agents, and surfactants [138]. **Table 2.5** summarized the most commonly available membrane chemical cleaning agents with their reaction mechanisms.

Table 2.5. The major chemical cleaning agent used with usual reaction [136, 135].

Cleaning agent	Chemical	Reactions
Base	Caustic soda (NaOH)	Hydrolysis and solubilisation, saponification
Oxidant	Hypochlorite (HOCl), Hydrogen Peroxide (H_2O_2)	Oxidation and Disinfection
Acid	Hydrochloric (HCl), Sulphuric Acid (H_2SO_4), Nitric Acid (HNO_3)	Solubilisation
Alkaline chelate	EDTA	Chelation
Surfactants	Proprietary	Emulsifying, dispersion and surface conditioning

The type of cleaning agent and cleaning conditions in chemical cleaning mainly depend on the kind of feed deposited, and on the chemical and thermal resistance of the membrane. Cleaning agents are often applied without pressure to prevent deeper penetration of the foulants into the membranes [141].

Chemicals are often selected depending on foulant types. Caustic solution after rinsing with clean water was found to be efficient in flux recovery of PVDF membrane that had been

fouled with HA [142]. Flushing the membrane surface with water, water/NaOH and with water/NaOH/HCl was performed on bioreactor PVDF membrane system that was severely fouled with wastewater reclamation [143]. Levitsky et al. [144] studied the effects of cleaning a bovine serum albumin (BSA) fouled PVDF membrane by using NaOCl. Sodium hydroxide (NaOH) and sodium hypochlorite (NaOCl) are both commonly used in the membrane cleaning study [139,140, 145].

Cleaning agent application sequence affects the degree of permeability recovery [137]. A comparable study of cleaning NOM fouled polysulfone membrane surface, by using single cleaning agent (NaClO) and the combination of NaOH and NaClO in sequence, regarding cleaning efficiency [146]. The largest recovery in water permeability was observed when the combination of acids and NaClO was used as demonstrated in **Fig. 2.14**. As NOM removal occurred through NOM hydrolysis and solubilisation effect of both acid and base, see **Table 2.5**.

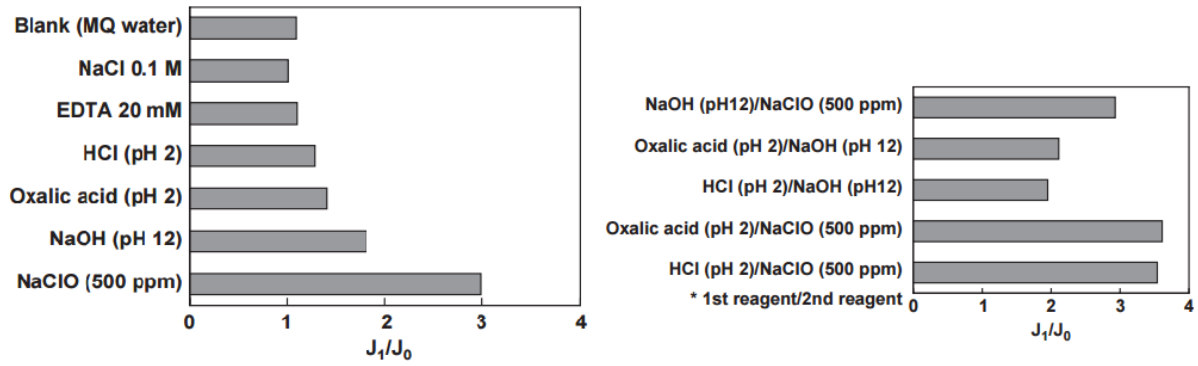

Fig. 2.14. A comparison study of the Effect of chemical membrane cleaning between single and combining cleaning agent. Where J_0 is pure water flux before chemical cleaning and J_1 pure water flux after chemical cleaning [146].

Studies have been performed to investigate cleaning sequences, and results suggested that an alkali followed by an acid cleaning sequence is more efficient than the reverse for membranes treating surface water [137]. Lee et al. [147] used a combination of NaOH and HCl in sequence for cleaning NOM fouled PES nanocomposite membrane, results showed 100%

flux recovery, with NaOH hydrolyzing the HA then HCl oxidizing and breaking down the functional groups of organic foulant and detached them from the membrane surface [135].

Membrane chemical cleaning mechanisms can be divided into six steps as following [137,148]:

1. Reactions (hydrolysis and other) of cleaning reagents occur

2. Cleaning agent reached the membrane surface

3. Cleaning agent breaks through foulants layers to membrane surface

4. Solubilization and detachment of the foulants occurred by cleaning reactions

5. Detached foulants-cleaning agent waste complex reached the interface

6. Foulants-cleaning agent waste complex diffuse to cleaning (bulk) solution from retention side of the membrane, see the **Fig. 2.15**.

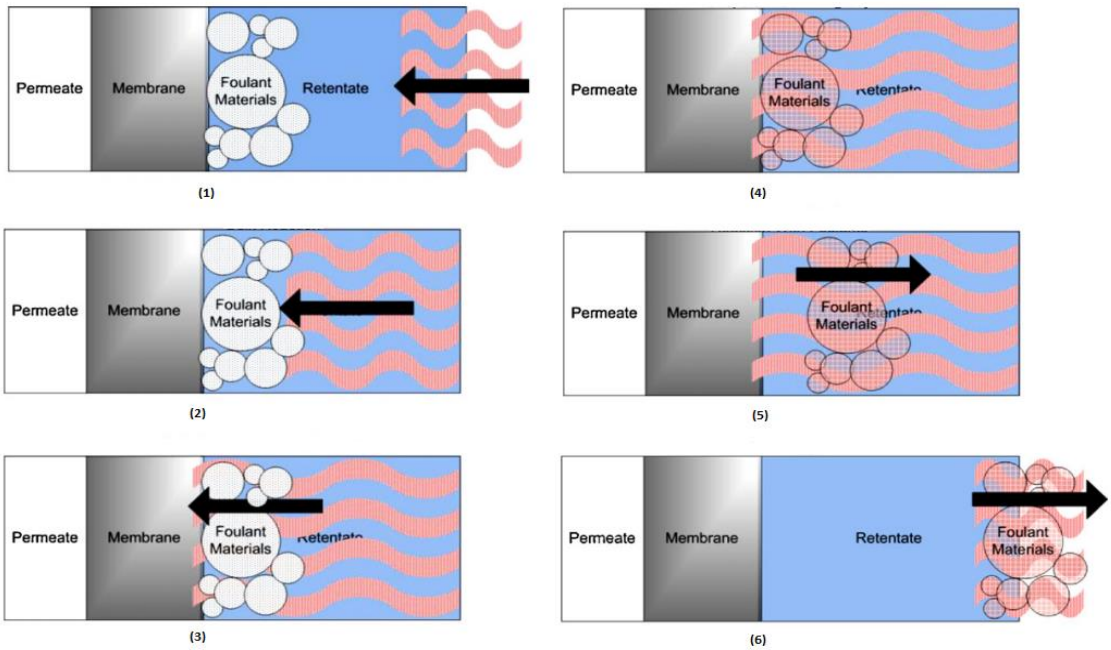

Fig. 2.15. Equilibrium model for membrane cleaning [137]**.**

2.12. Summary

In this review, a general overview of membranes types, material, and production methods were firstly considered. Then the properties of base polymer (PVDF) were discussed, as it is considered to be one of the most promising UF membrane materials for industrial applications regarding its outstanding properties such as high mechanical strength, excellent thermal stability, and chemical resistance to radiation.

The fabrication process of PVDF by phase inversion technique which is one of the most versatile, economical and flexible membrane fabrication processes used to develop porous membranes was reviewed and the several factors affecting the fabrication process including the solvent type, PVDF concentration, coagulation bath medium and temperature and non-solvent additives. The addition of non-solvent in the membrane casting solution is one of the methods to improve membrane morphology, increase the hydrophilicity, porosity and enhance the membrane performance such as water flux and rejection. Several additives were reviewed including inorganic slats and polymeric additives of which dopamine which was recently discovered and proved to be a promising novel bio-inspired polymer used for membrane modifications due to its amazing capability of adhesion to almost any surface. The use of dopamine as a membrane modifier was fully reviewed.

Other interesting additives used recently to membrane modification is nanoparticles of which carbon nanotubes (CNTs) have been paid more attention due to outstanding properties with large surface area, unique mechanical properties (stiffness and flexibility), high electrical and thermal conductivities as well as exceptional water treatment capabilities which were proven to work effectively against both chemical and biological contaminants, we reviewed the use of CNT as a membrane modified and specifically for PVDF-UF membranes, however few researchers studied the effects of carbon nanotubes (CNTs) addition to PVDF-based ultrafiltration membranes to improve hydrophilicity and anti-fouling properties, these studies were reviewed in this paper.

Membrane fouling is considered as the main determinant of the filtration systems nowadays. T An extensive research studied the fouling; we reviewed the types of membrane fouling and make a special concentration on the organic foulants of which NOM represents the main fraction found in aquatic, the mechanisms of fouling were reviewed and the physical, as well as chemical methods of membrane cleaning, were investigated.

References

[1] Lawrence K. et al., (2011). Membrane and Desalination Technologies, volume 10, Springer Science, Business Media, London. ISBN: 978-1-58829-940-6.

[2] Tarleton S., Wakeman R., (2011). Solid/Liquid Separation: Scale-up of Industrial Equipment, Elsevier, Technology & Engineering, ISBN-10 1856174204.

[3] Pinnau I., Freeman B.D., (2000). Formation and Modification of Polymeric Membranes : Overview. Academic press.

[4] Lalia B.S. et al., (2013). A review on membrane fabrication: Structure, properties and performance relationship. Desalination, 326, pp.77–95.

[5] Fan Z. et al., (2008). Preparation and characterization of poly (aniline)/poly (sulfone) nanocomposite ultrafiltration membrane. Journal of Membrane Science, 310(1-2), pp. 402–408.

[6] Crozes G., White P., Marshall M., (1995). Enhanced coagulation: its effect on NOM removal and chemical cost. Journal AWWA, 87, pp. 78-89.

[7] Mallevialle J., Anselme C., Marsigny O., (1989). Effects of humic substances on membrane processes, in: I.H. Suffet, P. MacCarthy (Ed.), Aquatic Humic Substances: Influence on Fate and Treatment of Pollutants, ACS, Washington, pp. 749-767.

[8] Zularisam A.W. et al., (2011). Role of natural organic matter (NOM), colloidal particles, and solution chemistry on ultrafiltration performance. Separation and purification Technology, 78(2), pp.189-200.

[9] Kabsch-Korbutowicz M., (2005). Application of ultrafiltration integrated with coagulation for improved NOM removal. Desalination.174 (1), pp. 13-22.

[10] Mao R.R., et al., (2013). Impact of various coagulation technologies on membrane fouling in coagulation/ultrafiltration process. Chemical Engineering Journal, 225, 387-393.

[11] Aoustin E., (2001). Ultrafiltration of natural organic matter. Separation and Purification Technology, 22-23(1-2), pp. 63–78.

[12] Elimelech M. and Phillip W.A., (2011). The future of sea water desalination: Energy, Technology, and the Environment Science, 333(6043), pp.712-717.

[13] Baker R.W., (2012). Membrane Technology and Applications, 3rd Edition. Chi Chester.

[14] Mulder M, (1996). Basic Principles of Membrane Technology. Dordrecht, the Netherlands: Kluwer.

[15] Harris J.F. Peter, (2009). Carbon Nanotube Science. United Kingdom, the University press, Cambridge. ISBN 978-0-521-82895-6.

[16] Pinnau I., Freeman B. D., (2000). Membrane Formation and Modification, ACS, Washington DC, USA.

[17] Cheryan M., (1986). Ultrafiltration Handbook; Technomic Publishing: Lancaster, PA.

[18] Singh R., (2015). Membrane Technology and Engineering for Water Purification, Application, Systems Design and Operation. Elsevier Ltd publication. ISBN: 978-0-444-63362-0

[19] Lalia B.S. et al., (2013). A review on membrane fabrication: Structure, properties and performance relationship. Desalination, 326, pp.77–95.

[20] Hilal N., Ismail F.A., Wright C., (2015). Membrane Fabrication. First edition, CRC Press, ISBN 1482210460.

[21] Boussu K., Bruggen Van der B., Vandecasteele C., (2006). Evaluation of self-made nano-porous poly (ether sulfone) membranes, relative to commercial nanofiltration membranes, Desalination 200, pp. 416–418.

[22] Zhang P.Y. et al., (2013). Preparation and characterization of PVDF-P (PEGMA-r-MMA) ultrafiltration blend membranes via simplified blend method. Desalination, 319, pp.47–59.

[23] Liu F. et al., (2011). Progress in the production and modification of PVDF membranes. Journal of Membrane Science, 375(1-2), pp.1–27.

[24] Uragami T., Naito Y., Sugihara M., (1981). Studies on synthesis and permeability of special polymer membranes, Polymer Bulletin 4 (10), pp. 617–622.

[25] Munari S., Bottino A., Capannelli G., (1983). Casting and performance of poly (vinylidene fluoride) based membranes, Journal of Membrane Science 16, pp. 181–193.

[26] Wu L., Sun J., Wang Q., (2006). Poly (vinylidene fluoride)/poly(ether sulfone) blend membranes: effects of the solvent sort, poly(ether sulfone) and poly(vinyl pyrrolidone) concentration on their properties and morphology, J. Membrane. Sci. 285, pp. 290–298.

[27] Khayet M, Chowdhury G, Matsuura T., (2002). Surface modification of poly (vinylidene fluoride_ pervaporation membranes. AIChE J; 48: pp.2833–43.

[28] Oh S.J., Kim N., Lee Y.T., (2009). Preparation and characterization of PVDF/TiO2 organic–inorganic composite membranes for fouling resistance improvement, J. Membrane. Sci. 345, pp. 13–20.

[29] Cao X. et al., (2006). Effect of TiO2 nanoparticle size on the performance of PVDF membrane, Appl. Surf. Sci. 253, pp. 2003–2010.

[30] Wei Y. et al., (2011). Effect of TiO2 nanowire addition on PVDF ultrafiltration membrane performance, Desalination 272, pp. 90–97.

[31] Wang Z. et al., (2012). Novel GO-blended PVDF ultrafiltration membranes, Desalination 299, pp. 50–54.

[32] Zhang J. et al., (2013). Improved hydrophilicity, permeability, antifouling and mechanical performance of PVDF composite ultrafiltration membranes tailored by oxidized low- dimensional carbon nanomaterials, J. Mater. Chem. A 1 3101.

[33] Shao L. et al., (2014). Tuning the performance of poly (pyrrole)-based solvent-resistant composite nanofiltration membranes by optimizing polymerization conditions and incorporating graphene oxide, J. Membr. Sci. 452, pp. 82–89.

[34] Liu F., Zhu B.K., Xu Y.Y., (2006). Improving the hydrophilicity of poly (vinylidene fluoride) porous membranes by electron beam initiated surface grafting of AA/SSS binary monomers, Appl. Surf. Sci. 253, pp. 2096–2101.

[35] Rahimpour A. et al., (2009). Preparation and characterization of modified nano-porous PVDF membrane with high anti- fouling property using UV photo-grafting, Appl. Surf. Sci. 255, pp. 7455–7461.

[36] Kaur S. et al., (2007). Plasma-induced graft copolymerization of poly (methacrylic acid) on electro spun poly (vinylidene fluoride) nanofiber membrane, Langmuir 23, pp. 13085–13092.

[37] Liu F. et al., (2007). Surface immobilization of polymer brushes onto porous poly (vinylidene fluoride) membrane by electron beam to improve the hydrophilicity and fouling resistance, Polymer 48, pp. 2910–2918.

[38] Chiang Y.C. et al., (2009). Sulfobetaine-grafted poly (vinylidene fluoride) ultrafiltration membranes exhibit excellent antifouling property, J. Membr. Sci. 339, pp. 151–159.

[39] A Q.F. et al., (2011). Multilayered poly (vinylidene fluoride) composite membranes with improved interfacial compatibility: correlating pervaporation performance with free volume proper- ties, Langmuir 27, pp.11062–11070

[40] Chuanqi Z. et al., (2013). Effect of graphene oxide concentration on the morphologies and antifouling properties of PVDF ultrafiltration membranes. Journal of Environmental Chemical Engineering, 1(3), pp.349–354.

[41] Ameduri B., (2009). From vinylidene fluoride (VDF) to the applications of VDF-containing polymers and copolymers: recent developments and future trends. Chem. Rev.109, pp.6632–6686.

[42] Cui Z., Drioli E., Lee Y.M., (2014). Recent progress in fluoropolymers for membranes. Progress in Polymer Science, 39(1), pp.164–198.

[43] Shirkova V.V., Tretyakova S.P., (1997). Physical and chemical basis for the manufacturing of fluoropolymer track membranes, Radiation Measurements 28 (1–6), pp. 791–798.

[44] Grasselli M., Betz N., (2005). Making porous membranes by chemical etching of heavy-ion tracks in [beta]-PVDF films, Nuclear Instruments and Methods in Physics Research Section B: Beam Interactions with Materials and Atoms 236 (1–4), pp. 501–507.

[45] Bottino A. et al., (1991). The formation of micro- porous poly (vinylidene difluoride) membranes by phase separation, Journal of Membrane Science 57 (1), pp. 1–20.

[46] Shih H.C., Yeh Y.S., Yasuda H., (1990). Morphology of microporous poly(vinylidene fluoride) membranes studied by gas permeation and scanning electron microscopy, Journal of Membrane Science 50 (3), pp. 299–317.

[47] Ahmad A.L., Ramli W.K.W., (2013). Hydrophobic PVDF Membrane via Two-stage Soft Coagulation Bath System for Membrane Gas Absorption of CO2. Separation and Purification Technology 103: 230–240. doi:10.1016/j.seppur.2012.10.032

[48] Tomaszewska M., (1996). Preparation and Properties of Flat-Sheet Membranes from Poly (Vinylidene Fluoride) for Membrane Distillation. Desalination 104(1–2), pp. 1–11. Doi: 10.1016/0011-9164(96)00020-3.

[49] Buonomenna MG. et al., (2007). Poly (vinylidene fluoride) membranes by phase inversion: the role the casting and coagulation conditions play in their morphology, crystalline structure, and properties. European Polymer Journal, 43(4), pp.1557–1572.

[50] Hongchen S. et al., (2012). Natural organic matter removal and flux decline with PEG-TiO2-doped PVDF membranes by integration of ultrafiltration with photocatalysis. Journal of Membrane Science, 405-406, pp.48–56. Available at: http://dx.doi.org/10.1016/j.memsci.2012.02.063.

[51] Albrecht W. et al., (2001). Formation of hollow fiber membranes from poly (ether imide) at wet phase inversion using binary mixtures of solvents for the preparation of the dope, J. Membr. Sci. 192, pp. 217–230.

[52] Kimmerle K., Strathmann H., (1990). Analysis of the Structure- Determining Process of Phase Inversion Membranes, Desalination, 79, pp. 283-302

[53] Young T.-H., Chen L.-W., (1995). Pore Formation Mechanism of Membranes from Phase Inversion Process. Desalination 103(3), pp. 233–247.

[54] Sukitpaneenit P., Chung T.S., (2009). Molecular elucidation of morphology and mechanical properties of PVDF hollow fiber membranes from aspects of phase inversion, crystallization and rheology, J. Membr. Sci 340 (1–2), pp. 192–205.

[55] Lin D.-J. et al., (2006). Preparation and Characterization of Microporous PVDF/PMMA Composite Membranes by Phase Inversion in Water/DMSO Solutions. European Polymer Journal 42(10), pp. 2407–2418. doi:10.1016/j.eurpolymj.2006.05.008.

[56] Wu T. et al., (2014). Facile and low-cost approach towards a PVDF ultrafiltration membrane with enhanced hydrophilicity and antifouling performance via graphene oxide/water-bath coagulation. RSC Adv., 5(11), pp.7880–7889.

[57] Cheng L.P., (1999). Effect of temperature on the formation of microporous PVDF membranes by precipitation from 1-octanol/DMF/PVDF and water/DMF/PVDF systems, Macromolecules 32 (20), pp. 6668–6674.

[58] Fontananova E. et al., (2006). Effect of Additives in the Casting Solution on the Formation of PVDF Membranes. Desalination 192(1–3), pp. 190–197. doi:10.1016/j.desal.2005.09.021.

[59] Uragami T., Naito Y., Sugihara M., (1981). Studies on synthesis and permeability of special polymer membranes, Polymer Bulletin 4 (10), pp. 617–622

[60] Lee H., Rho J., Messersmith P.B., (2009). Facile conjugation of biomolecules onto surfaces via mussel adhesive protein inspired coatings, Advanced Materials 21 (4), pp. 431–434.

[61] Arena J.T. et al., (2011). Surface modification of thin film composite membrane support layers with polydopamine: Enabling use of reverse osmosis membranes in pressure retarded osmosis. Journal of Membrane Science, 375(1-2), pp.55–62.

[62] Shao L. et al., (2014). A facile strategy to enhance PVDF ultrafiltration membrane performance via self-polymerized polydopamine followed by hydrolysis of ammonium fluotitanate. Journal of Membrane Science, 461, pp.10–21.

[63] Shi C. et al., (2013). Synthesis of Highly Water-Dispersible Poly (dopamine)-Modified Multi-walled Carbon Nanotubes for Matrix-Assisted Laser Desorption/ Ionization Mass Spectrometry Analysis.

[64] Postma A. et al., (2009). Self-polymerization of dopamine as a versatile and robust technique to prepare polymer capsules, Chemistry of Materials 21 (14), pp. 3042–3044.

[65] Fei B. et al., (2008). Coating carbon nanotubes by spontaneous oxidative polymerization of dopamine, Carbon 46 (13), pp. 1795–1797.

[66] Yang L. et al., (2011). Biomimetic, Approach to enhancing interfacial interactions: polydopamine-coated clay as reinforcement for epoxy resin, ACS Appl. Mater. Interfaces 3, pp. 3026–3032.

[67] Jiang J.-H. et al., (2014). Improved hydrodynamic permeability and antifouling properties of poly (vinylidene fluoride) membranes using polydopamine nanoparticles as additives. Journal of Membrane Science, 457, pp. 73–81. doi:10.1016/j.memsci.2014.01.043

[68] Zhao, S. et al., (2011). PSf/PANI nanocomposite membrane prepared by in situ blending of PSf and PANI/NMP. Journal of Membrane Science, 376(1-2), pp.83–95.

[69] Guillen G.R. et al. (2010). Pore-structure, hydrophilicity, and particle filtration characteristics of polyaniline–polysulfone ultrafiltration membranes, J. Mater. Chem. 20, pp.4621–4628.

[70] Fan Z.F., (2008). Performance improvement of polysulfone ultrafiltration membrane by blending with polyaniline nanofibers, J. Membr. Sci. 320 (2008) 363–371.

[71] Gupta Y., Hellgardt K., Wakeman R.J., (2006) Enhanced permeability of polyaniline-based nano-membranes for gas separation, J. Membr. Sci. 282, pp. 60–70.

[72] Lee Y.M., Nam S.Y., Ha S.Y., (1999). Pervaporation of water/isopropanol mixtures through polyaniline membranes doped with poly (acrylic acid), J. Membr. Sci. 159, pp. 41–46.

[73] Wang P. et al., (2002). Preparation and characterization of semi-conductive poly (vinylidene fluoride)/polyaniline blends and membranes, Appl. Surf. Sci. 193 (2002) 36–45.

[74] Fan, Z. et al., (2008). Preparation and characterization of polyaniline/polysulfone nanocomposite ultrafiltration membrane. Journal of Membrane Science, 310(1-2), pp.402–408.

[75] Kaner R.B., (2002). Gas, liquid and enantiomeric separations using polyaniline, Synth. Met. 125, pp.65–71.

[76] Gospodinova, N. & Terlemezyan, L., (1998). Conducting polymers prepared by oxidative polymerization: polyaniline. Progress in Polymer Science, 23(8), pp.1443–1484.

[77] Zhao, S. et al., (2011). Comparison study of the effect of PVP and PANI nanofibers additives on membrane formation mechanism, structure and performance. Journal of Membrane Science, 385-386, pp.110–122.

[78] Ma J. et al., (2013). Role of oxygen-containing groups on MWCNTs in enhanced separation and permeability performance for PVDF hybrid ultrafiltration membranes. Desalination, 320, pp. 1–9.

[79] Liang S. et al., (2012). A novel ZnO nanoparticle blended poly (vinylidene fluoride) membrane for anti-irreversible fouling, J. Membr. Sci. 394, pp. 184–192.

[80] Cui A.H. et al., (2010). Effect of micro-sized SiO_2-particle on the performance of PVDF blend membranes via TIPS, J. Membr. Sci. 360, pp. 259–264.

[81] Yu S.L. et al., (2009). Effect of SiO_2 nanoparticle addition on the characteristics of a new organic–inorganic hybrid membrane, Polymer 50 (2009) 553–559.

[82] Yan L. et al., (2006). Effect of nano-sized Al_2O_3-particle addition on PVDF ultrafiltration membrane performance, J. Membr. Sci. 276, pp. 162–167.

[83] Bottino A., Capannelli G., Comite A., (2002). Preparation and characterization of novel porous PVDF–ZrO_2 composite membranes, Desalination 146, pp. 35–40.

[84] Huang Zheng-Qing et al., (2012). The performance of the PVDF-Fe_3O_4 ultrafiltration membrane and the effect of a parallel magnetic field used during the membrane formation. Desalination Volume 292, pp. 64–72.

[85] Lin D.J. et al., (2003). Effect of salt additive on the formation of microporous poly (vinylidene fluoride) membranes by phase inversion from $LiClO_4$/water/DMF/PVDF system, Polymer 44, pp. 413–422.

[86] Botes M., Cloete T.E., (2010). The potential of nanofibers and nanobiocides in water puri- fication, Crit. Rev. Microbiol. 36, pp. 68–81.

[87] Iijima S., (1991). Helical microtubules of graphitic carbon. Nature, 354, pp. 56–58.

[88] Celik E., Liu L., Choi H., (2011). Protein fouling behavior of carbon nanotube/poly (ether sulfone) composite membranes during water filtration. Water Research, 45(16), pp. 5287–5294

[89] Lu L.Y. et al., (2006). Novel graphite-filled PVA/CS hybrid membrane for pervaporation of benzene/cyclohexane mixtures, J. Membr. Sci., pp. 281 245.

[90] Upadhyayula V. K. K. et al., (2009). Application of carbon nanotube technology for removal of contaminants in drinking water: A review. Science of the Total Environment, 408(1), pp. 1–13.

[91] Baj-rossi, C., Micheli, G. De, Carrara, S., (2005). for Personalized Medicine.

[92] Peng X. et al., (2005). Nanoparticles supported nanotubes for removal of arsenate in water. Mater Lett 59, pp. 399-403.

[93] Yang K., Zhu L., Xing B., (2006). Adsorption of polycyclic aromatic hydrocarbons by carbon nanomaterials. Environ Sci Technol; 40, pp.1855–61.

[94] Hyung H., Kim JH., (2008). Natural organic matter (NOM) adsorption to multi walled carbon nanotubes: effect on NOM characteristics and water quality parameters. Environ Sci Technol; 42:44, pp.16–21.

[95] Sears K. et al., (2010). Recent Developments in Carbon Nanotube Membranes for Water Purification and Gas Separation. Materials, 3(1), pp. 127–149.

[96] Saleh N.B., L.D. Pfefferle, M. Elimelech., (2008). Aggregation Kinetics of Multi-Walled Carbon Nanotubes in Aquatic systems: Measurements and Environmental Implications. Environmental Science& Technology, 42(21), pp. 7963-7969.

[97] Zhao J. et al., (2003). Noncovalent functionalization of carbon nanotubes by organic molecules, Appl. Phys. Lett. 82 3746.

[98] Rastogi R. et al., (2008). Comparative study of carbon nanotube dispersion using surfactants. Journal of Colloid and Interface Science, 328(2), pp. 421–8.

[99] Yin J., and Deng B., (2015). Polymer-matrix nanocomposite membranes for water treatment. Journal of Membrane Science, 2015. 479(0), pp. 256-275.

[100] Li W. et al., (2008). Preparation and shear properties of carbon nanotubes/poly (butyl methacrylate) hybrid material, Polym. Compos. 29 (9), pp. 972–977.

[101] Vaisman L., Wagner, H. D., & Marom, G. (2006). The role of surfactants in dispersion of carbon nanotubes. Advances in Colloid and Interface Science, 128-130, pp. 37–46.

[102] Lu K.L. et al., (1996). Mechanical damage of carbon nanotubes by ultrasound. Carbon, 34, pp. 814–816.

[103] Hilding J. et al., (2003). Dispersion of carbon nanotubes in liquids. J Dispers Sci Technol, pp. 24:1-41.

[104] Kim S. W. et al., (2012). Surface modifications for the effective dispersion of carbon nanotubes in solvents and polymers. Carbon, 50(1), pp. 3–33.

[105] Vatanpour V. et al., (2011). Fabrication and characterization of novel antifouling nanofiltration membrane prepared from oxidized multi-walled carbon nanotube/poly

(ether sulfone) nanocomposite. Journal of Membrane Science, 375(1-2), pp. 284–294.

[106] Yin J., Zhu G., Deng B., (2013). Multi-walled carbon nanotubes (MWNTs)/poly (sulfone) (PSU) mixed matrix hollow fiber membranes for enhanced water treatment. Journal of Membrane Science, 437, pp. 237–248.

[107] Majeed S. et al., (2012). Multi-walled carbon nanotubes (MWCNTs) mixed poly (acrylonitrile) (PAN) ultrafiltration membranes. Journal of Membrane Science, 403-404, pp. 101–109.

[108] Celik E. et al., (2011). Carbon nanotube blended poly (ether sulfone) membranes for fouling control in water treatment. Water Research, 45(1), pp. 274–282.

[109] Wang M. et al., (2006). The preparation and characterization of novel charged poly (acrylonitrile)/PES-C blend membranes used for ultrafiltration. Journal of Membrane Science, 274(1-2), pp. 200–208.

[110] Qiu S. et al., (2009). Preparation and properties of functionalized carbon nanotube/PSF blend ultrafiltration membranes. Journal of Membrane Science, 342(1-2), pp. 165–172.

[111] Daraei P. et al., (2013). Fabrication of PES nanofiltration membrane by simultaneous use of multi-walled carbon nanotube and surface graft polymerization method: Comparison of MWCNT and PAA modified MWCNT. Separation and Purification Technology, 104, pp. 32–44.

[112] Kim E.S. et al., (2012). Development of nanosilver and multi-walled carbon nanotubes thin-film nanocomposite membrane for enhanced water treatment. Journal of Membrane Science, 394-395, pp.37–48.

[113] Zhang J.X. et al., (2009). The synthesis of functionalized carbon nanotubes by hyperbranched poly (amine-ester) with liquid-like behavior at room temperature, Polymer 50, pp. 2953–2957.

[114] Zhao X. et al., (2012). Hyperbranched-polymer functionalized multi-walled carbon nanotubes for poly (vinylidene fluoride) membranes: From dispersion to blended fouling-control membrane. Desalination, 303, pp. 29–38.

[115] Sianipar, M. et al., (2016). Potential and performance of a polydopamine-coated multiwalled carbon nanotube/polysulfone nanocomposite membrane for ultrafiltration application. Journal of Industrial and Engineering Chemistry, 34(2016), pp.364–373.

[116] Kim, K.J. et al., (1992). Fouling mechanisms ultrafiltration of membranes during protein. , 68, pp.79–91.

[117] Anselme C. and Jacobs E. P., (1996). Ultrafiltration", chapter 10 in Water treatment membrane processes, J. Mallevialle, P. E. Odendaal and M. R. Wiesner, Eds., McGraw Hill; New York, NY,

[118] Hermia J., (1982). Constant pressure blocking filtration laws: Applications to Power-law non-Newtonian fluids, J. Trans. Inst. Chem. Eng., 60, pp. 183-187.

[119] Bowen W. R., Calvo J. I, Hernandez A., (1995). Steps of membrane blocking in flux decline during protein microfiltration. J. Membr. Sci., 101, pp. 153-165.

[120] Aoustin, E., (2001). Ultrafiltration of natural organic matter. Separation and Purification Technology, 22-23(1-2), pp.63–78.

[121] Hyeok Choi et al., (2005). Effect of permeate flux and tangential flow on membrane fouling for wastewater treatment, Separation and Purification Technology 45, pp. 68–78

[122] Baker R.W, (2004). Membrane Technology and Applications, John Wiley Son, Ltd, England.

[123] Guo, W., Ngo, H.H., Li, J., (2012). A mini-review on membrane fouling. Bioresource Technology, 122(2012), pp.27–34.

[124] Peña-méndez, M.E., Havel, J. & Patočka, J., (2005). Humic substances – compounds of still unknown structure: applications in agriculture, industry, environment, and biomedicine. J. Appl. Biomed., 3, pp.13–24.

[125] Matilainen A. et al., (2011). An overview of the methods used in the characterisation of natural organic matter (NOM) in relation to drinking water treatment. Chemosphere 83 (11), pp.1431-1442.

[126] Wiesner M.R. and Aptel P., (1996). Mass transport and permeate flux and fouling in pressuredriven processes, Chapter 4 in Water treatment: Membrane processes, McGraw Hill, New York, NY

[127] Schnitzer M. and Khan A.U., (1972) "Humic substances in the environment", Marcel Dekkerjnc, New York, NY,

[128] Martin-Mousset B. et al., (1997). Distribution and characterization of dissolved organic matter of surface waters. Water Res. 31, pp.541-553.

[129] Huber S.A, F.H. Frimmel, (1994). Direct gel chromatographic characterization and quantification of marine dissolved organic carbon using high-sensitivity DOC detection. Environ. Sci. Technol. 28, pp.1194-1197.

[130] Mallevialle J., Anselme C., and Marsigny O., (1989). Effects of humic substances on membrane processes, Advances in Chemistry, 219, pp. 749-767.

[131] Kennedy M.D. et al., (2005). Natural organic matter (NOM) fouling of ultrafiltration membranes: fractionation of NOM in surface water and characterization by LC-OCD, Desalination, 178 (1- 3), pp. 73-83.

[132] Cho J.et al., (1999). Characterization of clean and natural organic matter (NOM) fouled NF and UF membranes and foulants characterization, Water Supply, 17 (1), pp.183-190.

[133] Stevenson F.J., (1982). Humus chemistry genesis, composition, reactions. Willey-Interscience, New York.

[134] M. Cheryan, (2000). Ultrafiltration and Microfiltration Handbook, 2nd ed., CRC, Florida, USA.

[135] Liu, C. et al., (2001). Membrane Chemical Cleaning: From Art to Science. American Water Works Association, pp.1- 25.

[136] Hilal, N. et al., (2005). Methods employed for control of fouling in MF and UF membranes: a comprehensive review. Sep. Sci. Technol. 40, pp. 1957–2005.

[137] Porcelli, N., Judd, S., (2010). Chemical cleaning of potable water membranes: A review. Separation and Purification Technology, 71(2), pp.137–143.

[138] Deqian R., (1987). Cleaning and regeneration of membranes, Desalination, 62, pp. 363-371.

[139] Rabuni, M.F. et al., (2015). Impact of in situ physical and chemical cleaning on PVDF membrane properties and performances. Chemical Engineering Science, 122, pp.426–435.

[140] Lin, J.C.-T., Lee, D.-J. & Huang, C., 2010. Membrane Fouling Mitigation: Membrane Cleaning. Separation Science and Technology, 45(7), pp.858–872.

[141] Tragardh. G, (1989). Membrane cleaning, Desalination, 71 (3), pp. 325-335,

[142] Srisurichan, R. Jiraratananon, A.G. Fane, (2005). Humic acid fouling in the membrane distillation process, Desalination, 174, pp. 63–72.

[143] Zuo D.-Y. et al., (2010). A study on submerged rotating MBR for wastewater treatment and membrane cleaning, Korean J. Chem. Eng., 27, pp. 881–885.

[144] Levitsky, A. et al., (2011). Understanding the oxidative cleaning of UF membranes J. Membr. Sci., 377, pp. 206–213.

[145] Wang, Z. et al., (2010). Effect of hypochlorite cleaning on the physiochemical characteristics of polyvinylidene fluoride membranes. Chem. Eng. J., 162, pp. 1050–1056.

[146] Kimura K.et al., (2004). Irreversible membrane fouling during ultrafiltration of surface water, Water Res., 38 (14-15), pp. 3431-3441.

[147] Lee, J. et al., (2016). High flux and high selectivity carbon nanotube composite membranes for natural organic matter removal. Separation and Purification Technology, 163, pp.109–119.

[148] Shorrock C.J., Bird M.R., (1998). Membrane cleaning: chemically enhanced removal of deposits formed during yeast cell harvesting, Food Bioprod. Process. 76, pp. 30–38.

Chapter 3. Materials, Methods and characterization

3.1 Poly (vinylidene fluoride) / Polydopamine/ MWCNT nanocomposite ultrafiltration membrane for natural organic matter removal

3.1.1 Materials: All chemicals used as received without any treatment.

Poly (vinylidene fluoride) (PVDF) Solef 6010 was purchased from Solvay Company. Ammonium peroxidisulfate (APS) and dopamine from Aldrich Company. N, N-Dimethylformamide (DMF) from Merck. Suwannee River humic acid (HA), standard II from (International Humic Substances Society), was used as a model of NOM compound. Hydroxylated-MWCNT was supplied from Bucky USA with the following characteristics: purity of 98 wt. %, diameters of 5-15 nm and lengths from 1-5μm.

3.1.2 Membrane preparation

3.1.2.1 Synthesis of MWCNT/PDA

Fig 3.1 shows the first step in membrane preparation which is the synthesis of MWCNT/PDA by in-situ polymerization of dopamine on MWCNT. MWCNT was dispersed in DMF solvent/pure water by probe ultrasonication (500 W) for 30 min, then dopamine and APS (0.8 wt. %) were added to the solution mixture which was stirred by a magnetic stirrer for 72 hr at room temperature.

3.1.2.2 Preparation of MWCNT/PDA/PVDF

In the final step of membrane preparation; 12 wt. % PVDF was added to MWCNT/PDA composite and stirred at 70 ^{0}C for 24 hrs. The resultant casting solution was degassed by ultrasonication for 30 min and after cooling to room temperature, it was cast on a glass plate using applicator with 300 µm thickness. The cast film was then immediately immersed in pure water coagulation bath to form a porous membrane at room temperature. **Table 3.1** shows the composition of different membrane casting solutions.

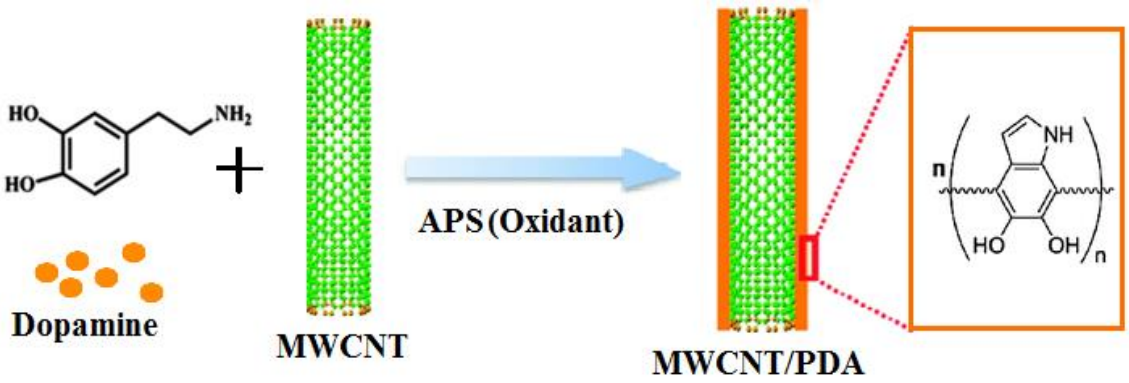

Fig 3.1 Synthesis of MWCNT/PDA

Table 3.1 Composition of membrane casting solutions

	PVDF (Wt. %)	**MWCNT (Wt. %)**	**Dopamine (Wt. %)**	**APS (Wt. %)**	**Water (Wt. %)**	**DMF (Wt. %)**
Pristine	12.5	0	0	0	0	87.5
P-PDA	12.5	0	2	1	3.0	81.5
PC-1	12.5	0.25	2	1	3.0	81.25
PC-2	12.5	0.5	2	1	3.0	81
PC-3	12.5	1.0	2	1	3.0	80.5
PC-4	12.5	1.5	2	1	3.0	80

3.2 Enhanced permeability and antifouling properties of Poly (vinylidene fluoride) ultrafiltration membranes using polyaniline as additives

3.2.1 Materials: All chemicals used as received without any treatment.

PVDF (solef 6010) was purchased from Solvay Company. Aniline hydrochloride and Ammonium peroxydisulfate (APS) from Aldrich Company. N, N-Dimethylformamide (DMF) from Merck. Suwannee River humic acid (HA), standard II from (International Humic Substances Society), was used as a model of NOM compound.

3.2.2 Membrane preparation

3.2.2.1 Synthesis of PVDF/PANI membranes

PVDF/PANI membranes were fabricated by two different methods: regular blending method referred as PP-X and *in-situ* polymerization method referred as PI-X. APS was used as an oxidant for aniline polymerization in both methods, as shown in **Fig. 3.2**.

Simple blending method: The composition of the blended membranes produced by this method with different aniline concentrations is summarized in **Table 3.2**. Aniline and APS were dissolved in DMF solution. Thus PANI polymerized in advance, and the mixture was stirred at 25 ^{0}C for 24 hrs. Then a fixed amount of PVDF was added to the mixture, which was stirred again at 60 ^{0}C for 24 hrs.

In-situ polymerization method: The composition of the blended membranes produced by this method with different aniline concentrations is summarized in **Table 3.2**. PVDF was dissolved in (N, N-Dimethylformamide) DMF, and aniline and APS were added to the solution. The mixture was stirred at 60 ^{0}C for 48 hr., and PANI *in-situ* polymerized in the casting membrane solution.

The casting solutions for pristine PVDF and modified membranes were degassed by ultrasonication for 30 min. After cooling to room temperature, it was cast on a glass plate

using applicator with 250 µm thickness. The cast film was then immersed into pure water coagulation bath to form a porous membrane at room temperature. After phase inversion, it was transferred and stored in a new pure water bath to remove any solvent or unpolymerized PANI.

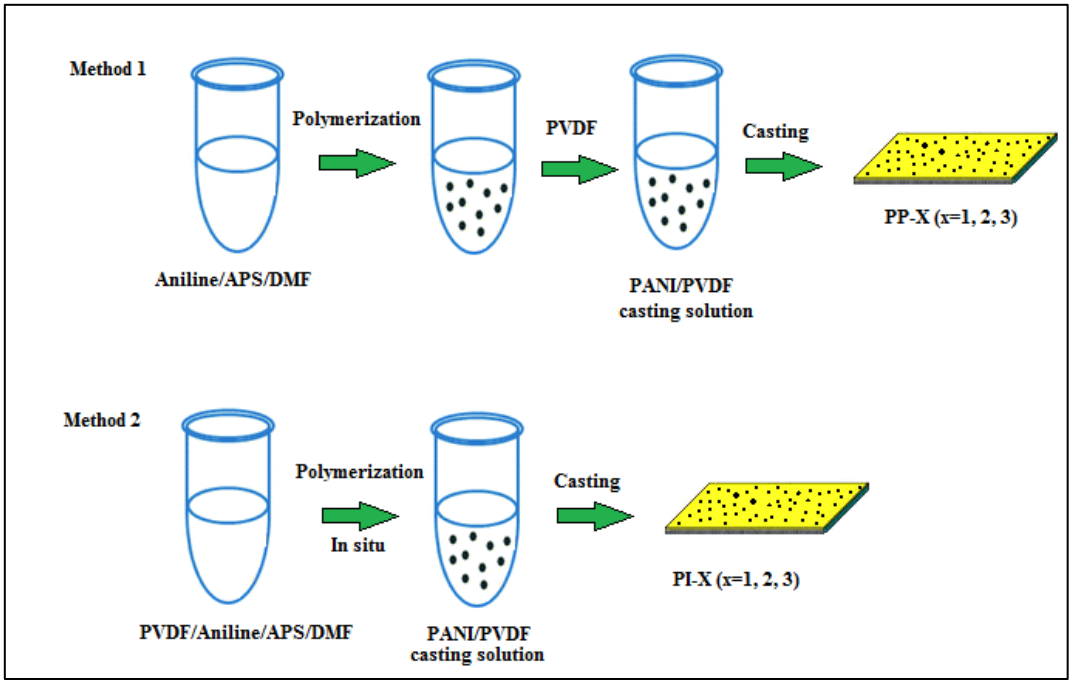

Fig 3.2. The two preparation methods used to fabricate PANI/PVDF modified membrane.

Table 3.2 Casting solution compositions for pristine, PP-X and PI-X membranes.

Membrane Type	PVDF (g)	Aniline (g)	APS (g)	DMF (g)	Total weight of casting (g)
Pristine	4.5	0	0	25.5	30
PP-1, PI-1	3.75	0.45	0.3	25.5	30
PP-2, PI-2	3.75	0.65	0.45	25.15	30
PP-3, PI-3	3.75	0.84	0.56	24.85	30

3.3 Poly (vinylidene fluoride) / Polyaniline/ MWCNT nanocomposite ultrafiltration membrane for natural organic matter removal

3.3.1 Materials

PVDF (solef 6010) was purchased from Solvay Company. Aniline hydrochloride and Ammonium peroxydisulfate (APS) from Aldrich Company. N, N-Dimethylformamide (DMF) from Merck. Suwannee River humic acid (HA) standard II from (International Humic Substances Society) was used as a model of NOM compound. Hydroxylated-MWCNT was supplied from Bucky USA with the following characteristics: purity of 98 wt. %, diameters of 5-15 nm and lengths from 1-5μm.

3.3.2 Membrane preparation

3.3.2.1 Synthesis of MWCNT/PANI

The first step of MWCNT/PANI *in-situ* polymerization synthesis is shown in **Fig. 3.3**. First MWCNT was dispersed in DMF solvent by probe ultrasonication (500 W) for 30 min. Then 1.3 g of aniline hydrochloride and APS (0.9 g); Ammonium peroxidisulfate used as radical initiators; were added to the mixture which was stirred for 72 hr at room temperature.

3.3.2.2 Fabrication of MWCNT/PANI/PVDF

In the final step of membrane preparation; 12.5 wt % of PVDF was added to MWCNT/PANI composite and stirred at 60 ^{0}C for 24 hrs. The resultant casting solution was degassed by ultrasonication for 30 min., after cooling to room temperature, it was cast on a glass plate using applicator with 250 μm thickness. The cast film was then immersed into pure water coagulation bath to form a porous membrane at room temperature. **Table 3.3** shows the composition of different membrane casting solutions.

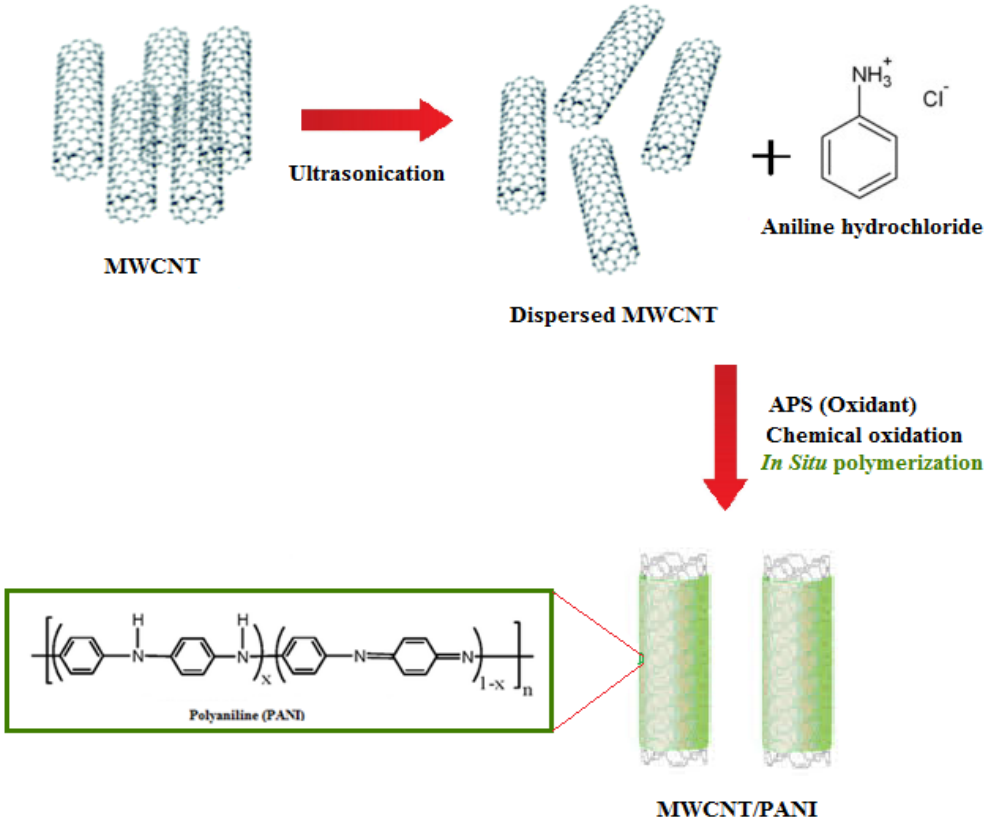

Fig. 3.3 Synthesis of MWCNT/PANI.

Table 3.3 The composition of membrane casting solutions.

	PVDF (Wt. %)	MWCNT (Wt. %)	Aniline hydrochloride (Wt. %)	APS (Wt. %)	DMF (Wt. %)
Pristine	12.5	0	0	0	87.5
PIC-0.25	12.5	0.25	2.2	1.5	83.6
PIC-0.5	12.5	0.5	2.2	1.5	83.3
PIC-1	12.5	1	2.2	1.5	82.8
PIC-1.5	12.5	1.5	2.2	1.5	82.3
PIC-2	12.5	2	2.2	1.5	81.8
P-CN	12.5	1	0	0	86.5

3.4 Membranes Characterization

3.4.1 Characterization and dispersion of the casting solution and the modified membrane sheets

Fourier-transformation infrared spectroscopy (FTIR Model Nicolet 6700) was used to characterize the modified MWCNT/PDA/PVDF membrane compared with PVDF pristine and to investigate the incorporation of PANI within PVDF modified membranes**.**

Ultraviolet Spectrophotometer (UV-2450, Shimadzu) was used to check the characterization and dispersion of MWCNT/ PDA between 250-500 nm wavelengths. Also to characterize the dispersity and interaction between PANI and MWCNT composite as PANI/MWCNT complex.

3.4.2 Membrane hydrophilicity measurement (contact angle)

Membrane hydrophilicity measurement was carried out with 1 µL sessile droplets of Milli-Q water with Krüss Easy Drop goniometer. Dry membrane was cut into 5 ×15 mm pieces and fixed on to 25× 75× 1 mm slide. The water drop volume ranged from 2.5 to 5 µL. The reported contact angles are the results of the average of five measurements at different points of a membrane sample.

3.4.3 Membrane surface (porosity and pore size)

Membrane porosity was determined by the gravimetric method. The wet membrane was cut into 5×5 cm piece and placed in a glass tray; then it was put into an oven to dry [1, 2]. The membrane samples were weighed before and after drying and then mass loss was measured (porosity ε) was calculated by the following equation (3.1):

$$\varepsilon = \frac{(W_W - W_d)/\rho_{water}}{(W_W - W_d)/\rho_{water} + W_d/\rho_p} \quad (3.1)$$

Where W_W is the weight of the wet membrane (g), W_d is the weight of the dry membrane (g), ρ_{water} is the pure water density (0.998 g·cm^{-3}) and $\rho_p$is the polymer density (as the inorganic content in the membrane matrix is small and ρ_p is approximate to ρ_{PVDF}, namely 1.765 g·cm^{-3}).

The mean pore size of the fabricated membrane was measured using two methods; the average pore size calculation method [1, 3]; this method was used in chapter 4 and 5. The N_2 adsorption/desorption isotherm (Brunauer-Emmett-Teller (BET)) method was used for Chapter 6 and partly in chapter 5 [4, 5]. BET method is considered to be more accurate method. The calculated mean pore size (r) was determined as follows:

$$r = [8\times(2.9 - 1.75\varepsilon)\cdot \eta LF/3600\varepsilon\Delta P]^{1/2} \quad (3.2)$$

Where r in (m), η was the viscosity of water ($8.9\times10^{-4} Pa\ s$), L is the membrane thickness (m), F is water flux($m^3/m^2.h$), and ΔP is the working pressure (Pa).

The top surface and cross-sectional images of the modified membranes were taken by Field Emission scanning electron microscopy (FE-SEM, Hitachi S4500), to obtain the cross-sectional images samples were fractured in liquid nitrogen to preserve the real pore structure. Samples were sputter coated with gold before the examination.

3.4.4 Zeta potential

The surface charge of membrane surface was measured by using the streaming potential technique (Anton Paar electrokinetic analyzer). Zeta potentials were calculated from streaming potentials versus pressure graphs using the Helmholtz-Smolushowski equation [6]. The experiment was run at an ionic strength of 0.001 M KCl and pH ranging from 3 to 6, at room temperature (25±0.5^{0}C).

3.4.5 Mechanical properties

The tensile strength and elongation-at-break of the membranes were determined at room temperature (25±0.5^{0}C) using Instron 5943 (Buckinghamshire, United Kingdom). Dry membrane was cut into dumbbell shapes with the length of 16 mm and thickness of 12 mm, and the tensile rate was 2 mm/min. For each specimen, three runs were performed and then averaged.

3.4.6 Membrane performance

3.4.6.1 Water permeability and rejection efficiency of membranes

The pure water flux and HA rejection were measured by high pressure stirred cell (HP 4750, Sterlitech) equipment. The rejection was carried out with an aqueous solution of HA (5 ppm at pH 5.5). All experiments were conducted at room temperature and under the feed pressure of 0.1 Mpa. The concentrations of HA in the permeation and feed solution were determined by UV- spectrophotometer (Shimadzu UV-2450, Japan) at a wavelength of 254 nm. The permeation flux and rejection were calculated using formulae (3.3) and (3.4), respectively:

$$\mathrm{F} = \frac{\mathrm{V}}{\mathrm{A}\times \Delta \mathrm{t}} \tag{3.3}$$

$$R = \left(1 - \frac{C_p}{C_F}\right) \times 100\% \tag{3.4}$$

Where F is the permeation flux of membrane for pure water (L·m^{-2}·h^{-1}), V is the volume of pure permeate water (L), A is the effective surface area of the membrane (=14.6 cm^2), and Δt is the permeation time (hr). R is the rejection of HA (%), C_P and C_F are the concentrations of HA in the permeation and feed solution (mg/L), respectively.

3.4.7 Flux recovery by chemical cleaning

HA was used as a model for natural organic matter (NOM) to evaluate the anti-fouling performance of the modified membranes. Anti-fouling properties of the modified membranes were investigated using a filtration test which was done as follow: initially permeation was done with pure water, then filtration with Humic acid (5 ppm); and then the membrane was cleaned by rinsing it with 0.1 M HCl for 1.5 hr then with 0.1 M of NaOH for another 1.5 hr, and then the permeation of pure water was done again [7]. The flux recovery (FR_w) and total fouling ratio (R_t) were calculated by the following equations:

$$FR_w(\%) = \left(\frac{F_{w2}}{F_{w1}}\right) \times 100 \tag{3.5}$$

$$R_t(\%) = \left(1 - \frac{H_p}{F_{w1}}\right) \times 100 \tag{3.6}$$

Where F_{w1}= pure water permeability, F_{w2}= pure water permeability of cleaned membrane, H_p= HA solution permeability.

3.5 Variables selection for the membrane casting procedure

The membrane casting variables such as the concentration of base polymers, the concentration of additives, the thickness of membrane films and casting techniques were determined based on measurement and literature. The selection of the component concentration depends on literature studies with a principle of 10-18 wt. % for PVDF and 0-4 wt. % additives of PDA and PANI.

Song et al. studied PVDF concentration between (10-18) wt. %, he observed that the casting solution became too viscous to produce a membrane when the PVDF content transcended 18 wt. % but when PVDF content was 12 wt. %, the membrane had a good combination of membrane flux and rejection [8]. Generally, membrane concentration should not be too low to avoid brittle membranes or too high to avoid the formation of the low porous (tight) membrane. Thus, in this research, 12.5 % of PVDF was used.

In Chapter 4 to determine the optimal PDA concentration to be used in the fabricated membranes, a comparison between 3 concentrations (1.5, 2, 2.5 wt. %) was done, as using concentration greater than 2.5 wt. % leads to the formation of extra big pores with resultant very low HA rejection and using concentration less than 1.5 wt. % leads to a very limited effect on the membrane performance. **Fig. 3.4** illustrates the effect of different dopamine concentrations on both pure water permeability and HA rejection with a constant amount of PVDF (12 wt. %). The water flux was found to increase with the increase of dopamine concentration, which might be due to large pore formation as dopamine is a pore forming agent. HA rejection appeared to decrease with the increase of dopamine concentration. As shown from the results the best combination of flux and HA rejection was observed when dopamine concentration was 2 wt. % and therefore dopamine concentration were fixed at 2 wt. % in PDA/MWCNT/PVDF fabrication experiments.

Jiang et al. studied the addition of dopamine to PVDF membrane with three different methods. He noticed that in-situ polymerization of PDA in casting solution is the most efficient method to form surface pores and inner three-dimensionally connected pores which result in a relatively high permeate flux and tensile strength in comparison to the other methods used [7].

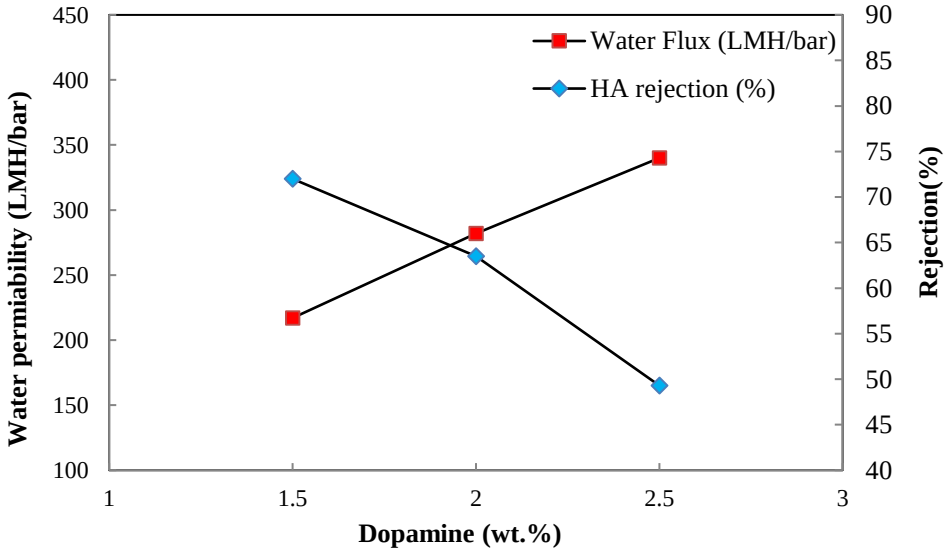

Fig. 3.4 Effect of dopamine content on membrane performance.

Two methods of blending PANI with PVDF in the fabricated membrane presented in chapter 5 with different aniline concentrations. The results indicate that *in situ* polymerization method of PANI on PVDF showed more uniform and homogeneous structure with better performance enhancement in comparison to simple blending method, and upon this results; we used *in situ* polymerization method of PANI/MWCNT in fabrication procedure in chapter 6 in order to obtain the best enhanced membrane performance results and also for overcoming MWCNT aggregation seen in simple blending method. Moreover, depending on the results of chapter 5, PI-2 showed a combination of the good permeability and HA rejection. Therefore PI-2 concentration (2.16 wt. %) was used in PANI/MWCNT/PVDF fabrication in chapter 6.

The casting was conducted at room temperature (25 ± 0.5^{0}C). The casting solution was poured over a clean, and smooth glass plate, and the membrane film was shaped by dragging gently over the solution where the membrane thickness kept in the range of 200 to 300 µm. The glass plate then immersed immediately into pure water coagulation bath at room temperature, in this step exchange between the non-solvent (pure water) and the solvent (DMF) occurred immediately, and the membrane sheet peeled off from the glass plate. The glass plate then cleaned carefully and rinsed thoroughly with tap water and ultrapure water. Each membrane was fabricated at least three times to confirm the permeability and HA rejection results.

References

[1] Ma, Jilan et al., (2013). Role of Oxygen-Containing Groups on MWCNTs in Enhanced Separation and Permeability Performance for PVDF Hybrid Ultrafiltration Membranes. Desalination 320. Elsevier B.V., pp.1–9.

[2] Li J.F., Xu Z.L., Yang H. (2008). Microporous polyethersulfone membranes prepared under the combined precipitation conditions with non-solvent additives, Polym. Adv. Technol. 19, pp. 251–257.

[3] Zhang L.P., et al., (2009) Preparation and characterization of composite membranes of poly (sulfone) and microcrystalline cellulose, Journal of Applied Polymer Science. 112, pp. 550–556.

[4] Lee S. et al., (2002). Determination of membrane pore size distribution using the fractional rejection of nonionic and charged macromolecules. Journal of Membrane Science 201(1–2), pp. 191-201.

[5] Sing, K., 2001. The use of nitrogen adsorption for the characterization of porous materials. Colloids Surf. A, 187-188, pp.3–9.

[6] Nystrom M., Lindstrom M. and Matthiasson E., (1989). Streaming potential as a tool in the characterization of ultrafiltration membranes. Colloids Surfaces, 36, pp. 297-312

[7] Jiang, J.-H. et al., (2014). Improved hydrodynamic permeability and antifouling properties of poly (vinylidene fluoride) membranes using polydopamine nanoparticles as additives. Journal of Membrane Science, 457, pp.73–81.

[8] Hongchen S. et al., (2012). Natural organic matter removal and flux decline with PEG-TiO2-doped PVDF membranes by integration of ultrafiltration with photocatalysis. Journal of Membrane Science, 405-406, pp.48–56.

CHAPTER 4. Poly(vinylidene fluoride) / MWCNT Polydopamine/ nanocomposite ultrafiltration membrane for natural organic matter removal

4.1 Results and discussion

4.1.1 Characterization of MWCNT/PDA in the polymer matrix

4.1.1.1 MWCNT/PDA dispersion (PDA coated MWCNT)

UV-vis spectroscopy of MWCNT/ PDA was performed to investigate the interaction and the dispersion of MWCNT in PDA; to check the ability of PDA to overcome MWCNT aggregation. Absorbance spectra of MWCNT/PDA and MWCNT were performed (in the range of 250-500 nm). It showed that MWCNT/PDA complex has a strong absorbance band at around 263 nm as seen in **Fig. 4.1** indicating the presence of PDA and the coating of the MWCNT surface to form separate MWCNT bundles with stable incorporation and dispersion [1-4], while no strong peak was observed in the same range when dispersing MWCNT in DMF.

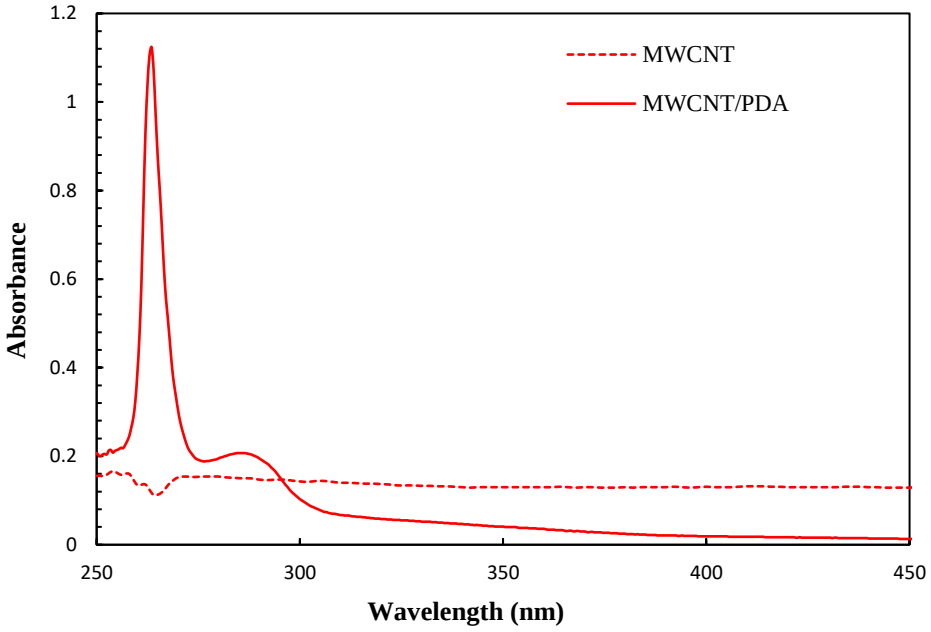

Fig.4.1. UV-vis spectra of MWCNT and MWCNT/PDA composite.

To check the dispersion status of the MWCNT; UV-vis absorbance spectra were measured at 263 nm for MWCNT/PDA and MWCNTs dissolved in DMF. The pristine MWCNTs agglomerated and precipitated immediately after ultrasonication (within 30 min) due to strong van der Waals interactions [1] and its absorbance spectrum dropped, while MWCNT/PDA formed a homogeneous solution, and the dispersion was stable for 12 hrs as shown in **Fig. 4.2**. This excellent dispersion stability of MWCNT/PDA is attributed to the strong π–π stacking interactions of dopamine with MWCNT, which improved the dispersibility of MWCNTs in the aqueous reaction solution [3]. **Fig. 4.3** shows the dispersion of MWCNT/PDA and MWCNT in DMF after 12 hr.

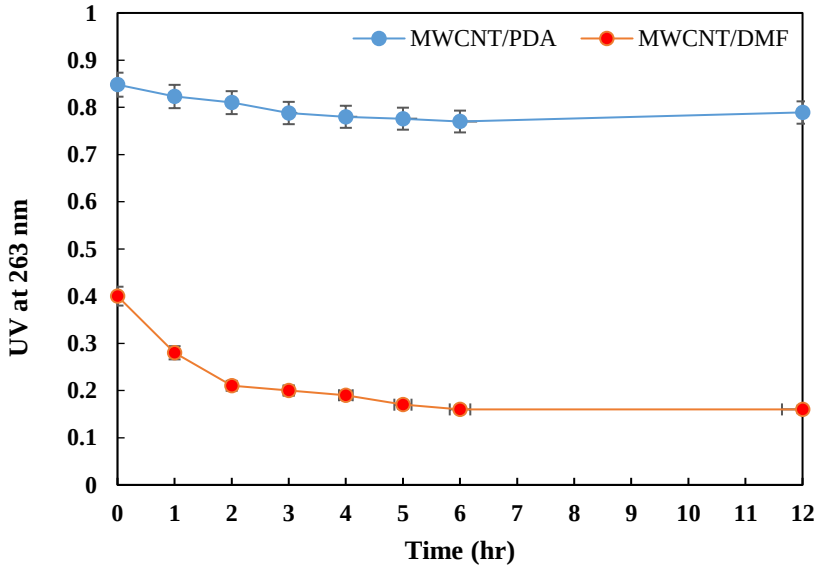

Fig.4.2. Stability of MWCNT and MWCNT/PDA dispersion over time (UV/Vis. spectra of MWCNT and MWCNT/PDA composite at 263 nm for 12 hrs).

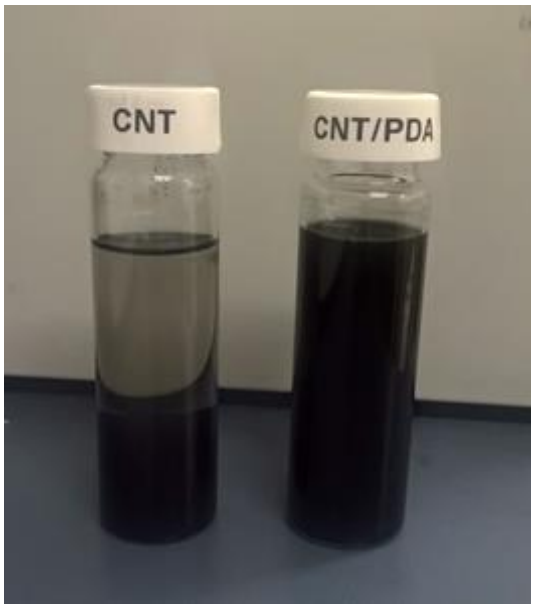

Fig. 4.3. Photo of MWCNT/PDA and MWCNT in DMF mixtures showing the dispersion status with time (after 12 hr.).

4.1.1.2 FTIR spectrophotometer

FTIR was used to characterize the modified MWCNT/PDA/PVDF membrane compared to pristine PVDF membrane. **Fig. 4.4** showed the spectra of both membranes, in the absorption spectrum of modified membrane it is noticed that there are a new absorption band peaks at 1658 cm^{-1} and 1536 cm^{-1} which are likely represent the stretching vibration of C = C in the aromatic ring and the N-H bending vibration respectively. These results indicate that blended PVDF membrane has been successfully modified by PDA/MWCNT complex via the oxidative polymerization method of dopamine, and these results showed agreement with the previous reports [5, 6].

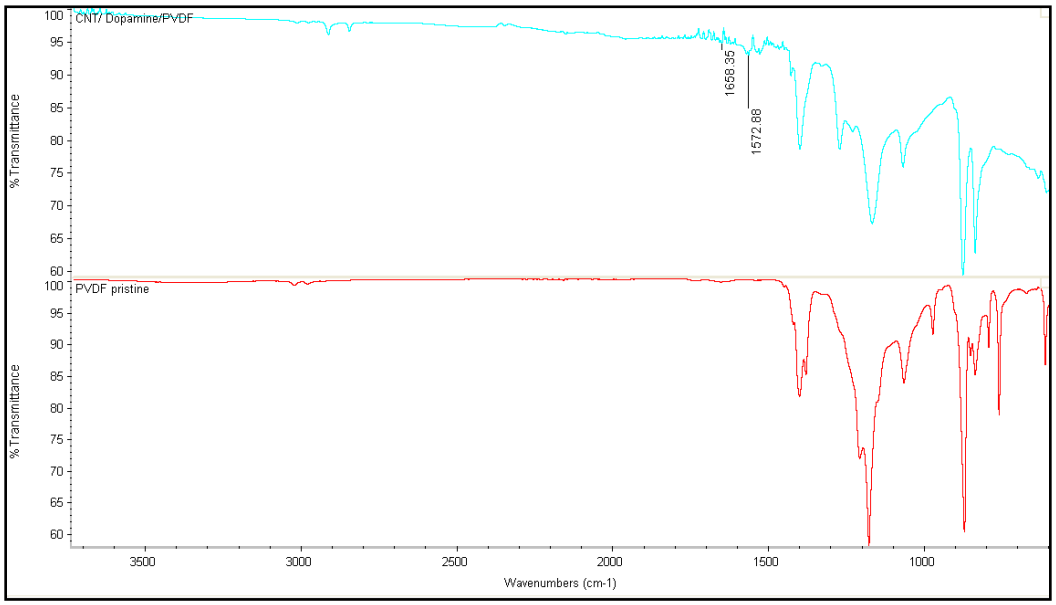

Fig. 4.4. FTIR spectra for pristine PVDF and MWCNT/PDA/PVDF membranes.

4.1.2 Membrane surface and Morphology

4.1.2.1 Hydrophilicity

The hydrophilicity of the samples was determined by measuring the contact angle (CA). Hydrophilicity measurement results which are shown in **Fig. 4.5** demonstrated that the CA decreased with increasing the amount of MWCNT, suggesting an increase in hydrophilicity of the membrane surface. Thus, played a major role in water permeation of the resultant modified membranes [7].

The CA of pristine PVDF was 91 and decreased with PDA addition to reaching 82.2, with MWCNT inclusion CA decreased further and reached 66.4 for 1 wt. % MWCNT PC-3 membrane, this decline in CA indicated an increase in the hydrophilicity which enhanced the water permeability of the blended membrane. However, with the further increase in the MWCNT to 1.5 wt. % for PC-4 membrane, a slight increase in CA was seen, this might be due to the high viscosity of the solution due to high MWCNT concentration in the membrane matrix; and so decreased the uniformity and irregular dispersion of MWCNT in the membrane structure during membrane fabrication which leads to the formation of an aggregate and reduces the effectiveness of carbon nanotubes; same results were concluded by Ma et al. [7, 8].

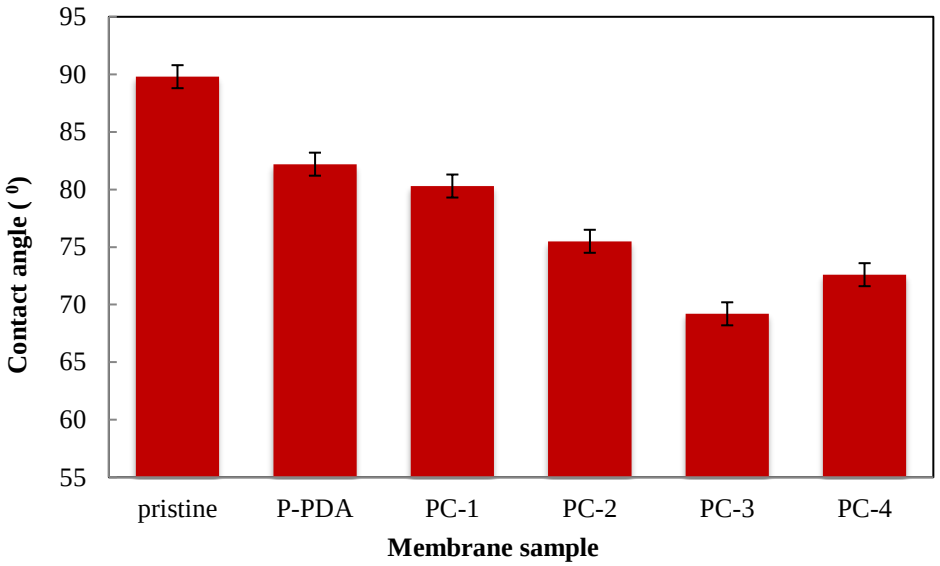

Fig. 4.5. Contact angle measurement for blended membranes.

4.1.2.2 Porosity and average pore size

The effect of MWCNT/PDA inclusion on the porosity and pore size of the fabricated membranes is shown in **Table 4.1**. Results indicated that the porosity increased with the addition of MWCNT/PDA. The porosity of the fabricated membranes ranged from 84.5 to 86.3%., it reached its maximum value of 86.3% in the PC-3 membrane (1 wt.% MWCNT). This increase in the porosity can be attributed to the hydrophilic effect of MWCNT/PDA inclusion which accelerates the diffusion rate between non-solvent (water) and the solvent (DMF) exchange leading to the formation of more porous structure resulting in an increase in porosity [8].

Furthermore, MWCNTs are hollow materials, which result in the formation of new macrovoids and porous structure as a consequence of the interaction of solid-liquid contacted in the polymer matrix compared with pristine PVDF, which contains less hydrophilic groups [7, 9]. Therefore, the inclusion of MWCNT is valuable to fabricate a membrane with higher porosity.

However, with the further increase in MWCNT concentration to 1.5 wt. % in PC-4 membrane, porosity decreased to 85.3 due to the growing viscosity of the casting solution with the excess

addition of MWCNT amount. Consequently, a denser layer with fewer finger-like structures was formed [7].

Table 4.1 Porosity and average pore size of the top layer of membrane.

Type of membrane	Porosity (%)	Calculated mean pore size (nm)
pristine	70.4	4.3
PC-1	84.0	6.6
PC-2	85.0	7.3
PC-3	86.3	9.5
PC-4	85.1	8.4

The average pore size (calculated as presented in chapter 3, section 3.4.3) showed a similar trend by changing the concentration of MWCNT/PDA; all the fabricated membranes exhibited larger pore size compared to pristine PVDF. When the MWCNT concentration increased to 1 wt. % in PC-3, the membrane pore size increased and reached the maximum value of 9.5 nm.

However, when the concentration of MWCNT further increased to 1.5 wt. % in PC-4, pore sizes decreased, and denser structure formation was noted, this was likely related to the increasing viscosity effect [8].

4.1.2.3 Zeta potential measurement

Measuring the electrokinetic properties such as zeta potentials for the membrane surface and the particles are important in understanding the nature and magnitude of membrane fouling caused by the membrane–particle interfacial interactions[10]. Zeta potential of the modified membranes was studied at pH 5.5 to investigate the surface charge of the membranes when using HA solution. The results of zeta potential measurements are shown in **Fig. 4.6;** stated that pristine

PVDF has a negative surface charge equal to -11.3 mV. With PDA addition to PVDF membrane, the negative charge of the membrane increased to -19.6mV, while with the addition of MWCNT, further increase in negative charge of the membrane surface to reach -25.85 mV was noticed.

HA is a negatively charged solution with zeta potential equal to -7 mV, and the fabricated membrane surface is negatively charged as shown from zeta potential results. Consequently, repulsion interactions [11] will occur between HA and the surface of the modified membranes, which lead to a reduction in membrane fouling as explained in the following sections.

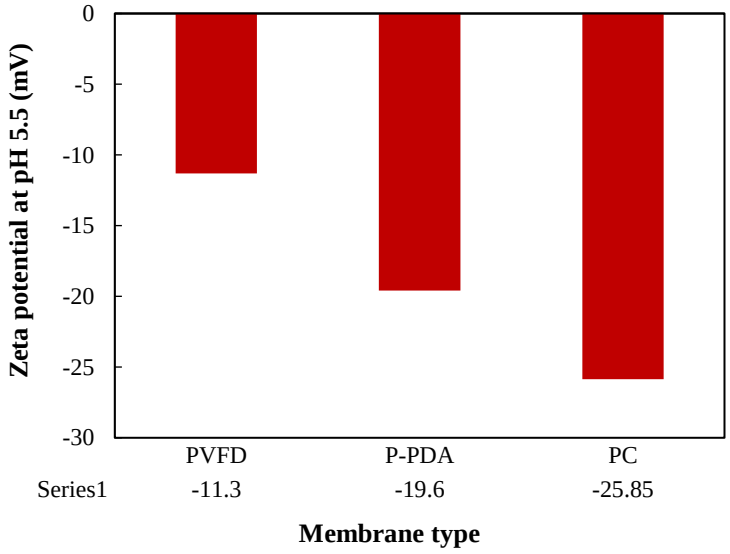

Fig. 4.6. Zeta potential of the membrane surface for pristine PVDF, P-PDA, and PC-1.

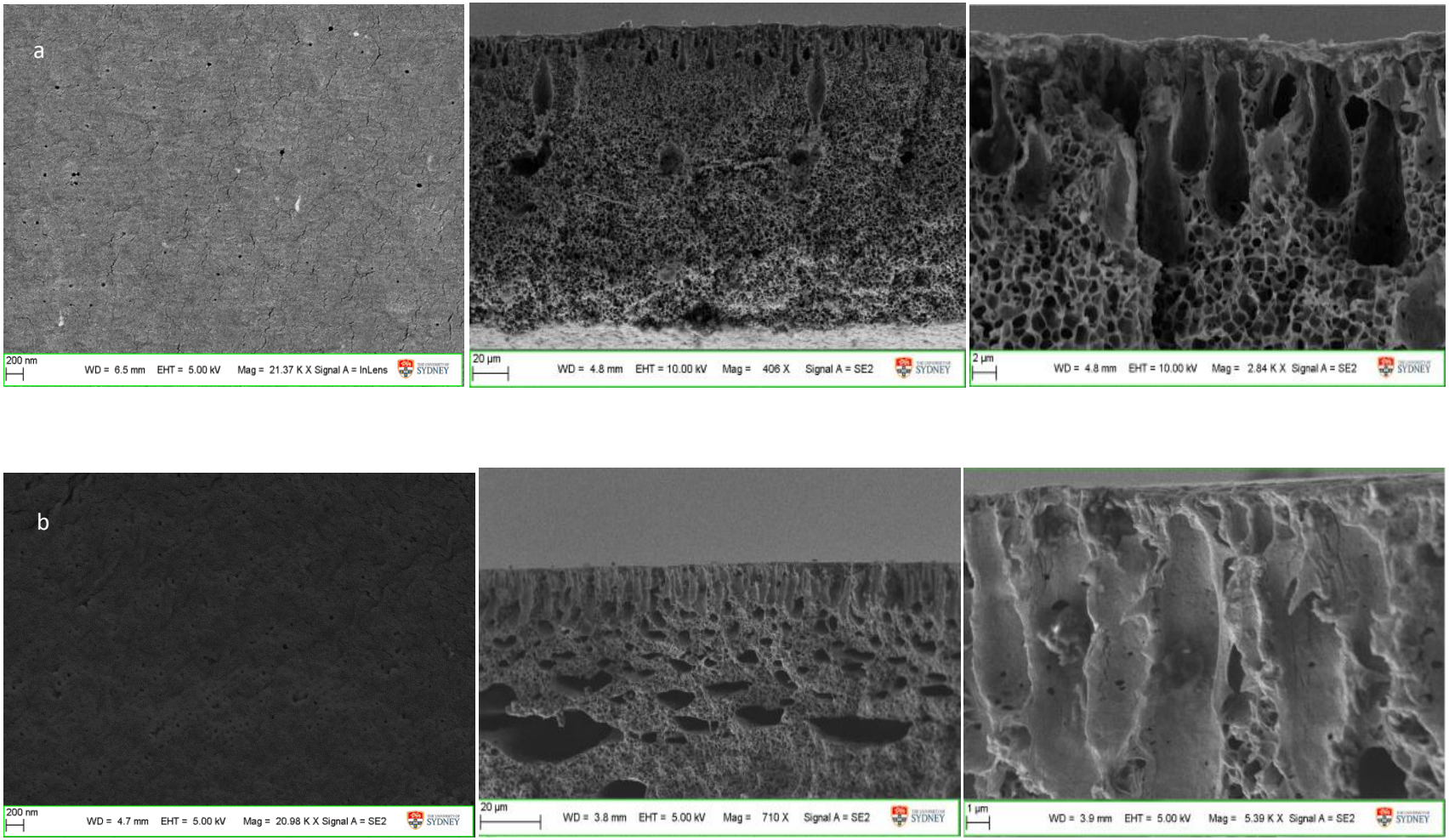

Fig. 4.7A. SEM images including the top surface and the cross-sectional views at 20 µm and 2µm respectively, of the blended membranes with different compositions; (a) pristine. (b) P-PDA.

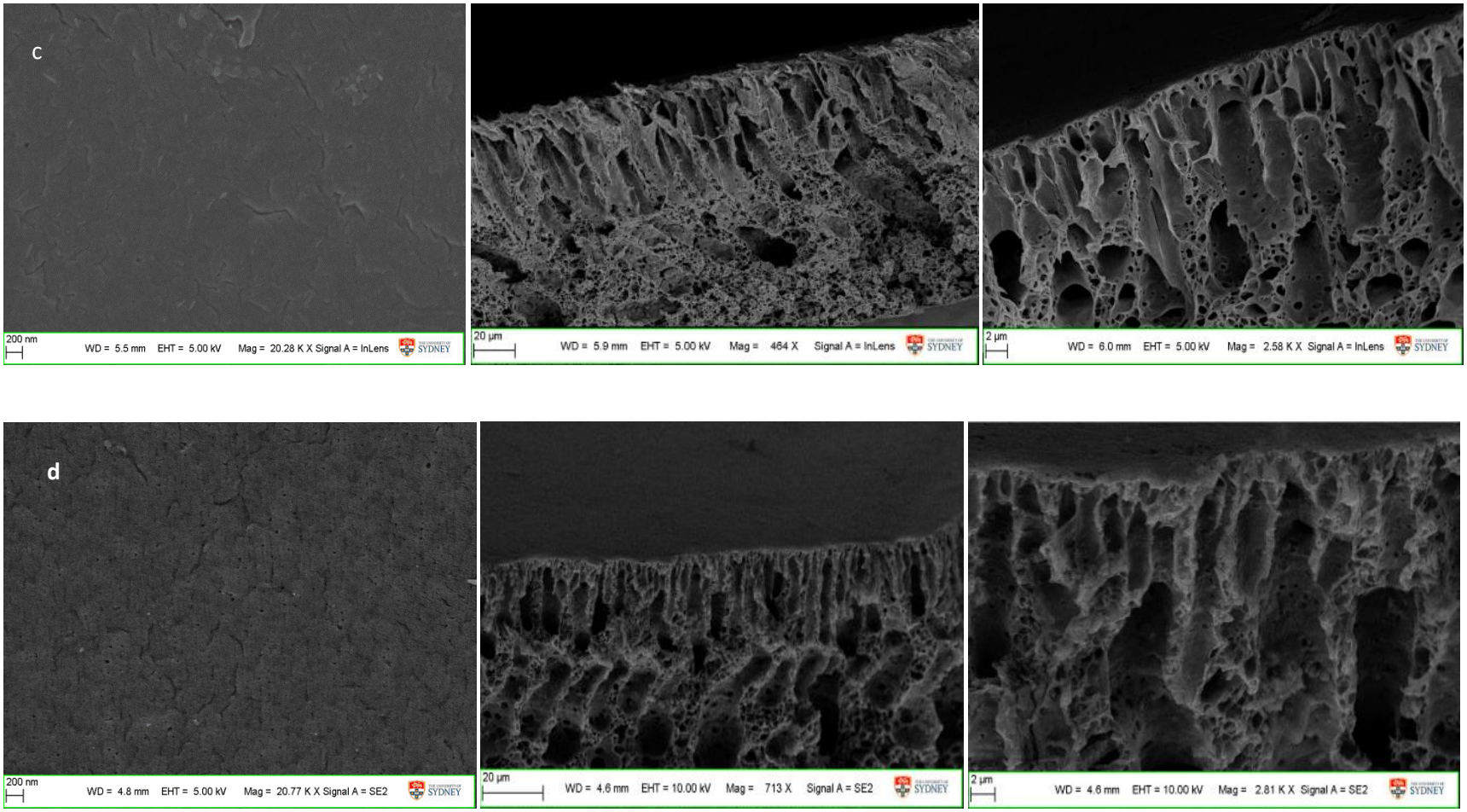

Fig. 4.7B. SEM images including the top surface and the cross-sectional views at 20 µm and 2µm respectively, of the blended membranes with different compositions; (c) PC-1 (d) PC-2.

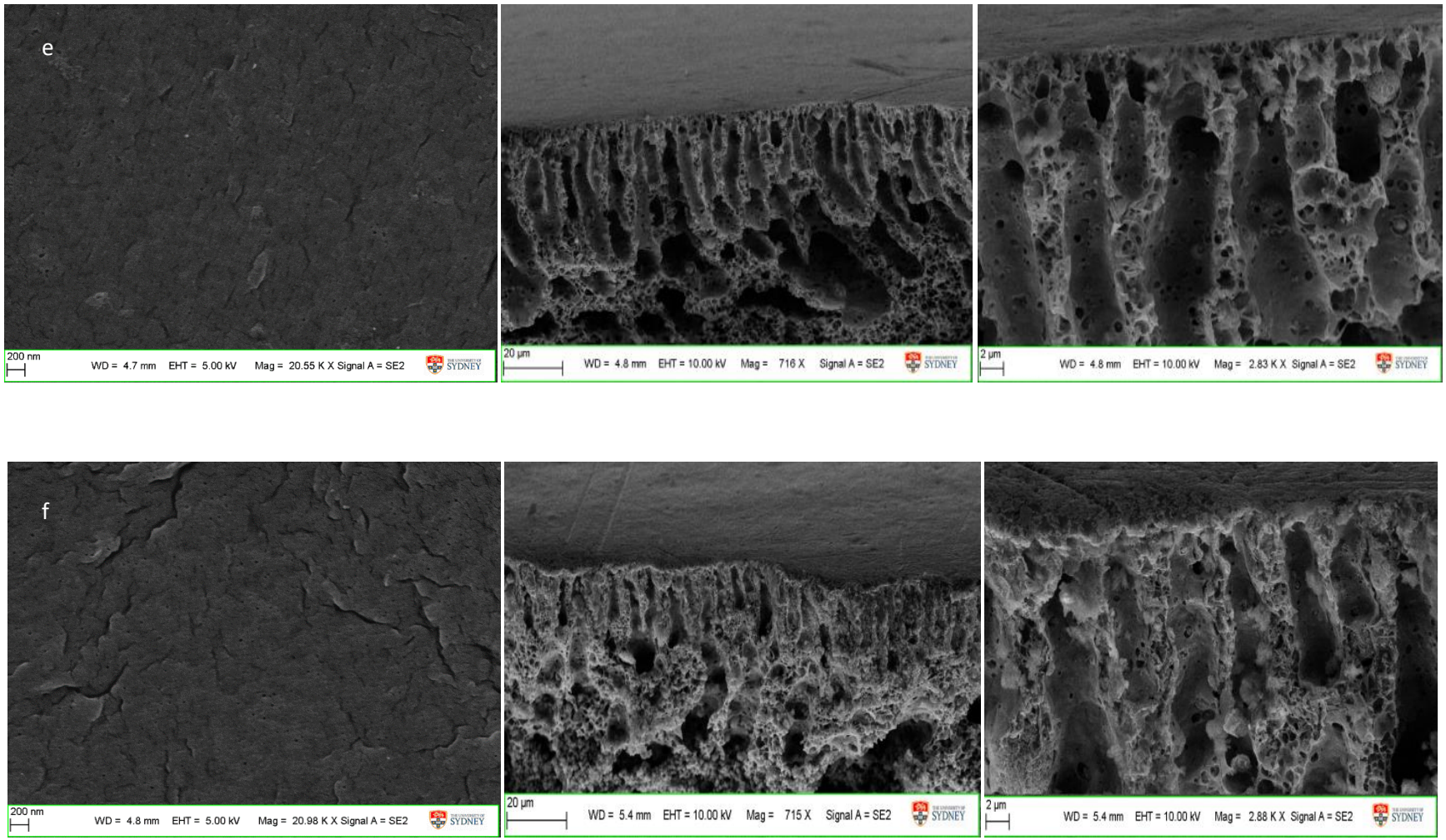

Fig. 4.7C. SEM images including a top surface and the cross-sectional views at 20 µm and 2µm respectively of the blended membranes with different compositions; (e) PC-3 (f) PC-4.

4.1.2.4 Membrane Structure

The top surface and cross sections of the fabricated membranes are shown in **Fig. 4.7A**, **B**, and **C** cross section images revealed that all membranes exhibited inhomogeneous asymmetric structure with large voids and finger-like cavities; this was due to the strong interaction between the non-solvent (water) and the solvent (DMF) which affected the demixing process significantly and accelerated exchange rate [12, 13]. As can be seen in **Fig. 4.7A**, **B**, and **C** the finger-like pores in the blended membrane are larger compared to pristine PVDF, and the size of those voids are increased with increased MWCNT content. Therefore water transfer is much easier through these modified membranes leading to an increase in their water permeability.

These results could be attributed to the hydrophilic MWCNT, which accelerated the exchange phase inversion process between solvent and non-solvent.

It can be seen from **Fig. 4.7C** (e) that PC-3 membrane with 1 wt. % MWCNT showed the most evident changes in the morphology with more finger-like voids and larger pores compared to pristine PVDF. However, by increasing MWCNT to 1.5 wt. % in the PC-4 membrane, the solution viscosity increased and thus slowed down the phase separation which resulted in the membrane with smaller finger-like cavities and pores as can be seen in **Fig. 4.6C** (f).

4.1.3 PVDF/MWCNT/PDA mechanical properties

Mechanical properties of the fabricated membranes were determined by measuring the tensile strength and the elongation at the point of breakage. The results are shown in **Fig. 4.8.** Compared to pristine PVDF membrane, the tensile strength of all of the fabricated membranes was enhanced. The tensile strength of PVDF membrane initially increased on adding PDA from 1.1 MPa to 1.7 MPa. It was further increased with MWCNT/PDA inclusion to 2.3 MPa for PC-2 membrane, but when the MWCNT concentration was increased to 1 wt. % for the PC-3

membrane, the tensile strength decreased from to 1.8 MPa, further increase in MWCNT to 1.5 wt. % for PC-4 membrane decreased the tensile slightly to 1 MPa, but it is still more than the pristine PVDF membrane.

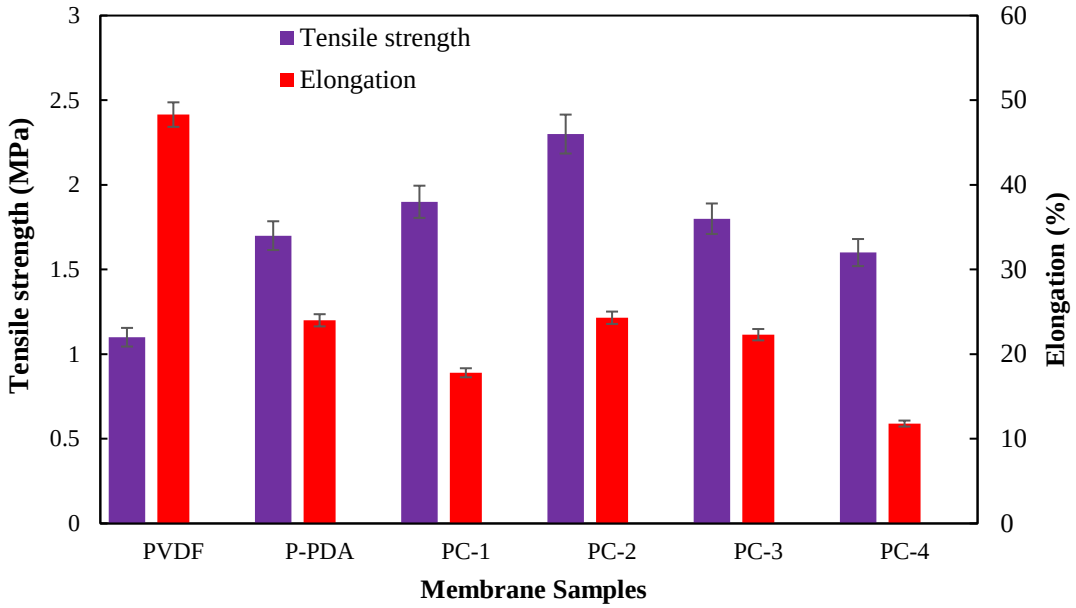

Fig. 4.8. Mechanical properties of PVDF blended membranes.

This may be attributed to aggregation caused by increasing the amount of MWCNT, which accelerates the fracture of the membranes [14] as well as the formation of large finger-like pores within the membrane.

The elongation of the blended membranes decreased significantly on adding MWCNT/PDA complex; this may be attributed to the high rigidity of the modified membranes. Also, it might be due to the weak compatibility between the hydrophilic MWCNT/PDA complex and the hydrophobic PVDF matrix, which lead to a decrease in mechanical strength [6, 7].

These results demonstrated that adding MWCNT/PDA to the PVDF membranes could increase tensile strength but reduced membrane elasticity.

4.1.4 Membrane performance

4.1.4.1 Water permeability

A comparison between pure water permeability of different membrane types (pristine PVDF, PVDF/PDA, PVDF/CNT and PVDF/PDA/MWCNT) is presented in **Fig. 4.9** which showed that pristine PVDF has the lowest permeability results (30 LMH/bar) and this is expected due to the relatively smaller average pore sizes and disribution, low porosity, and decreased hydrophilicity.

P-CN membrane which is simple blended 1 wt.% PVDF/MWCNT showed low permeability results (107 LMH/bar) compared to PC-3 (1 wt. % PVDF/PDA/MWCNT) membrane which has the highest permeability (502 LMH/bar). The low permeability of P-CN can be attributed to aggregation and low dispersion of MWCNT in P-CN membrane; leading to reduced porosity and blockage of membrane pores. While for PC-3 membrane the dispersion and aggregation problem of MWCNT was solved by the inclusion of MWCNT as MWCNT/PDA complex in the polymer matrix and this enhanced the fabricated membrane performance for water permeability as seen in **Fig. 4.9**.

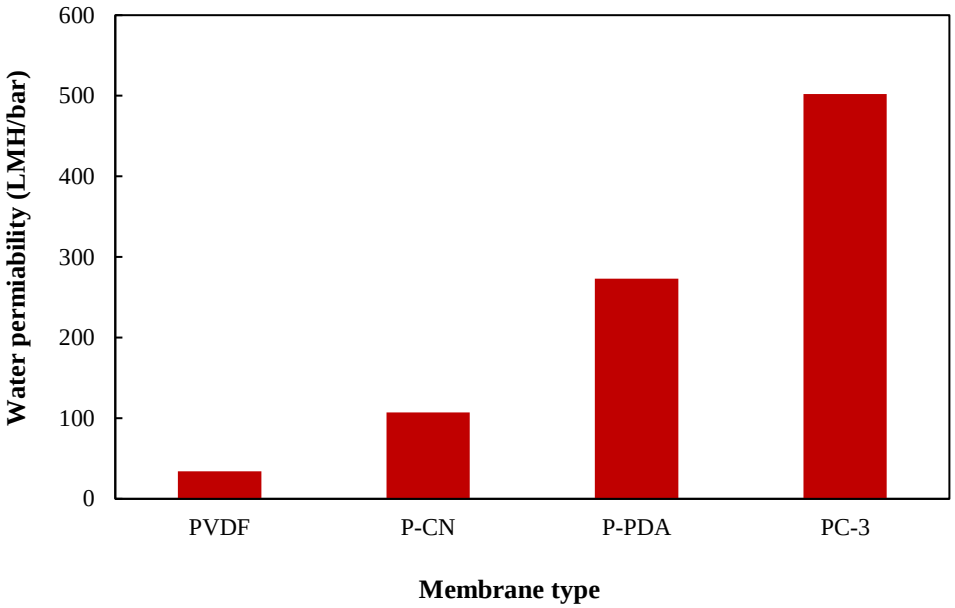

Fig. 4.9 Water permeability for pristine PVDF, P-CN simple blended 1% CNT with PVDF, P-PDA membrane fabricated by in-situ polymerization of PDA/PVDF, PC-3 membrane fabricated by *in-situ* polymerization of PDA/ 1% MWCNT/PVDF.

P-PDA which was obtained by PDA addition to PVDF as PVDF/PDA membrane showed water permeability reached to 275 LMH/bar; which is 9 times greater compared with pristine PVDF membrane; this is due to the dopamine polymerization on PVDF polymer, a thus fraction of unpolymerized dopamine and a polymerized dopamine (PDA) released from the membrane structure during membrane fabrication forming pores in the modified PVDF membrane [6].

Jiang et al. [6] studied the preparation of PVDF/PDA membranes under different polymerization conditions, and their membranes showed permeability up to 100 LMH/bar with 15% rejection, while for our membrane the performance significantly improved (permeability: 272 LMH/bar, rejection: 63%).

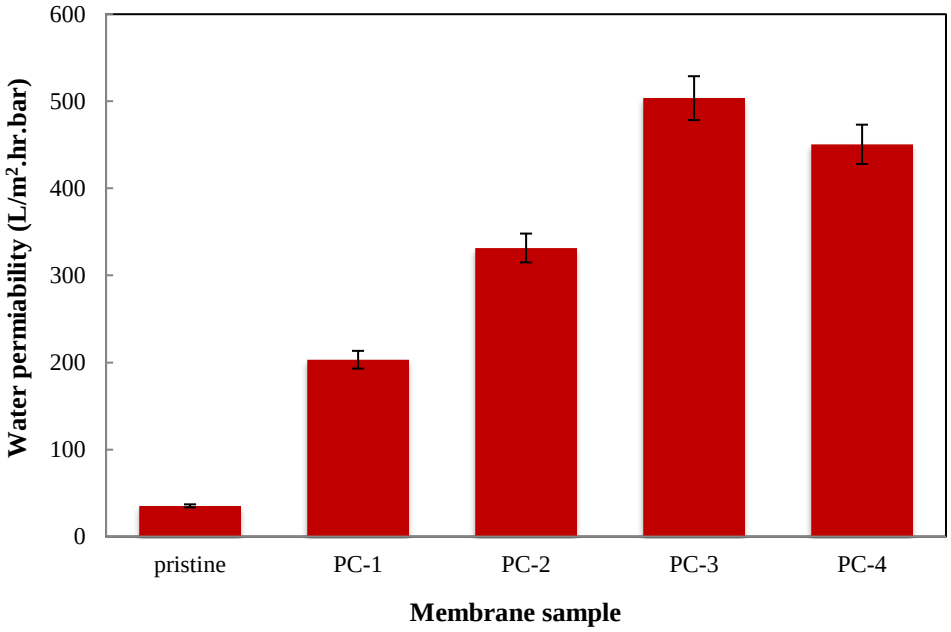

Fig. 4.10 Effect of MWCNT concentration on water permeability.

A comparison between water permeability of modified PVDF/PDA/MWCNT (PC) membranes with different MWCNT concentrations is illustrated in **Fig. 4.10**. The results shown in **Fig. 4.10** are consistent with the characterization results obtained in the previous sections.

For PC-1 (0.25 wt.% MWCNT) membrane, water permeability increased to 203.2 LMH/bar compared to 30 LMH/bar for the pristine membrane, when the concentration of MWCNT rose to 0.5 wt. % for PC-2 membrane; water permeability increased to 331.5 LMH/bar.

The maximum permeability was achieved with the addition of 1 wt. % MWCNT for PC-3; in this case water permeability reached 506 LMH/bar which is 16 times more permeable than pristine PVDF membrane. This improvement in permeability is consistent with the porosity and pore size measurement shown in **Table 4.1**; as higher porosity decreases the hydraulic resistance and so increases water passage through the membrane. Furthermore, increased the hydrophilic surface due to the MWCNT/PDA addition increased the overall surface hydrophilicity, which

causes water molecules preferentially adsorb inside membrane pores surface with less interaction making their passage through the membrane easier and as a result increasing water permeability. Moreover, the hydrophilic MWCNT/PDA additives accelerate exchange phase inversion process between solvent and non-solvent through the fast exchange of the demixing process and thus leading to form a porous layer with uniformity of MWCNT in the membrane which helps in improving water permeability [3, 9, 12, 15]. It is also evident that with increasing MWCNT, the average pore size and porosity increased (**Table 4.1**), and hence water permeability increased.

Further increase in MWCNT concentration to 1.5 wt. % in PC-4 membrane showed a decrease in water permeability which can be attributed to increased viscosity of the casting solution due to high amount of MWCNT [8, 15]. This high viscosity casting solution delayed the exchange between solvent and non-solvent with a resultant membrane of less MWCNT uniformity and relatively dense top layer with smaller average pore size and smaller finger-like cavities [3, 8, 11] as can be seen in **Table 4.1** and **Fig.4.7C** (f).

The addition of 1 wt. % of MWCNT used in PC-3 proved to be the optimum concentration which resulted in the highest water permeability for the modified membranes, see **Fig. 4.10**.

4.1.4.2 HA rejection efficiency of membranes

A comparison between HA rejection efficiency of different membrane types (pristine PVDF, PVDF/PDA, PVDF/CNT and PVDF/PDA/MWCNT) is shown in **Fig. 4.11**. MWCNT coating with PDA as MWCNT/PDA complex successfully overcame the dispersion problem in the polymer matrix and enhanced the results of the fabricated membrane rejection performance; this can be concluded by comparing the high rejection efficiency of PC-3 (up to 81%) to P-CN (up to 30%). The low rejection efficiency of P-CN is attributed to agglomeration and low dispersion of MWCNT on the membrane surface.

As the adsorption of HA is governed by the high surface area of MWCNT [16], consequently, the simple blended MWCNT/PVDF membrane was less effective in increasing the adsorption ability of MWCNT [17].

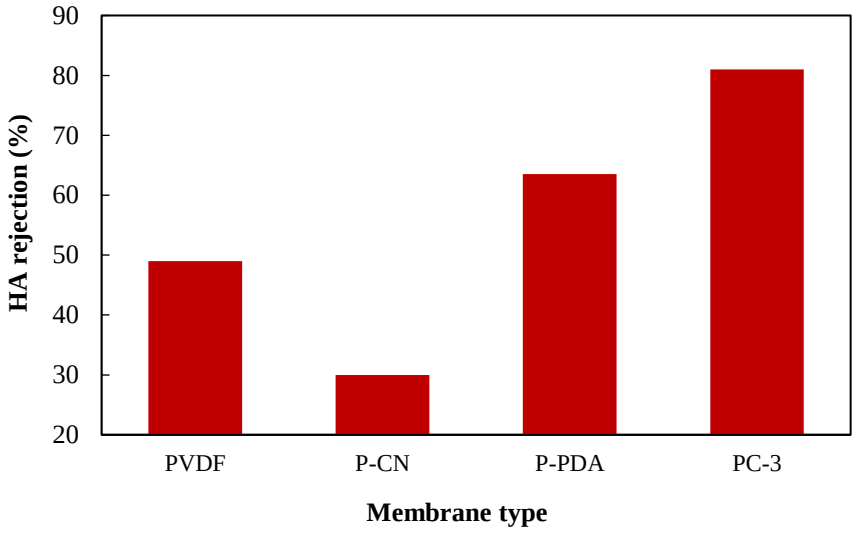

Fig. 4.11 HA rejection for pristine PVDF, P-CN simple blended 1% MWCNT with PVDF, P-PDA Membrane fabricated by in-situ polymerization of PDA/PVDF, PC-3 Membrane fabricated by *in-situ* polymerization of PANI/ 1% MWCNT/PVDF.

The HA rejection efficiency results for modified membranes with different MWCNT concentrations are shown in **Fig. 4.12**.

As can be seen, HA rejection increased significantly with the inclusion of MWCNT; HA rejection reached 86 % for 0.25 wt. % MWCNT in the PC-1 membrane, with 37 % HA rejection increase compared to the pristine membrane.

As the MWCNT concentration increased to 1 wt. % for PC-3 membrane, HA rejection slightly decreased to 81%. This reduction is possibly due to the highest permeability results (502 LMH/bar) which make the contact time between the feed solution and the membrane surface in

the filtration test not lengthy enough for HA adsorption on the membrane surface; besides that the larger average pore size will allow HA to pass easily with the high flux [17, 3].

However, when the concentration of MWCNT increased to 1.5 wt % in PC-4, the rejection increased again to 88 %; likely due to the high density of MWCNT, which caused increased viscosity that delayed the exchange between solvent and non-solvent, resulting in a smaller pores membrane and more.

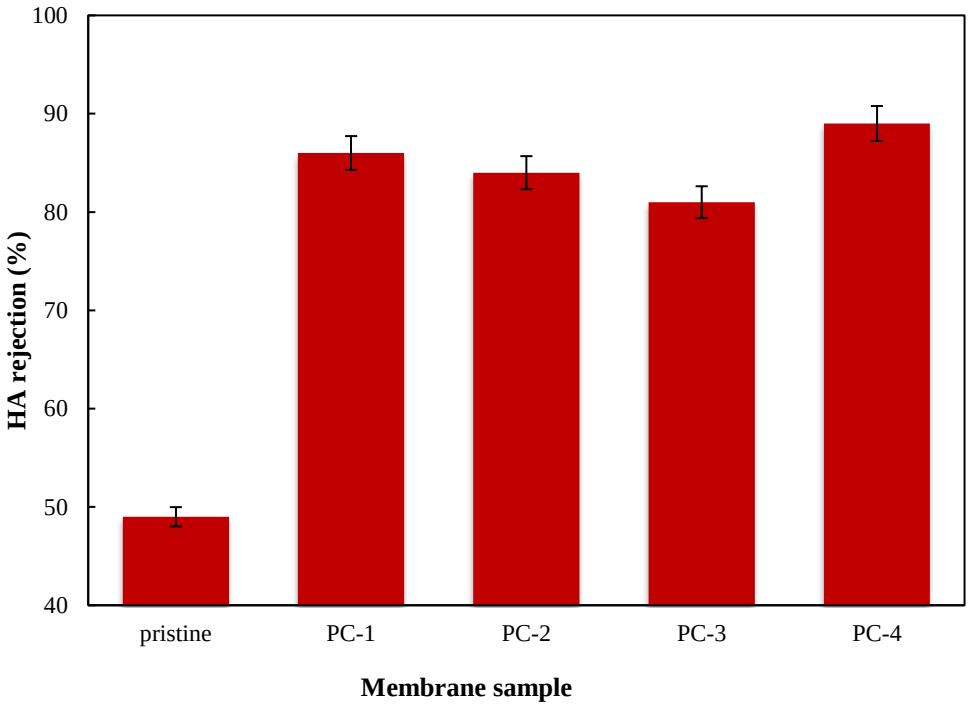

Fig. 4.12 Effect of MWCNT on HA rejection.

HA removal mechanism depends on the average pore size of the membrane and the adsorption of HA on the membrane surface.

As the HA molecule sizes are less than the modified membrane average pore size; (HA molecule size is less than 1 nm and the modified membranes measured pore sizes are between (6.6 – 9.5

nm), hence, the membrans are not able to reject HA by pore sieving, thus the high HA separation property is mainly attributed to the adsorptin capacity of the membrans. Inclusion of MWCNT as MWCNT/PDA enhanced the adsorption capacity of the modified membranes, as MWCNTs have high adsorption capacity to organic matters which is mainly due to the π-π bonds between bulk π system on CNT surfaces and the HA molecules [18].

Moreover, the high separation of HA in the modified membranes might be due to the aggregation of HA on the membrane surface by the steric hindrance effect for their relatively large molecules [19, 20]. Furthermore, HA is a negatively charged molecule (contains mainly carboxylic groups and phenolic hydroxyl groups with a zeta potential of -7 mV at pH 5.5). The membrane surface is also negatively charged as found by zeta potential measurements (-25.8 mV at pH 5.5), as showen in**Fig. 4.6**, thus a repulsion interaction occurs between HA, and the membrane surface, however, from the rejection results shown, PDA was able to show a balance between permeability and HA rejection performance which is considered to be largely responsible for the high HA rejection efficiency noticed in this study [3, 19].

When the particle size is less than the membrane average pore size as in this case where HA particles less than membrane average pore size; HA particles deposited on the internal pores decreased the pore diameters, and is expected to have a standard blocking model or blocking cake layer on the membrane surface [21, 22, 23], thus leading to flux decline. **Fig. 4.13** showed the pure water permeability of all modified membrane, and as comparison (**Fig. 4.14)** which showed the flux decline of HA rejection with time.

Jucker and Clark [20, 24] suggested that the membrane pores are the preferable place for organic adsorption. This HA deposition on the membrane surface would explain severe flux decline of NOM fouling compared to other colloidal particles.

When HA adsorbed and covers the membrane surface then the membrane reached its capacity, desorption might happen and decrease HA rejection efficiency. Repulsion between HA particles itself may also occur, and as explained before some adsorption causes pore narrowing or blocking or even cake layer on the membrane surface. However, even when the membrane reached its adsorption capacity, rejection rate drops slightly [17].

A filtration test with HA solution was performed to check the adsorption capacity of the membrane for a run of (24 hrs) as seen in **Fig. 4.15**; HA rejection was measured every 6 hrs results showed a marginal decrease in HA removal over 24 hrs for the PC-3 membrane, which means that the membrane does not reach its adsorption capacity yet, while for the pristine membrane it showed a drop in HA efficiency from 49 % to 21%.

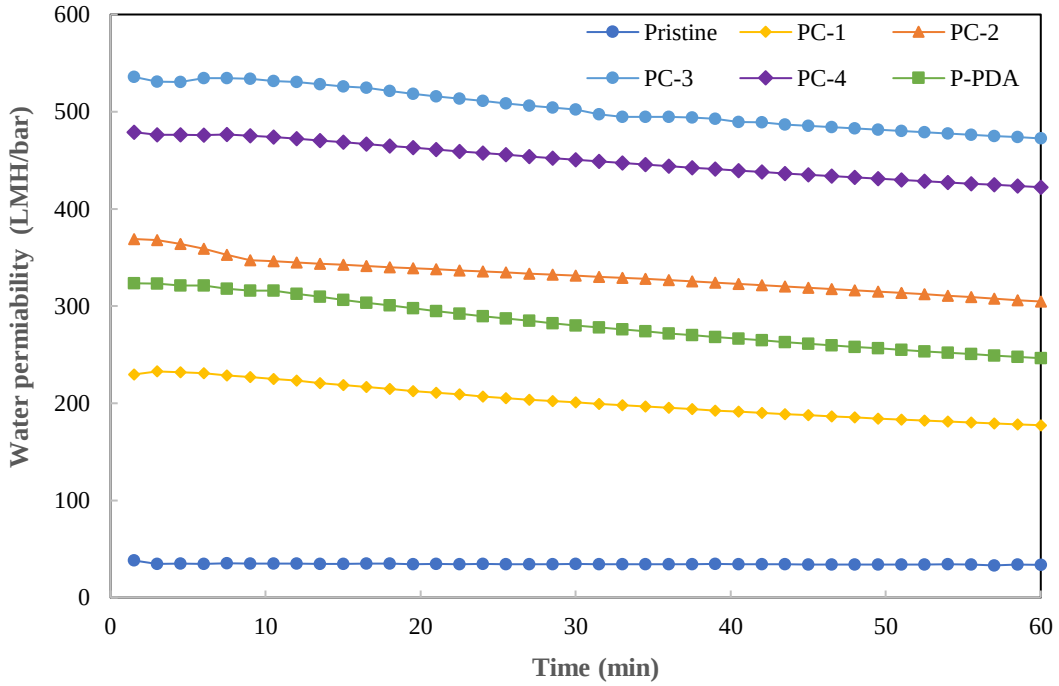

Fig. 4.13 Water permeability behavior for pristine and modified membranes PIC.

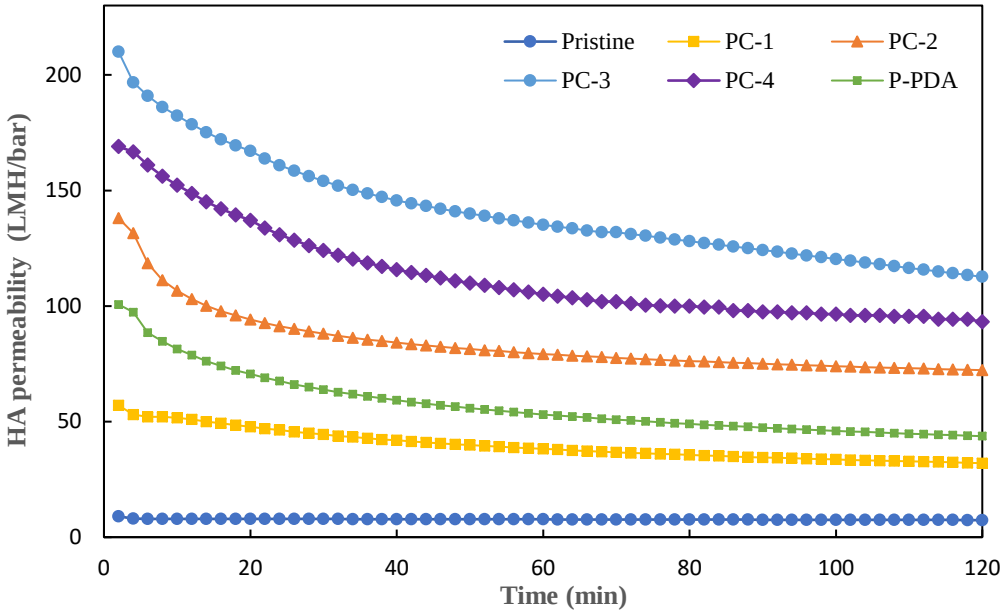

Fig. 4.14 HA permeability decline behavior for pristine and modified membranes PIC.

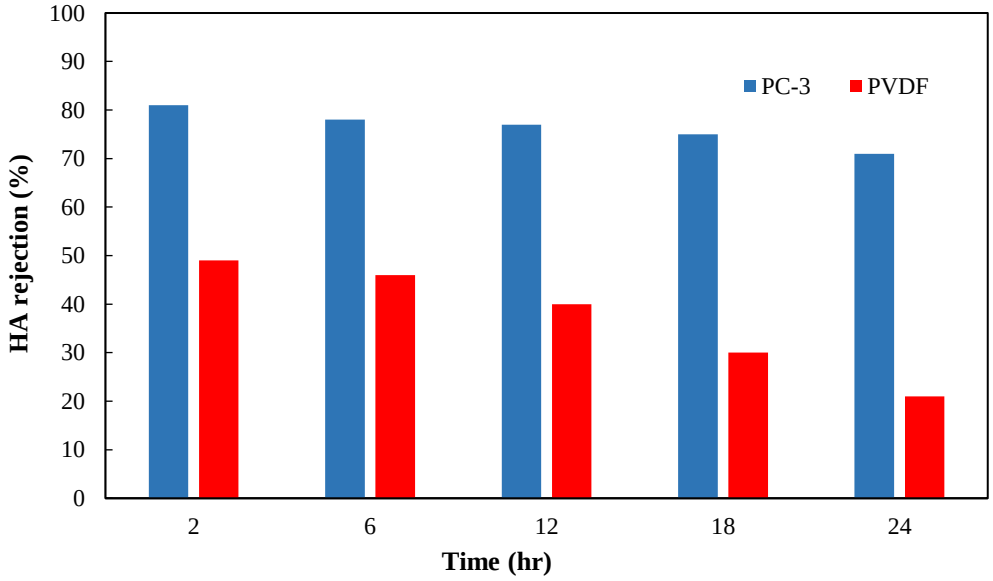

Fig. 4.15 HA rejection behavior for PC-3 and pristine PVDF with time.

4.1.5 Flux recovery after chemical cleaning

Flux recovery and a decline in flux test for HA and its cleaning method were conducted. As shown in **Fig. 4.13 and 4.14**, the flux of HA rapidly decreased compared to the flux of pure water due to fouling. The permeation of pure water and HA for modified membranes was enhanced compared to pristine PVDF this is because of higher porosity and hydrophilicity, which reduced the resistance of the membrane to water flux [6].

HA removal from the membrane surface was accomplished by cleaning the membrane surface with both acid (HCl) and base (NaOH). HA removal occurred through hydrolysis and solubilization effect. First, NaOH hydrolyzing the HA with carboxylic and phenolic functional groups as it can change the configuration of NOM to a looser fouling layer with an open structure. Then HCl is oxidizing and breaking down the functional groups of organic foulant to soluble carboxyl, ketonic and aldehyde groups, and then they detached from the membrane surface [11, 25].

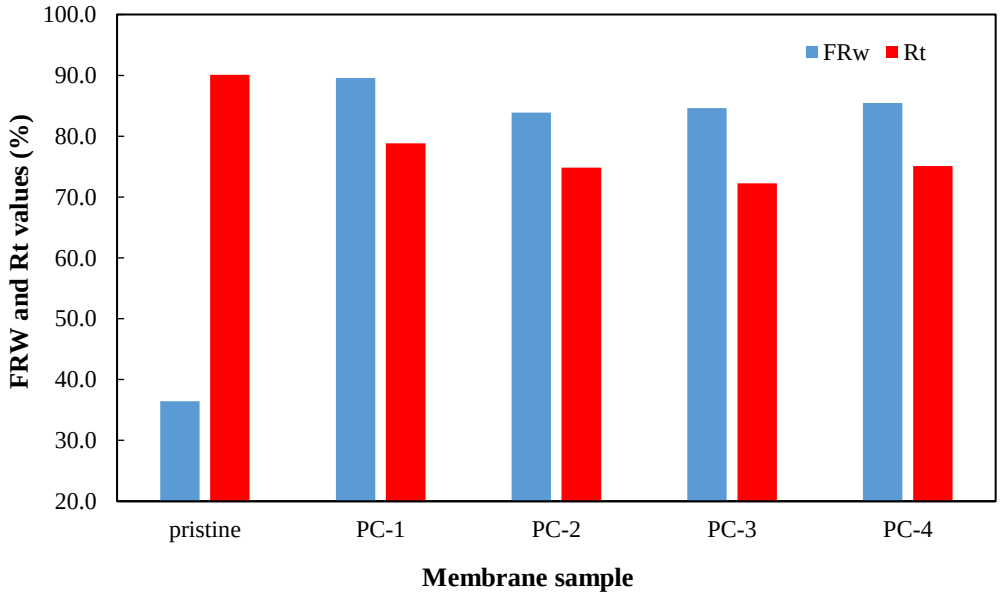

Fig. 4.16 Flux recovery and total fouling ratio for pristine and modified membranes.

As can be seen from **Fig. 4.16** The modified membranes showed higher recovery flux F_{Rw} and lower total flux R_t in comparison to pristine PVDF membrane. HA adsorption usually caused a significant fouling found to be (70-74) %, and flux recovery for all membranes after cleaning by acid and base is between (85.4-89.6)%. This high flux recovery of the membranes indicates that HA has a weak tendency to interact with membrane surface due to increased negative charge of membrane surface as a result of the PDA/MWCNT additives, which exhibits higher electrostatic repulsion to negatively charged HA. Therefore, more fouling resistant; consequently, decreasing membrane fouling and easier HA removal from the membrane surface [11, 26].

Most of the HA adsorbed on the membrane surface can be easily removed using both acid and base with water flux recovery and HA recovery up to 90 %.

4.2 Conclusion

MWCNT/PDA/PVDF ultrafiltration membrane was fabricated by in-situ polymerization using phase inversion method with improved water permeability and antifouling properties. The effect of MWCNT/PDA on the performance of PVDF blended membrane was investigated. In-situ synthesis of PDA on MWCNT was found to be valuable to form a porous membrane with larger finger like cavities which results in high water permeability.

The synthesized MWCNT/PDA/PVDF membrane showed higher porosity, hydrophilicity, and larger pore size compared to the pristine membrane. The significant performance enhancement reflected as 20 times permeability increase of the modified membranes compared to pristine PVDF membrane and 12.5% increase in HA rejection when the membrane was blended with 1 wt. % of MWCNT (PC-3); therefore, the addition of 1wt. % of MWCNT and 2wt. % fixed amount of PDA was recommended concentrations for PVDF membrane modification to obtain the optimal results. However, the mechanical property of the blended membrane was slightly reduced.

Humic acid was used as a model for natural organic matter (NOM) to evaluate the performance of the modified membranes. Improvement in HA rejection was shown with the inclusion of MWCNT/PDA; which is due to the repulsion interaction between negatively charged HA and the negatively charged membrane surface and the excellent adsorption properties for MWCNT, rejection reached up to 89% in PC-4 with 40% increase compared to pristine PVDF membrane.

References

[1] Wang, J.-L. et al., (2014). Facile fabrication of robust superhydrophobic multilayered film based on bioinspired poly (dopamine)-modified carbon nanotubes. Physical chemistry chemical physics: PCCP, 16(7), pp.2936–43.

[2] Lin, M. et al., (2013). High loading of uniformly dispersed Pt nanoparticles on polydopamine coated carbon nanotubes and its application in simultaneous determination of dopamine and uric acid. Nanotechnology, 24(6), p.065501.

[3] Sianipar, M. et al., (2016). Potential and performance of a polydopamine-coated multiwalled carbon nanotube/polysulfone nanocomposite membrane for ultrafiltration application. Journal of Industrial and Engineering Chemistry, 34(2016), pp.364–373.

[4] Peng, H.P. et al., (2013). General preparation of novel core-shell heme protein-Au-polydopamine- Fe3O4 magnetic bio-nanoparticles for direct electrochemistry. Journal of Electroanalytical Chemistry, 700(2013), pp.70–76.

[5] Shi C. et al., (2013). Synthesis of Highly Water-Dispersible Poly (dopamine)-Modified Multi-walled Carbon Nanotubes for Matrix-Assisted Laser Desorption/ Ionization Mass Spectrometry Analysis.

[6] Jiang, J.-H. et al., (2014). Improved hydrodynamic permeability and antifouling properties of poly (vinylidene fluoride) membranes using polydopamine nanoparticles as additives. Journal of Membrane Science, 457, pp.73–81.

[7] Majeed, S. et al., (2012). Multi-walled carbon nanotubes (MWCNTs) mixed polyacrylonitrile (PAN) ultrafiltration membranes. Journal of Membrane Science, 403-404, pp.101–109.

[8] Ma J. et al., (2013). Role of oxygen-containing groups on MWCNTs in enhanced separation and permeability performance for PVDF hybrid ultrafiltration membranes. Desalination, 320, pp. 1–9.

[9] Zhang J.G. et al., (2013). Improved hydrophilicity, permeability, antifouling and mechanical performance of PVDF composite ultrafiltration membranes tailored by oxidized low- dimensional carbon nanomaterials, Journal of Mater. Chem. A, 1 (9), pp. 3101–3111.

[10] Salgin, S., Salgı, U. & Soyer, N., 2013. Streaming Potential Measurements of Polyethersulfone Ultrafiltration Membranes to Determine Salt Effects on Membrane Zeta Potential. Int. J. Electrochem. Sci, 8(2013), pp.4073–4084.

[11] Liu, Charles et al., (2001). Membrane Chemical Cleaning: From Art to Science. American Water Works Association, pp. 1-25.

[12] Hilal N., Ismail F.A., Wright C., (2015). Membrane Fabrication. First edition, CRC Press, ISBN 1482210460.

[13] Liu, F. et al., (2011). Progress in the production and modification of PVDF membranes. Journal of Membrane Science, 375(1-2), pp.1–27.

[14] Zhang L.P. et al., (2009). Preparation and characterization of composite membranes of poly (sulfone) and microcrystalline cellulose, J. Appl. Polym. Sci. 112, pp. 550–556.

[15] Mulder, M., (1996). Basic Principles of Membrane Technology. Dordrecht, the Netherlands: Kluwer.

[16] Hyung H., Kim J.-H., (2008). Natural organic matter (NOM) adsorption to multi-walled carbon nanotubes: effect of NOM characteristics and water quality parameters. Environ. Sci. Technol., 42 pp. 4416–4421.

[17] Lee, J. et al., (2016). High flux and high selectivity carbon nanotube composite membranes for natural organic matter removal. Separation and Purification Technology, 163, pp.109

[18] Pan, B. & Xing, B., (2008). Adsorption mechanisms of organic chemicals on carbon nanotubes. Environmental Science and Technology, 42(24), pp.9005–9013.

[19] Suhartono, Jono, and Chedly Tizaoui., (2015). Polyvinylidene Fluoride Membranes Impregnated at Optimised Content of Pristine and Functionalised Multi-Walled Carbon Nanotubes for Improved Water Permeation, Solute Rejection and Mechanical Properties. Separation and Purification Technology 154. Elsevier B.V., pp. 290–300.

[20] Teow, Y.H. et al., 2012. Preparation and characterization of PVDF/TiO2 mixed matrix membrane via in situ colloidal precipitation method. Desalination, 295(2012), pp.61–69.

[21] Aoustin, E., (2001). Ultrafiltration of natural organic matter. Separation and Purification Technology, 22-23(1-2), pp.63–78.

[22] Hermia J., (1982). Constant pressure blocking filtration laws: Applications to Power-law non-Newtonian fluids, J. Trans. Inst. Chem. Eng., 60, pp. 183-187.

[23] Bowen W. R., Calvo J. I, Hernandez A., (1995). Steps of membrane blocking in flux decline during protein microfiltration, J. Membr. Sci., 101, pp. 153-165.

[24] Clark, M. M., and C. Jucker (1993): Interactions between Hydrophobic Ultrafiltration Membranes and Humic Substances, Proceedings of the Membrane Technology Conference, Baltimore, MD

[25] Nguyen, Sy Thuy, and Felicity Anne Roddick. (2011). Chemical Cleaning of Ultrafiltration Membrane Fouled by an Activated Sludge Effluent. Desalination and Water Treatment 34, pp. 94–99.

[26] Daraei, P. et al., (2013). Enhancing antifouling capability of PES membrane via mixing with various types of polymer modified multi-walled carbon nanotube. Journal of Membrane Science, 444, pp.184–191.

CHAPTER 5. Enhanced permeability and antifouling properties of Poly(vinylidene fluoride) ultrafiltration membranes using polyaniline as additive

5.1 Results and Discussion

5.1.1 PVDF/PANI membrane characterization

5.1.1.1 FTIR spectrophotometer

In order to study the chemical changes of PVDF membrane surface after PANI addition, FTIR spectra analysis was performed to examine the new chemical composition bands, the neat PANI and PVDF spectra were also measured for comparison. As shown in **Fig. 5.1** PVDF showed absorption band at 1401 cm^{-1} and 876 cm^{-1} which are due to the C-F stretching vibration, and absorption band at 1168 cm^{-1} which was for C-C bond [1, 2]. PANI showed absorption band at 1558 cm^{-1} and 1496 cm^{-1} which were assigned for quinoid and benzenoid ring system in polyaniline [3]. The FTIR spectrum of PVDF/PANI membrane showed an overlapped absorption band for both PANI and PVDF, i.e. at 1558, 1457, 1398, 1169 and 877 cm^{-1} which confirm the polymerization of aniline to PANI in the membrane sheet coated the PVDF in the modified blended membranes [2, 3].

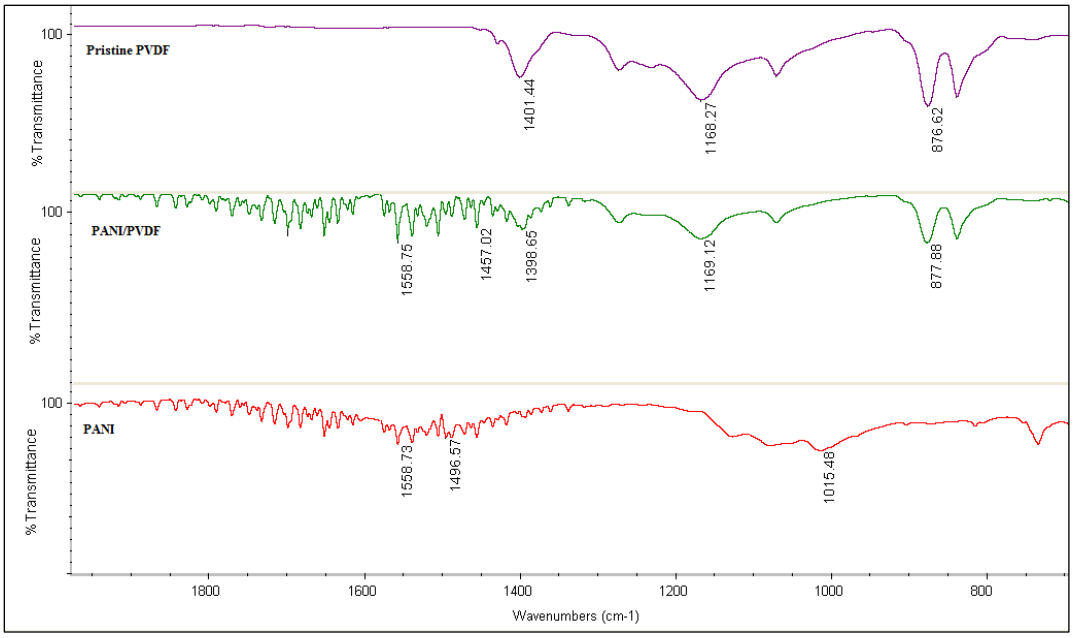

Fig.5.1 FTIR spectra for pristine PVDF, PANI and PANI/PVDF (PI-3) membrane.

5.1.2 Membrane surface and morphology

5.1.2.1 Hydrophilicity

The hydrophilicity of the samples was determined by measuring the contact angle (CA). The hydrophilicity measurement results, as shown in **Fig. 5.2**, demonstrated that the CA for PANI/PVDF modified membranes is lower than pristine PVDF. The CA of pristine PVDF was 90^{o} and decreased with PANI addition reaching 73^{o} for PP-3 membrane and 69^{o} for the PI-3 membrane, indicating hydrophilicity of the membranes surface increased due to the presence of nanospheres and oligomers of PANI in the blended membranes [4]. This increase in hydrophilicity leads to increase water permeability as going to be discussed later.

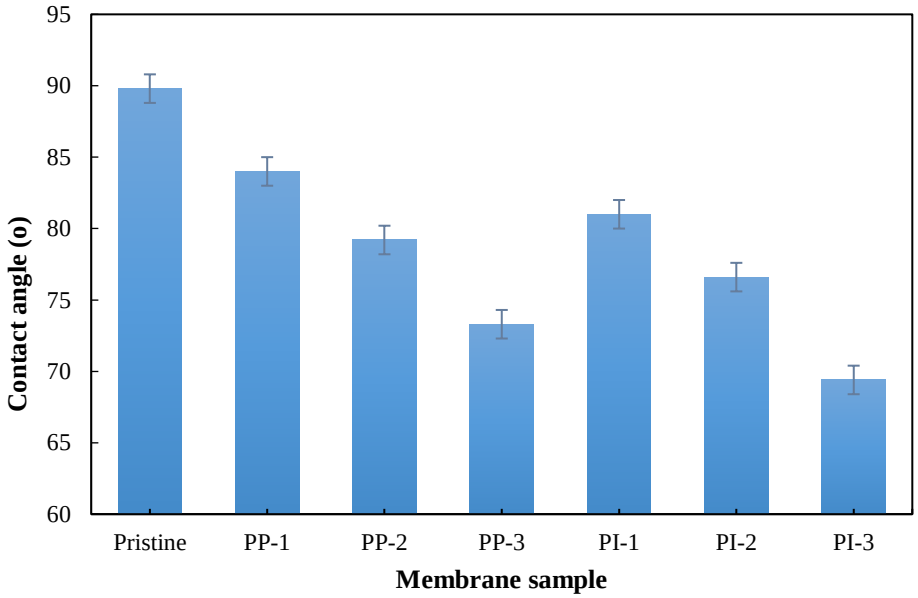

Fig. 5.2 Contact angle measurement for pure and modified membranes.

5.1.2.2. Porosity and average pore size

The average pore size was calculated (shown in chapter 3, section 3.4.3) and part of the membranes was measured by BET, approximate near results was noticed see **Table 5.1** and the Appendix. PVDF average pore size found to be 4.3 nm while the average pore sizes of the modified membranes are in the range of (4.6 -7.5 nm) for PP-X modified membranes and in the range of (5.0 - 8.8 nm) for PI-X membranes. It can be noticed that PANI/PVDF composite membranes showed larger average surface pore size than pristine PVDF membrane which resulted in an increase in water flux.

Table 5.1 Porosity and average pore size of the modified membrane.

Membrane type	Porosity (%)	Mean pore size (nm)
PVDF	70.4	4.3
PP-1	79.70	4.6
PP-2	80.03	5.8
PP-3	85.84	7.5
PI-1	74.43	5.0
PI-2	85.22	6.1
PI-3	89.81	8.8

As can be seen from **Table 5.1**, there is an increase in the membrane average pore size and porosity with increasing PANI content for PP and PI membranes. Also, it can be noticed that PI membranes showed a larger pore size and higher porosity than PP membranes; this might be for the larger fraction of unpolymerized aniline and PANI released from the membrane structure during membrane formation in water bath *in-situ* polymerization method for PI membranes; leading to larger pores formation in comparison to simple PANI blended method PP membranes by which less unpolymerized aniline released in the PVDF casting solution resulted in a smaller pore sizes [4, 5].

5.1.2.3 Zeta potential measurement

Zeta potential measurement is an important factor to understand the interaction type between the membrane surface and the feed solution. Thus it affects the membrane fouling and rejection [6].

Zeta potential of the modified membranes was studied at pH 5.5 to investigate the surface charge of the membrane when using HA solution (pH 5.5). As shown in **Fig. 5.3** and in the previous chapter, the results of zeta potential measurements of pristine PVDF is -11.3 mV. With the

addition of PANI by *in-situ* method for PI-2, zeta potential decreased to be equal to -6.1 mV, while for a simple blended method for PANI addition; slightly higher zeta potential value –7.5 mV.

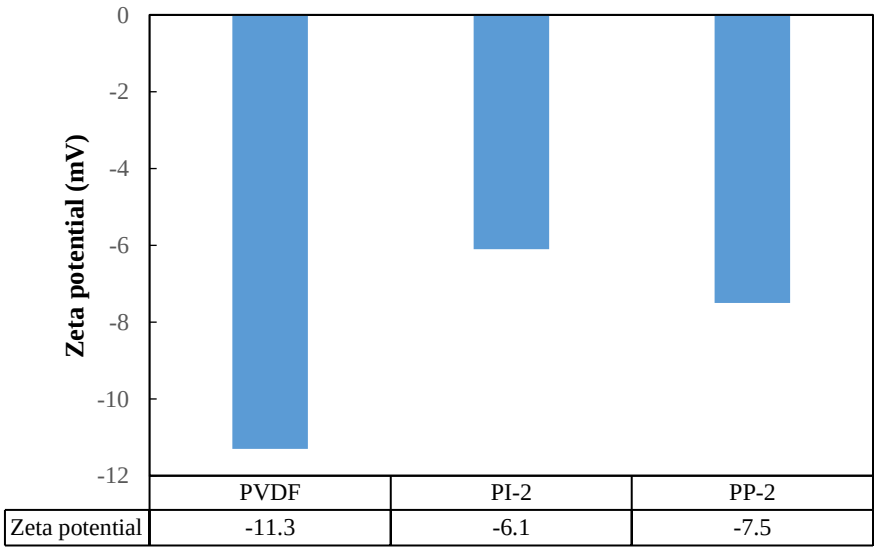

Fig.5.3 Zeta potential measurement of pristine PVDF, PI-2, and PP-2 at pH: 5.5.

HA is a negatively charged solution with zeta potential equal to -7 mV as shown in the previous chapter, and the membrane surface is negatively charged; Consequently, repulsion interactions [7] occur between HA and the surface of the modified membranes, with the expectation to decreased membrane fouling as going to be explained later.

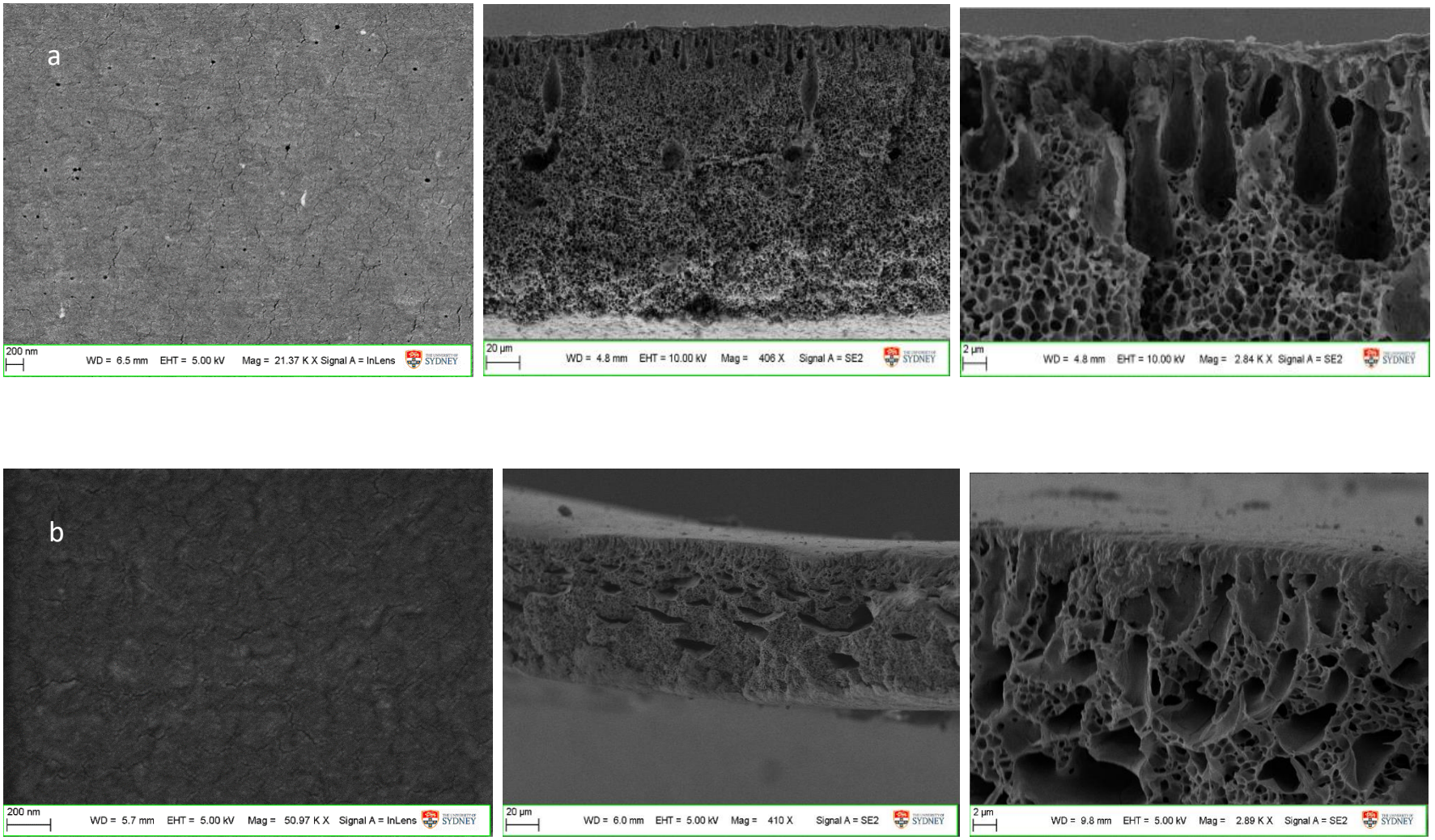

Fig. 5.4A. SEM images including top surface and the cross-sectional views at 20 µm and 2µm respectively with different compositions; (a) Pristine (b) PI-1.

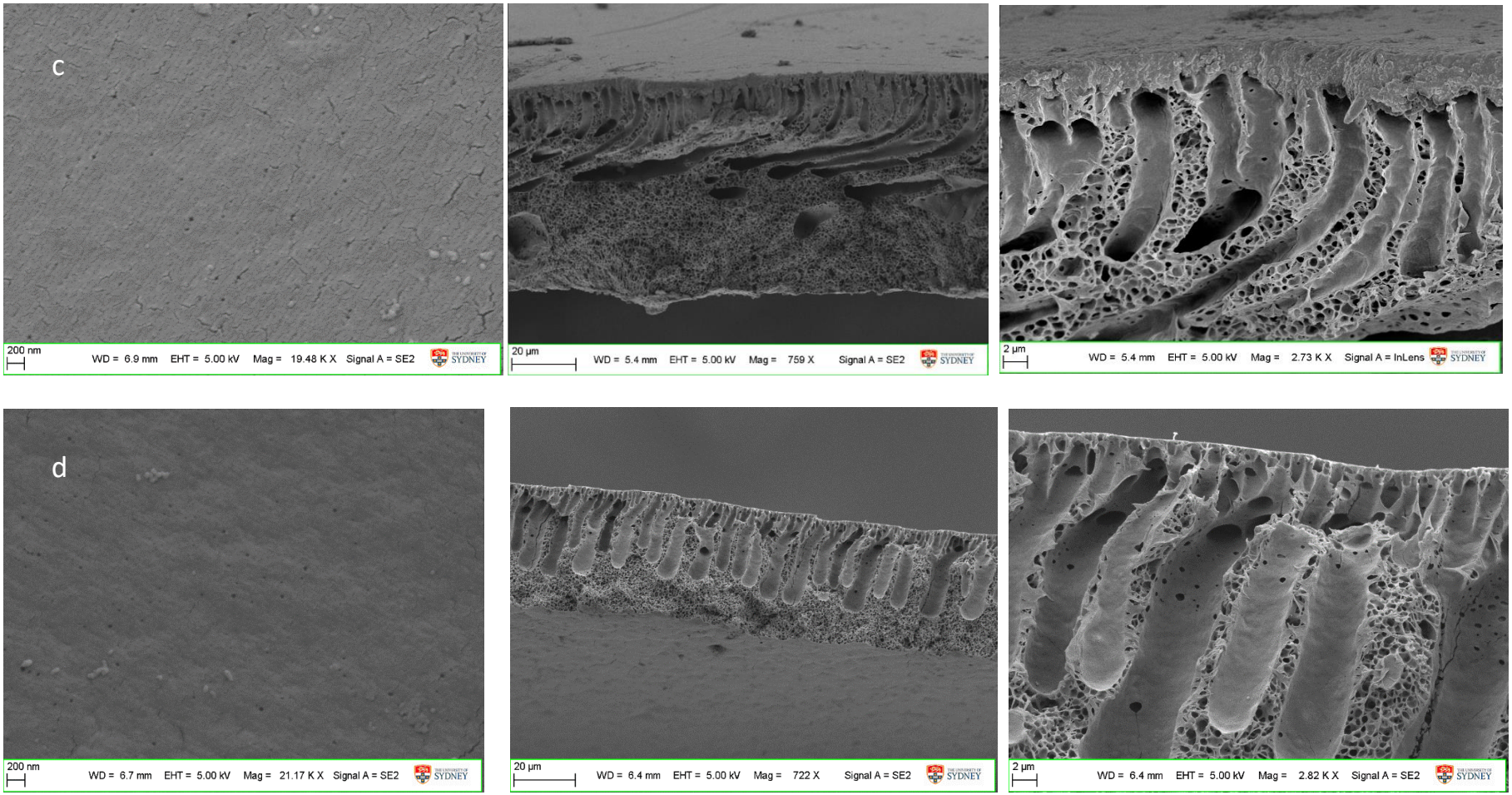

Fig. 5.4B. SEM images including top surface and the cross-sectional views at 20 µm and 2µm respectively with different PANI composition (c) PI-2. (d) PI-3

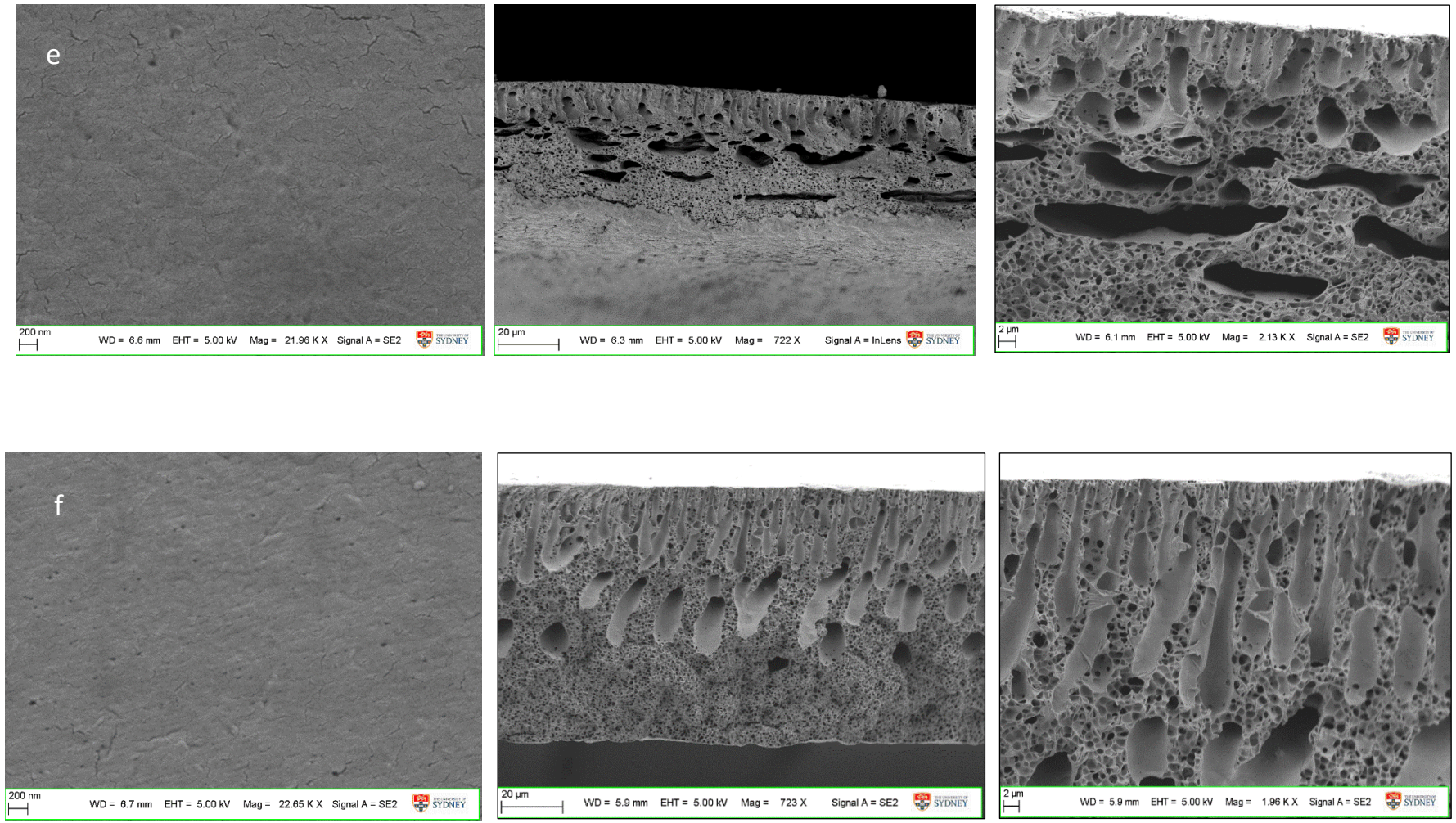

Fig. 5.4C. SEM images including top surface and the cross-sectional views at 20 µm and 2µm respectively, with different PANI composition (e) PP-1 (f) PP-2.

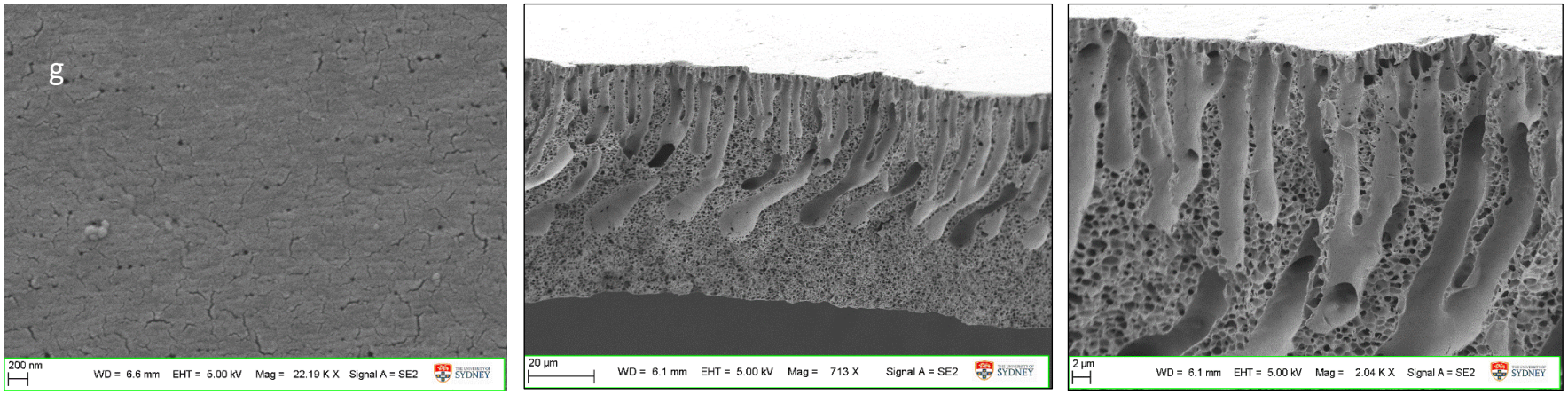

Fig.5.4D SEM images including the top surface and the cross-sectional views at 20 µm and 2µm respectively, with different PANI composition (g) PP-3.

5.1.2.4 Membrane morphology

As can be seen in **Fig. 5.4A, B** and **C;** the cross section images of the modified membranes show that all modified membranes exhibited asymmetric non-homogeneous structures with finger-like pores and cavities, probably due to the powerful interaction between the non-solvent (water) and the solvent (DMF) which affected the demixing process significantly and accelerated exchange rate [8, 9]. pristine PVDF showed shorter and smaller finger-like pores **Fig. 5.4** (a), however, with PANI addition to the PVDF matrix, it can be noticed that the finger-like pores size increased with macrovoids in the sub-layer **Fig. 5.4A**(b) and **Fig. 5.4C**(e). With further increase in PANI concentration, finger-like pores become longer and better vertically linked mostly for PI-3 and PP-3, resulting in easier water transfer through the membranes and increased water permeability. In comparison with pristine PVDF, the modified membrane showed larger pores under the top layer. These results could be attributed to PANI oligomers and PANI nanospheres migration during membrane fabrication which was advantageous to increase pore size, porosity, and the production of longer vertically-connected pores [4].

The addition of hydrophilic PANI accelerated the exchange phase inversion process between solvent and non-solvent; thus reduced the non-solvent tolerance and so the phase separation of the membrane surface happened at less polymer concentration, resulting in the formation of more pores, larger surface pore size, and larger pores below the skin layer [9, 10].

Furthermore, as can be seen in **Fig. 5.4B** (d) and **Fig. 5.4D (**g); *in-situ* polymerization method (PI) membranes showed a larger finger-like pores with a homogeneous distribution in comparison to PP membrane, which can be explained by the *in-situ* method, by which larger fraction of unpolymerized aniline and PANI released from the membrane structure during membrane formation in water bath, leading to larger pores formation in the PANI/PVDF membrane in comparison to simple PANI blended method by which less unpolymerized aniline released in the PVDF casting solution resulted in a smaller pore sizes [4].

Furthermore, PI membranes showed more uniform homogenized structure as shown in **Fig. 5.4B** (d) and **Fig. 5.4D (**g); results similar to that demonstrated by Bae et al. [11] who prepared Polystyrene with PANI by two blending methods *in-situ* polymerization and direct blending and revealed that *in-situ* polymerization method had a much better miscibility and homogeneous morphology.

5.1.3. PVDF/PANI mechanical properties

The mechanical properties of modified membranes were determined by tensile strength and elongation test at the point of breakage as shown in **Fig. 5.5** PANI/PVDF nanocomposite membranes showed higher tensile strength but with lower elongation in comparison to pristine PVDF membrane. As the amount of PANI additive increased the tensile strength increased from 1.3 for PP-1 to 1.65 MPa for PP-3 and from 1.37 for PI-1 membrane to 1.66 MPa for PI-3 membrane, as compared to 1.1 MPa for pristine PVDF.

This increment in tensile strength can be attributed to the PANI nanospheres and oligomers rigidity in the modified membranes. However, the elongations of blended membranes decreased with increasing PANI concentration from 34 % for PP-1 to 13.4 % for PP-3 as compared to 48 % for pristine PVDF; which is due to the reduction in flexibility of the modified membranes due to the hard structure resulted from PANI addition [4].

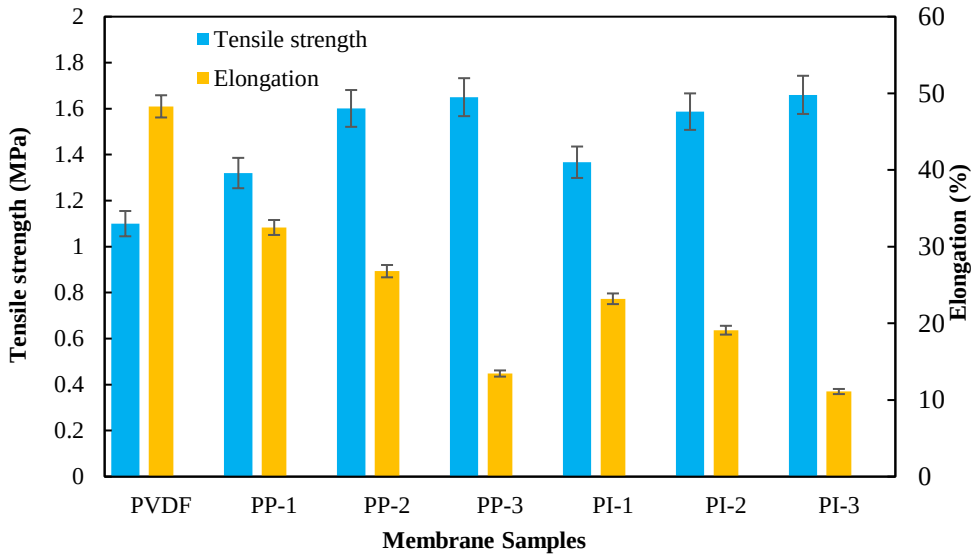

Fig. 5.5. Mechanical properties of pristine and modified PVDF membranes.

5.1.4. Membrane performance

5.1.4.1. Water permeability and rejection efficiency of membranes

The low water flux of pristine PVDF membrane is attributed to relatively small average pore size with small broad pore size distribution, low porosity and low hydrophilicity and so the lack of permeability. The permeate flux of water and HA rejection for PVDF/PANI modified membranes fabricated by both methods are improved in comparison to pristine PVDF membrane and the permeability increased with increasing the amount of PANI reaching 388 and 400 LMH/bar for PI-3 and PP-3 respectively which is about 13 times greater than the pristine PVDF membrane as showen in **Fig. 5.6**). This significant increase can be explained by the increase in surface hydrophilicity, increased porosity, longer and better linked finger-like pores and wider pores under the top layer of the modified membranes blended with hydrophilic PANI additive which not only increased the average surface pore size; due to the migration of PANI oligomers and nanospheres during membrane fabrication, but also increased the hydrophilicity of the membrane and speed up the phase inversion process [4].

Furthermore, the strong adsorption of water molecules and PANI reduced the binding force between water molecules, therefore few water clusters formed on the membrane surface which enabled to permeate quickly through the filtration process and enhance membrane water permeability [5, 12]. In literature Zhao, et al. [4] studied poly (sulfone) PS/PANI nanocomposite membrane by *in-situ* blending, and the results showed 300 LMH/bar (2-4 times faster water permeability than pure PS). Fan et al. [12] also studied PS/PANI membrane by blending PANI directly to PS, which resulted in water permeability 175 LMH/bar (1.6 times faster than PS).

HA rejection efficiency results for membranes are shown in **Fig. 5.7**. As the HA size (<1 nm) is much smaller than the pore size of PANI/PVDF modified membranes (4.6-7.7 nm), therefore, the separation of HA depends mainly on the interaction of membrane with feed [13].

Enhanced HA separation depends on the adsorption capacity of the membrane. As shown in zeta potential measurement PANI/PVDF is negatively membrane surface while HA is negatively charged due to carboxylic, phenolic group and carbonyls [14] and as measured previously (-7 mV). Therefore, an electrostatic repulsion between the membrane surface and the HA occur, however, a reduction in the membrane charge was shown with addition of PANI, and so the electrostatic repulsion decreased between the membrane surface and the HA, which allow HA to accumulate more densely on the membrane surface [15], thus increase HA adsorption on the membrane surface.

Furthermore, HA adsorption on the membrane surface enhanced by the steric hindrance of HA particles and the aggregation they formed on the membrane surface, because of their relatively large molecules [16, 17].

Maximum HA rejection was achieved in PP-1 membrane, with 75 % rejection and PI-1 membrane with 65%. It is noticed that with increasing PANI concentration the rejection efficiency decreased; where it reached 36% for PP-3 membrane and 32% for PI-3 membrane; this may be attributed to the bigger average pore size formed with high PANI concentration. Thus the permeability increased (according to Hagen-Poiseuille equation) and so reduced the contact time between the feed and the membrane surface, consequently, HA adsorption decreased [18].

Also, the membrane surface, which was covered with HA adsorption, may reduce more HA deposition due to the repulsion force of HA-HA. So HA adsorption decreased.

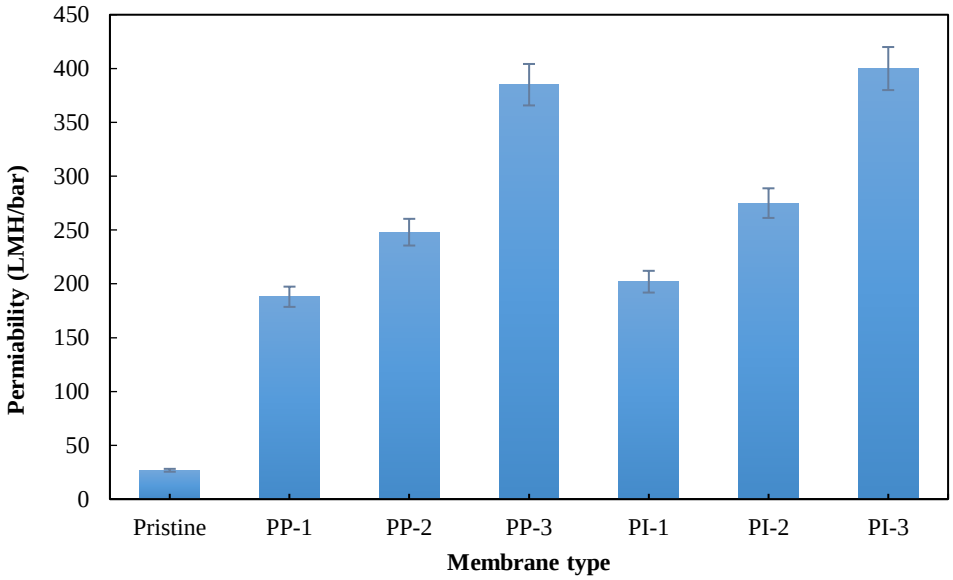

Fig. 5.6. Water permeability of pure and modified PVDF membranes.

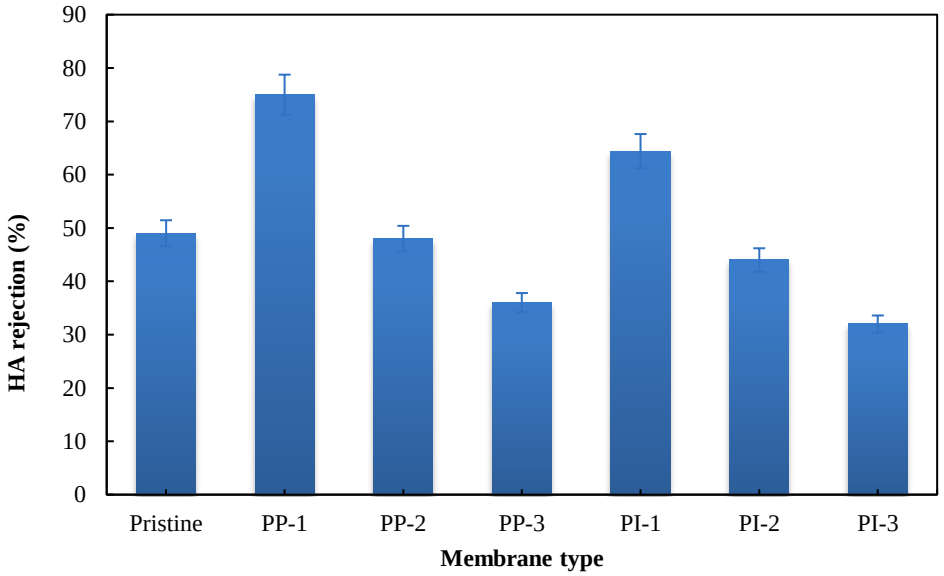

Fig. 5.7. Humic acid rejection for pure and modified PVDF membranes.

When the amount of PANI additives are similar, the permeate flux values of modified membranes showed more regularity for the membranes blended with *in-situ* polymerization method than simple blending method which suggests that *in-situ* polymerization method of PANI on PVDF is preferable to form larger pores and inner linked pores in the modified membranes, this also can be demonstrated by the cross-section SEM images showed in **Fig.**

5.4A, **B,** and **C** The longer and larger pore size of *in-situ* polymerization membranes are more evident in comparison to direct blending membranes as explained above.

5.1.5 Flux recovery after chemical cleaning

Flux decline behavior with HA and membrane proper cleaning method were examined. **Fig. 5.8** and **5.9** illustrate that modified membranes permeation of pure water and HA was much enhanced compared to the pristine PVDF; this is most likely due to the higher porosity and hydrophilicity, which reduced the resistance of the membrane to the water flux [5].

It can also be shown that there is considerable flux decline for PI-3 and PP-3 PANI/PVDF membranes with PI-3 **Fig. 5.8** (D) had the highest flux decline; which could be due to the larger average pore size, as larger pores probably allow HA to fill and block the pore more easily by pore adsorption (standard blocking model) [19] compared to smaller pore size, which leads to more significant flux decline as shown in**Fig. 5.8** and **5.9**, this results showed agreement with the results found by Li et al. [20]. Who studied the effect of membrane fouling with humic acid at different MWCOs, they suggested that membranes with larger MWCO had the highest flux decline in comparison with lower MWCO flux decline as shown in **Fig. 5.8** and **5.9** [4, 21].

(A)

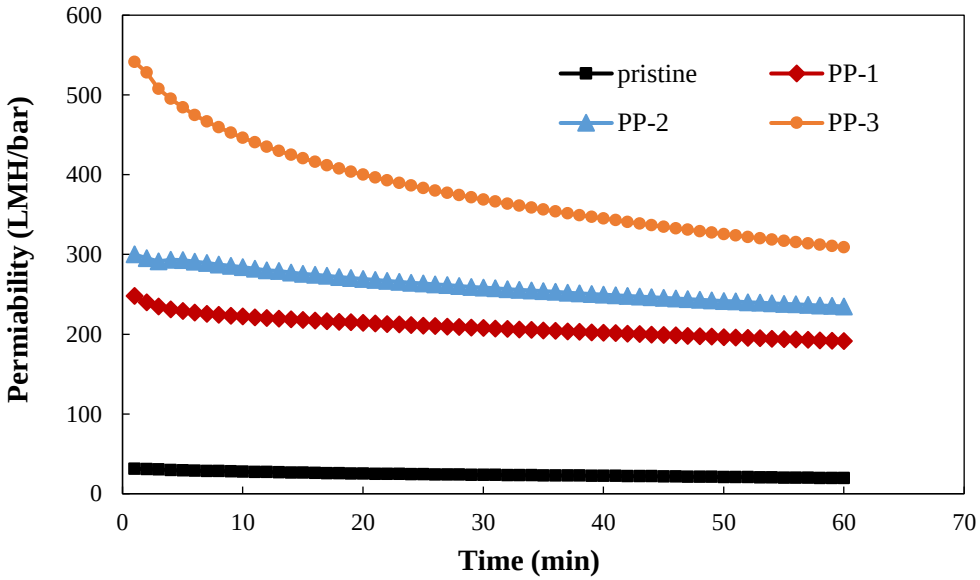

(B)

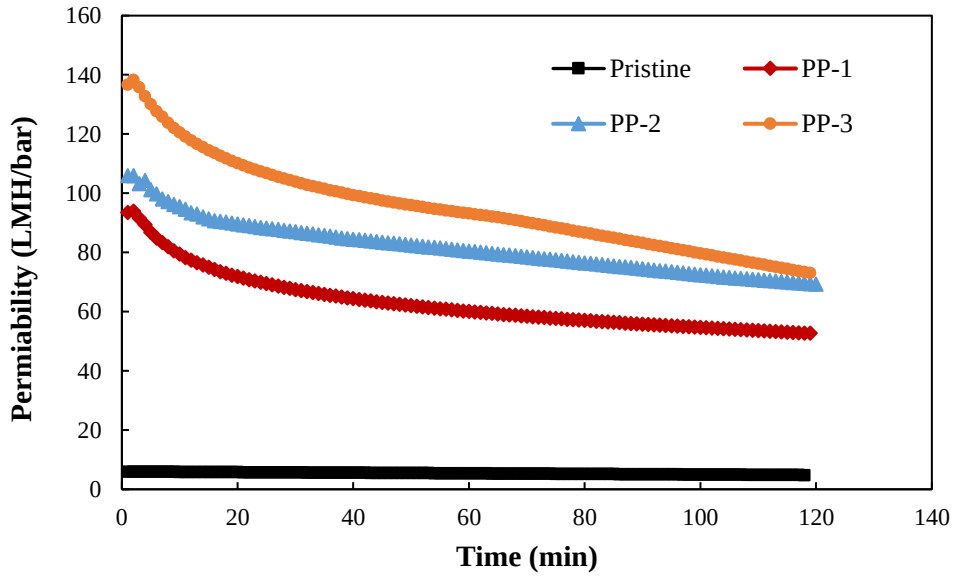

Fig. 5.8. Permeate flux for pristine and PP-(1, 2 and 3) modified membrane with (A) pure water then (B) HA solution.

(C)

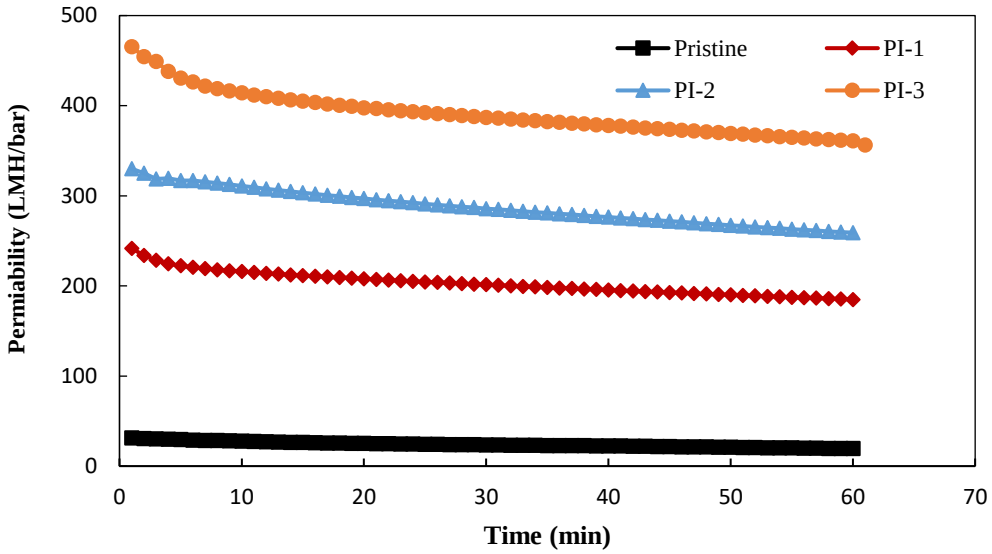

(D)

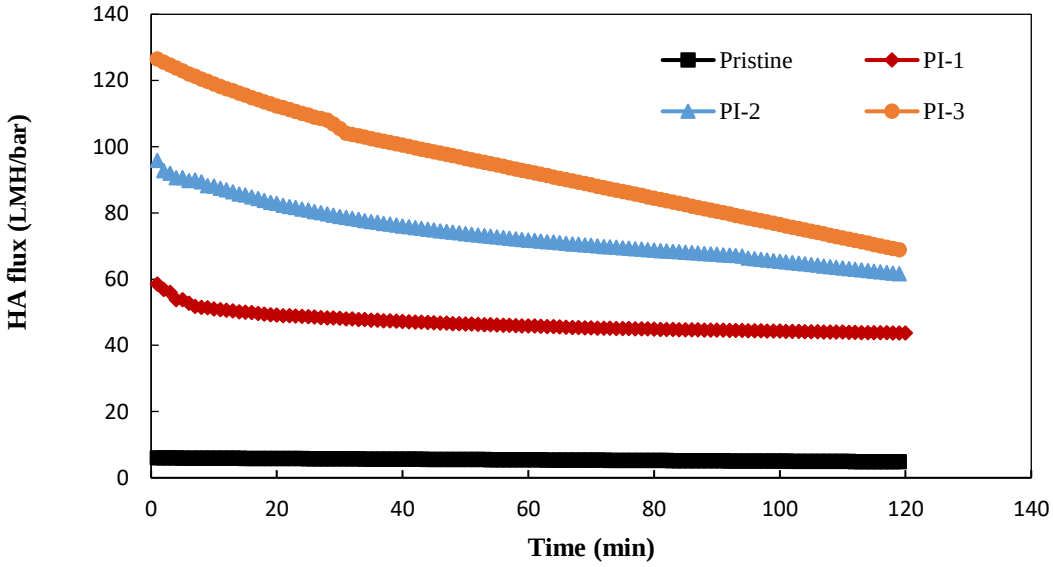

Fig. 5.9. Permeate flux for pristine and PI-(1, 2 and 3) modified membrane with (C) pure water then (D) HA solution.

All PANI/PVDF nanocomposite membranes showed higher flux recovery F_{Rw} and lower total fouling (R_t) in comparison with pristine PVDF.

This indicates that HA has a weak tendency to interact and adsorb on hydrophilic membrane surface resulted from hydrophilic PANI addition as the hydrophilic surface interacts tightly with water by hydrogen bond formation and also because of the negative charge of membrane surface which exhibits electrostatic repulsion to negatively charged HA molecules. So this lead to increase fouling resistance. This HA-modified surface weak interactions suggesting that total membrane fouling (R_t) is reduced and HA can be washed away easily with cleaning in acid and base as demonstrated in **Fig. 5.10**.

It is noticed that PP-3 and PI-3 membranes have slightly lower F_{Rw} values, and this is likely due to their large pore size which permits easier pores adsorption and blocking as previously explained.

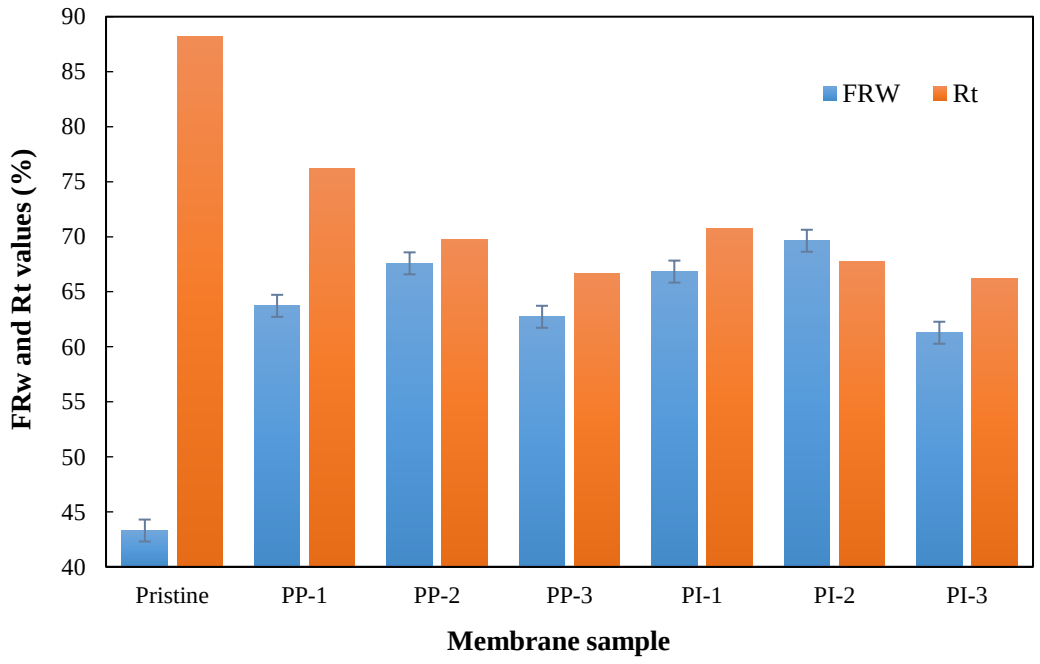

Fig. 5.10. Flux recovery ratio for pure and modified PVDF membranes.

5.2 Conclusion

PANI/PVDF ultrafiltration membranes were fabricated by two different blending methods of aniline using phase inversion technique. Greatly enhanced water permeability and antifouling properties were achieved. Water permeability of PANI /PVDF modified membranes was 7-16 times faster than pristine PVDF, with HA rejection ranged maximally from 78% for the PP-1 membrane to 32% for the PI-3 membrane. The effect of PANI on the performance of PVDF blended membrane was investigated.

The modified PANI/PVDF membranes showed higher porosity, hydrophilicity, and larger pore sizes. Cross-sectional structures of PANI/PVDF modified membranes showed larger pores under the top layer and longer finger-like pores with better vertically linked pores mostly seen for PI-3 and PP-3 membranes. PANI/PVDF membranes exhibited higher flux recovery after cleaning with acid and base and lower total fouling compared with pristine PVDF.

It can be concluded from the results that the *in-situ* polymerization blending method (PI) of PVDF/PANI contributed to the formation of membranes with larger pore sizes and more inter-linked finger-like pores, which resulted in higher water permeability and tensile strength in comparison to the membranes fabricated using the direct blending method (PP). For future studies, in-depth research of the addition of carbon nanotubes to further improve PVDF /PANI blended membranes will be carried out.

References

[1] Gregorio R., and Borges, D. S. (2008). Effect of crystallization rate on the formation of the polymorphs of solution cast poly (vinylidene fluoride). Polymer 49, 4009–4016.

[2] Merlini C. et al., (2015). Electrically Conductive Polyaniline-Coated Electrospun Poly (Vinylidene Fluoride) Mats. Frontiers in Materials, 2(February), pp.1–6.

[3] Khan R. et al., (2011). Spectroscopic, Kinetic Studies of Polyaniline-Flyash Composite. Advances in Chemical Engineering and Science, 01(02), pp.37–44.

[4] Zhao S. et al., (2011). PSf/PANI nanocomposite membrane prepared by *in situ* blending of PSf and PANI/NMP. Journal of Membrane Science, 376(1-2), pp.83–95.

[5] Jiang J.-H.et al., (2014). Improved hydrodynamic permeability and antifouling properties of poly (vinylidene fluoride) membranes using polydopamine nanoparticles as additives. Journal of Membrane Science, 457, pp.73–81.

[6] Salgin S., Salgı U., Soyer N., (2013). Streaming Potential Measurements of Polyethersulfone Ultrafiltration Membranes to Determine Salt Effects on Membrane Zeta Potential. Int. J. Electrochem. Sci, 8(2013), pp.4073–4084.

[7] Liu Charles et al., (2001). Membrane Chemical Cleaning: From Art to Science. American Water Works Association, pp. 1-25.

[8] Hilal N., Ismail F.A., Wright C., (2015). Membrane Fabrication. First edition, CRC Press, ISBN 1482210460.

[9] Liu F. et al., (2011). Progress in the production and modification of PVDF membranes. Journal of Membrane Science, 375(1-2), pp.1–27.

[10] Yang Y.N et al., (2008). The research of rheology and thermodynamics of organic–inorganic hybrid membrane during the membrane formation, J. Membr. Sci. 311, pp. 200–207.

[11] Bae W.J., Jo W.H., Park Y.H., (2003). Preparation of polystyrene/polyaniline blends by in situ polymerization technique and their morphology and electrical property. Synthetic Metals, 132(3), pp.239–244.

[12] Fan, Z. et al., 2008. Preparation and characterization of polyaniline/polysulfone nanocomposite ultrafiltration membrane. Journal of Membrane Science, 310(1-2), pp.402–408.

[13] Zularisam A.W. et al., (2007). The effects of natural organic matter (NOM) fractions on Fouling characteristics and flux recovery of ultrafiltration membranes, Desalination. 212, pp.191-208.

[14] Korshin G.V. et al., (1997). Monitoring the properties of natural organic matter through UV spectroscopy: A consistent theory. Water Res. 31, pp. 1787-1795.

[15] Gary L. Amy, (2001). NOM Rejection By, and Fouling Of, NF and UF Membranes. American Water Works Association, 2001 - Nanofiltration - 374 pages.

[16] Suhartono, Jono, and Chedly Tizaoui., (2015). Polyvinylidene Fluoride Membranes Impregnated at Optimised Content of Pristine and Functionalised Multi-Walled Carbon Nanotubes for Improved Water Permeation, Solute Rejection and Mechanical Properties. Separation and Purification Technology 154. Elsevier B.V., pp. 290–300.

[17] Teow, Y.H. et al., 2012. Preparation and characterization of PVDF/TiO2 mixed matrix membrane via in situ colloidal precipitation method. Desalination, 295(2012), pp.61–69.

[18] Lee, J. et al., (2016). High flux and high selectivity carbon nanotube composite membranes for natural organic matter removal. Separation and Purification Technology, 163, pp.109–119.

[19] Bowen W. R., Calvo J. I, Hernandez A., (1995). Steps of membrane blocking in flux decline during protein microfiltration. J. Membr. Sci., 101, pp. 153-165.

[20] Li C. W., Chen Y., (2004). Fouling of UF membrane by humic substance: Effects of molecular weight and powder-activated carbon (PAC) pre-treatment, Desalination 170, pp. 59-57.

[21] Amin, I.N.H.M. et al., 2010. Flux decline study during ultrafiltration of glycerin-rich fatty acid solutions. Journal of Membrane Science, 351(1-2), pp.75–86.

CHAPTER 6. Poly(vinylidene fluoride) / MWCNT/ Polyaniline Nanocomposite Ultrafiltration Membrane for natural organic matter removal

6.1 Results and discussions

6.1.1 Characterization of MWCNT/ PANI

6.1.1.1 MWCNT/PANI dispersion

In the membrane fabrication procedure, PANI stirred well with MWCNT and PVDF for 24 hr. in DMF, UV-Vis absorption measurements were used to test the dispersion of MWCNT/PANI compared to pristine MWCNT, and to characterize the interaction between PANI and MWCNT. The absorption spectra of MWCNT and PANI/MWCNT complex are shown in **Fig. 6.1**.

A charge-transfer complex formed between MWCNT and aniline; as aniline is good electron donor while CNT is good electron acceptor, a π-π interaction is occurred as evidenced by the UV-vis absorption spectra of MWCNT and MWCNT/PANI [1] **Fig. 6.1**.

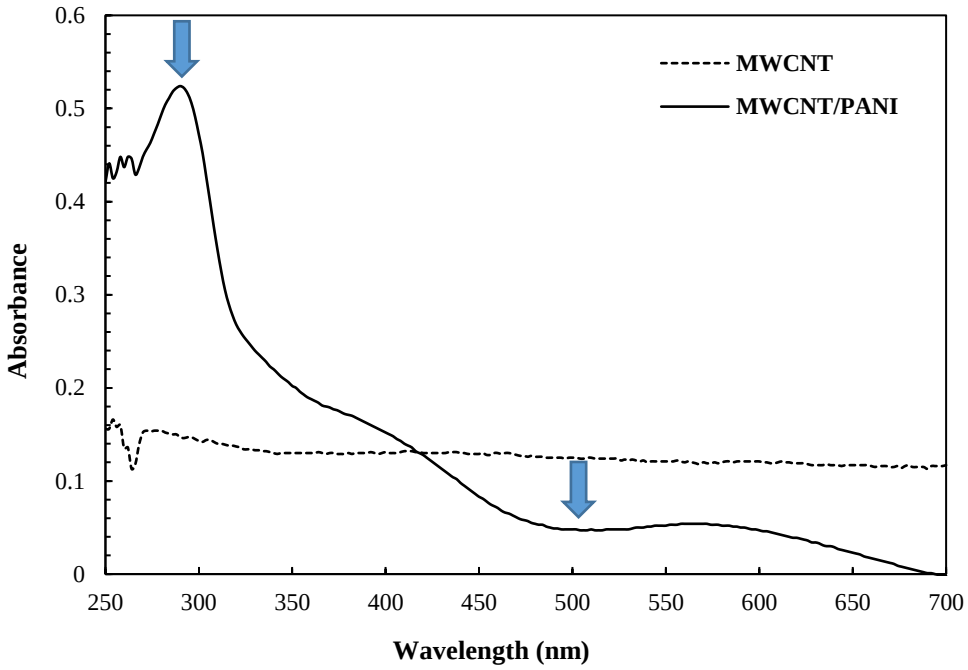

Fig. 6.1 UV- vis spectra of MWCNT and MWCNT/PANI composites.

In **Fig. 6.1** MWCNT/PANI showed new strong peak band at 290 and wide band at 508 indicating that the charge transfer of benzoid and quinoid excitation bands and suggesting the strong interaction between MWCNT and PANI as a charge transfer complex and a good compatibility between MWCNT and aniline. Which resulted in well-dispersed MWCNT within PVDF matrix (MWCNT/PANI enhance the dispersion of MWCNT). However for MWCNT in DMF solution, no characteristic absorption peaks were shown in range 250 - 700 nm [1, 2].

The dispersion status of MWCNT/PDA and MWCNT in DMF after 12 hrs. are shown in **Fig. 6.2**. MWCNT shows aggregation and settlement, while MWCNT/PDA stay dispersed over 12 hr.

Fig. 6.2. Photo of MWCNT/PANI and MWCNT in DMF mixtures showing the dispersion status with time.

To assure the dispersion of MWCNT by MWCNT/PANI complex, the dispersion of MWCNT in the PVDF membrane was observed by SEM. **Fig. 6.3** shows the SEM cross-sectional images in PVDF/MWCNT/PANI (PIC) membrane; the white arrows presented individual MWCNT particles, which is well dispersed and spread into PVDF matrix without agglomeration. Thus MWCNT/PANI enhances the dispersion of MWCNT in PVDF membrane by *in-situ* polymerization method.

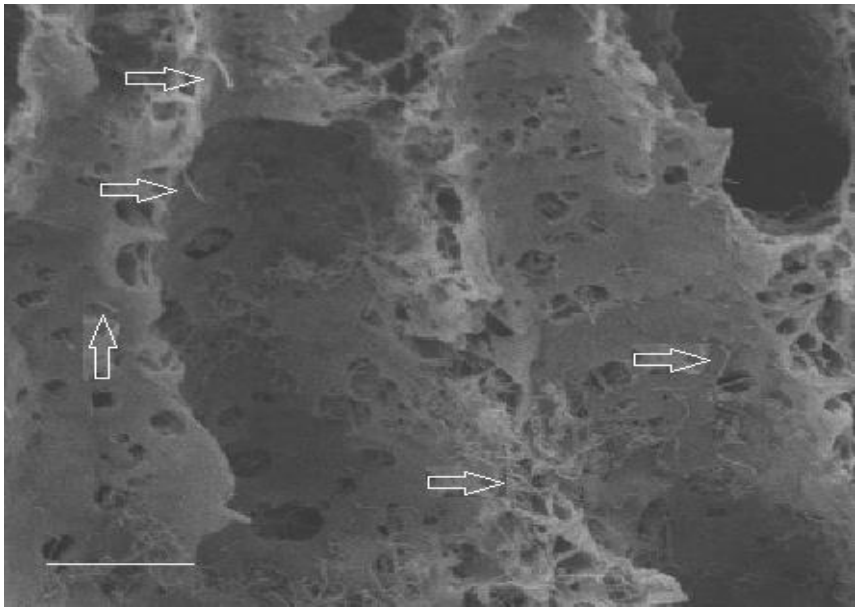

Fig. 6.3. SEM image for CNT dispersed in polymer matrix. (Arrows point to CNT particles dispersed in the membrane matrix). Scale bar: 2 µm.

6.1.2 Membrane surface and morphology

6.1.2.1 Hydrophilicity

Hydrophilicity of the modified membranes were determined by measuring Contact Angle (CA). Measurement results are illustrated in **Fig. 6.4** which shows that the CA for all MWCNT/PANI/PVDF (PIC) modified membranes is lower than pristine PVDF. The CA of pristine PVDF was 91^{o} and decreased with MWCNT/PANI complex addition to reaching 85^{o} in PIC- 0.25 (0.25 wt. % MWCNT) membrane. With increasing the comcentration of MWCNT inclusion in PVDF matrix, CA decreased further to minimum value and the highest hydrophilicity reaching 55^{o} for PIC-2 (2 wt. % MWCNT) indicating that hydrophilicity of the membranes surfaces increased as a result of modification with hydrophilic MWCNT in the form of MWCNT/PANI complex in the blended membranes. This hydrophilicity increase leads to enhancement in water permeability, as going to be discussed later in the next sections.

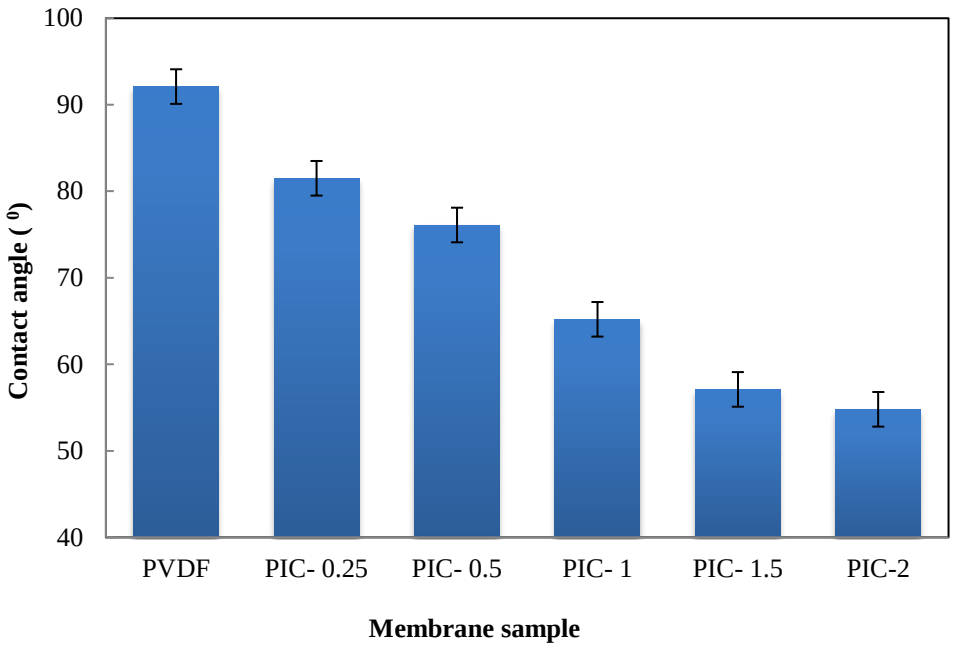

Fig. 6.4 Contact angle measurement for blended membranes.

6.1.2.2 Porosity and average pore size

The effect of MWCNT/PANI inclusion on the porosity and pore sizes of the fabricated membranes is illustrated in **Table 6.1**; all the fabricated membranes exhibited larger pore sizes and increased porosity in comparison to pristine PVDF.

From the results shown in **Table 6.1**; the porosity increased with the addition of MWCNT, the porosity of the fabricated membranes ranged from 84.7 % to 91.0%. In PIC-0.25 (0.25 wt. % MWCNT) membrane porosity increased by 14% compared to pristine PVDF. Further increase of MWCNT to 1.5% in PIC-1.5 resulted in the maximum porosity which reached 91%. This increase in the porosity can be attributed to MWCNT/PANI addition as they considered to be hydrophilic materials that accelerate the diffusion rate between non-solvent (water) and the solvent (DMF) exchange leading to the formation of the more porous structure resulting in an increase in porosity. Also, MWCNTs themselves are hollow materials, which result in the

formation of the new macro-voids porous structure as a consequence of the interaction of solid-liquid contacted in the polymer matrix [3, 4]. Therefore, and based on these results it is evident that modification of PVDF membrane with the addition of MWCNT/PANI complex is valuable to fabricate higher porosity membranes.

However, further addition MWCNT/PANI in PIC-2 membrane lead to a slight decrease in porosity; this may be due to the high concentration of MWCNT, which causes less MWCNT uniformity as a high concentration of MWCNT/PANI increased the viscosity of the mixture [5] which slow down the phase separation during membrane formation. Thus, the high viscosity casting solution reduces the water ability to get into the solution and so delay the demixing process resulting in a denser top layer with low porous membrane and fewer macrovoids pores [3, 4].

Table 6.1 Porosity and average pore size of the modified membrane.

Membrane type	Porosity (%)	Mean pore size (nm)
Pristine	70.4	4.3
PIC-0.25	84.7	4.8
PIC-0.5	87.1	6.3
PIC-1	90.6	7.4
PIC-1.5	91.0	5.3
PIC-2	88.4	4.7

The average pore sizes of all membranes were determined by BET, see the Appendix. The average pore size found to be in the range of 4.8 to 7.4 nm as shown in **Table 6.1**. The fabricated membranes pore sizes tend to increase with increase concentration of MWCNT/PANI; all the

modified membranes showed larger pore size in comparison to pristine PVDF. As the concentration of MWCNT/PANI increased the average pore size increased simultaneously to reach the maximum at 1% wt. MWCNT in PIC-1 (7.4 nm compared to 4.3 in pristine PVDF). With increase the MWCNT/PANI weight concentration more, this lead to a decrease in the average pore size to 5.3 nm for PIC-1.5, and 4.7 for PIC-2. Adding the hydrophilic MWCNT/PANI accelerate the diffusion rate between non-solvent (water) and the solvent (DMF) and so forming a more porous layer with bigger pores. But with the further increase, the viscosity of the casting solution increased and so delayed the diffusion rate resulting in a smaller average pore size [3, 4].

Many studies reported similar trend when adding nanomaterials to the polymer matrix [5, 6].

6.1.2.3 Zeta potential measurements

Measuring electrokinetic properties of the membrane such as Zeta potential is considered valuable to understand the interactions between the membrane surface and the solution in contact with the membrane as it has a significant effect on the membrane rejection and fouling performances. Zeta potential of the modified membranes was studied at pH 5.5. As shown in **Fig. 6.5**, the results of zeta potential measurements stated that pristine PVDF has a negative surface charge equal to -10.3 mV, with PANI addition to PVDF membrane, zeta potential value reduced to -6.1 mV. While with the addition of MWCNT to the membrane, zeta potential showed a positive charge membrane surface equal to + 12.3 mV.

The interaction between PANI and MWCNT resulted in dopant effect. Doping is a unique process in conducting polymers in which polymers are transforming to its conductive form by chemical oxidation, during the doping process, positive or negative charge are developed in the polymer by the effect of doping agent like chemical oxidants [7, 8]. Thus, the doping effect (chemical oxidation) of MWCNT/PANI complex during the membrane synthesis resulted in

changing the surface charge of MWCNT/PANI complex to be positively charged. Positively charged MWCNT/PANI complex converted negatively charged pristine PVDF membrane to the positively charged membrane. So as can be seen in **Fig. 6.3** by inclusion MWCNT/PANI complex, the zeta potential of the membrane surface became positive.

HA is a negatively charged solution with zeta potential equal to -7 mV; consequently, electrostatic interactions [9] occur between HA and the surface of the modified membranes, which result in more HA adsorption on the modified membrane surface; leading to enhanced HA rejection (about 37 %) higher than pristine PVDF membrane.

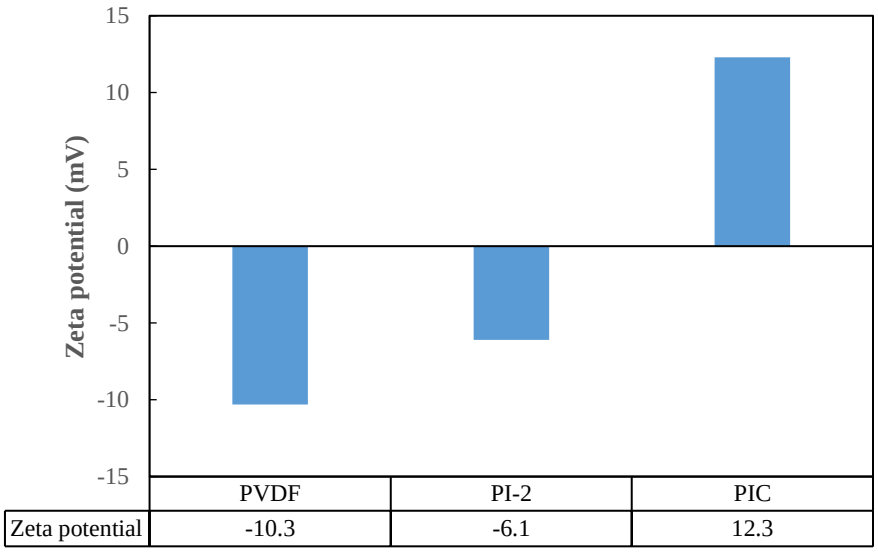

Fig. 6.5 Zeta potential of pristine PVDF, PI, and PIC-2.

6.1.2.4 Membrane morphology

The top surface and the cross sections of the fabricated membranes are shown in **Fig. 6.6A, B, and C**; the modified PVDF membranes showed larger surface pore size and finger-like structure compared with pristine PVDF membrane which is related to improved water permeability of the modified membranes.

MWCNT/PANI/PVDF (PIC) membranes showed asymmetric finger-like pores with large voids and cavities. Modified membranes formed smaller pores on the top layer connected to larger pores in the underneath layer structure, this resulted in higher water permeation and HA rejection [5].

The inclusion of hydrophilic MWCNT/PANI complex accelerates the diffusion rate between non-solvent (water) and the solvent (DMF) and so forming a more porous layer with bigger pores [4]. Increasing the concentration of MWCNT/PANI increased the pore size (as shown previously), and the width of the finger-like structure as can be seen in **Fig. 6.6A** (b) and **Fig. 6.6B** (c, d), however, with the further increase, the viscosity of the casting solution increased, and so delayed the diffusion rate resulting in a smaller average pore size and finger-like structure as shown in **Fig. 6.6C** (e, f) [3]. These results agree with studies reported by Ma et al. [3, 4].

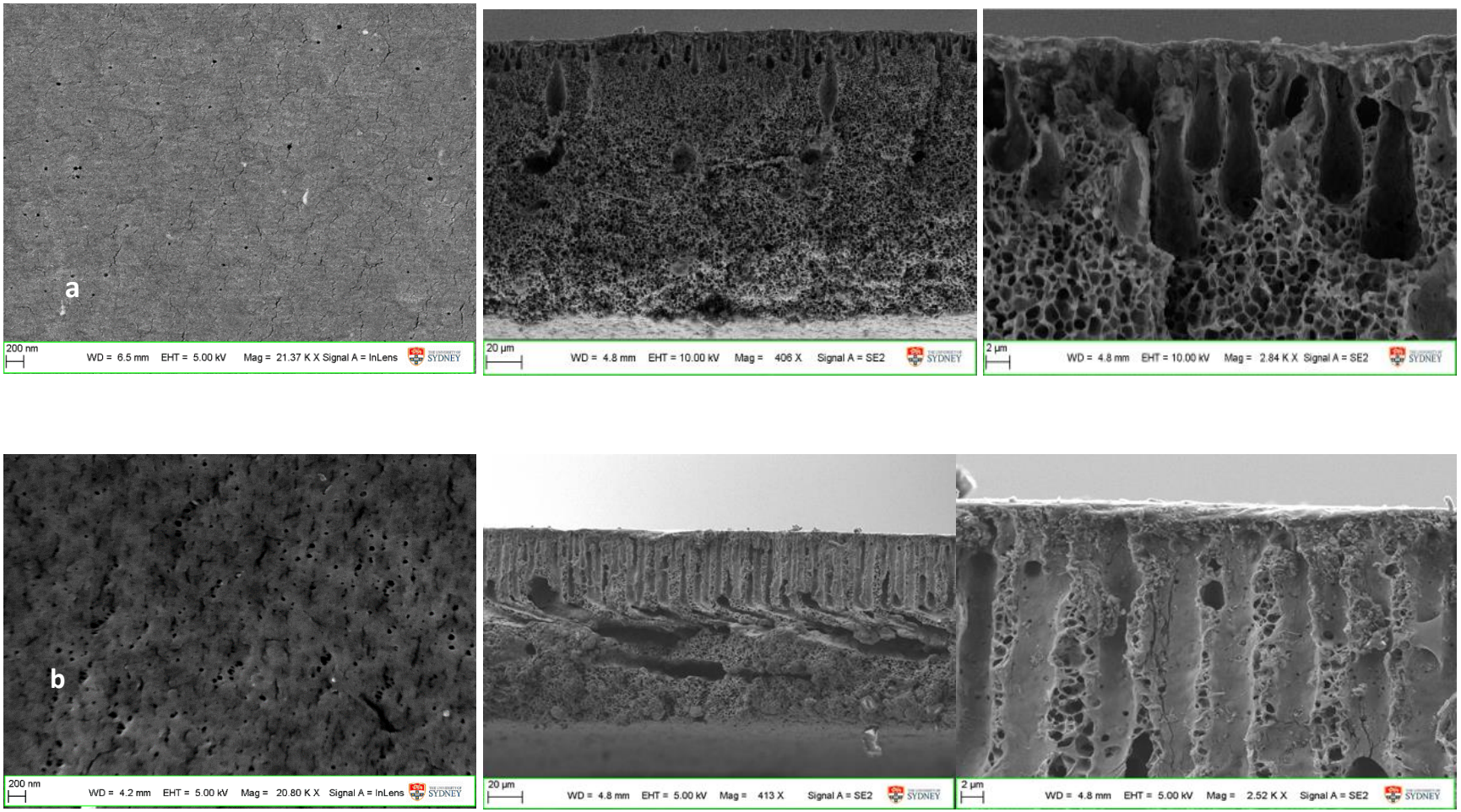

Fig. 6.6A. SEM images of the top surface and the cross-sectional views at 20 µm and 2µm respectively of the blended membranes with different compositions; (a) pristine, (b) PIC-0.25.

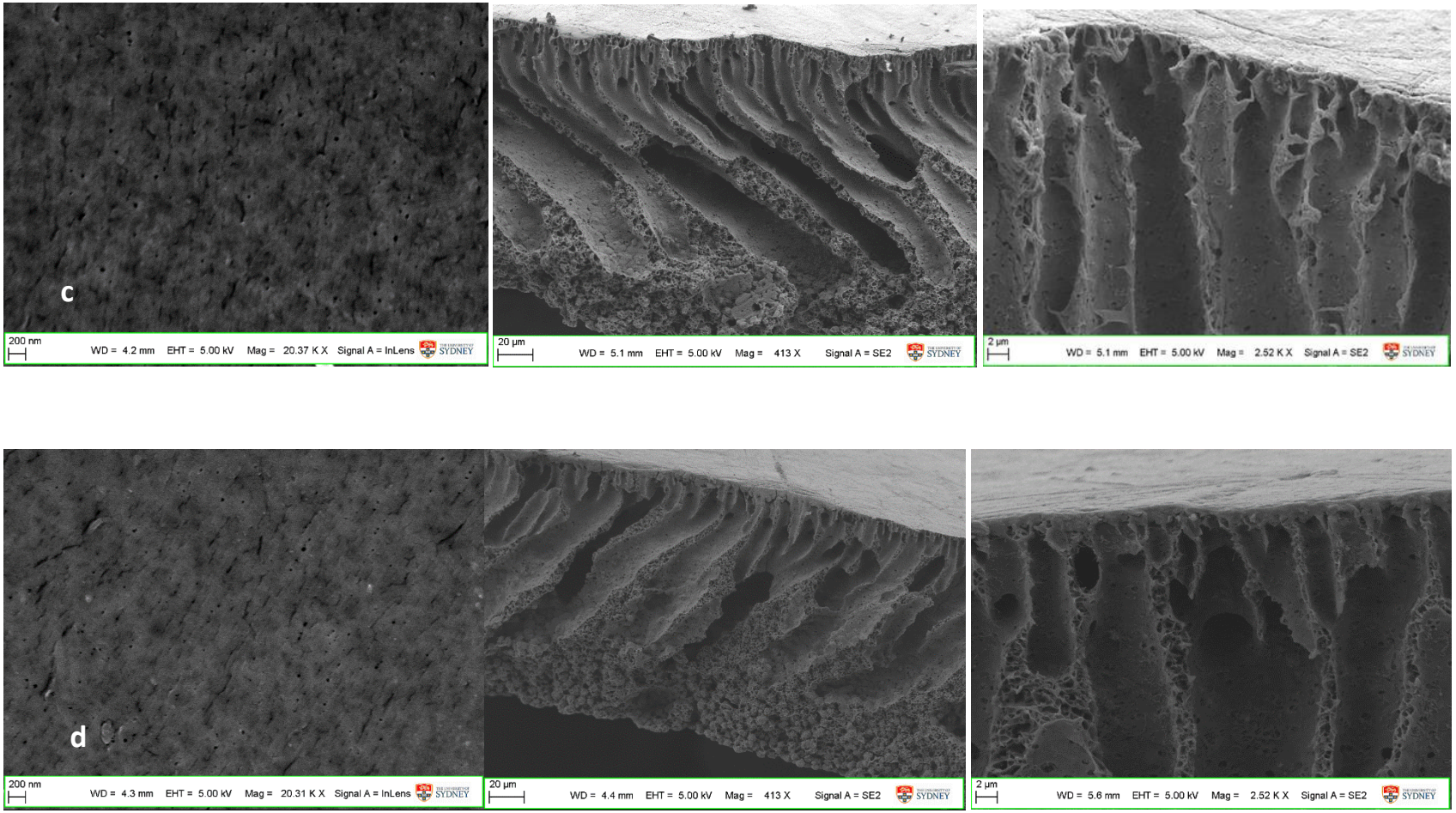

Fig. 6.6B. SEM images of the top surface and the cross-sectional views at 20 µm and 2µm respectively of the blended membranes with different compositions; (c) PIC-0.5, (d) PIC-1.

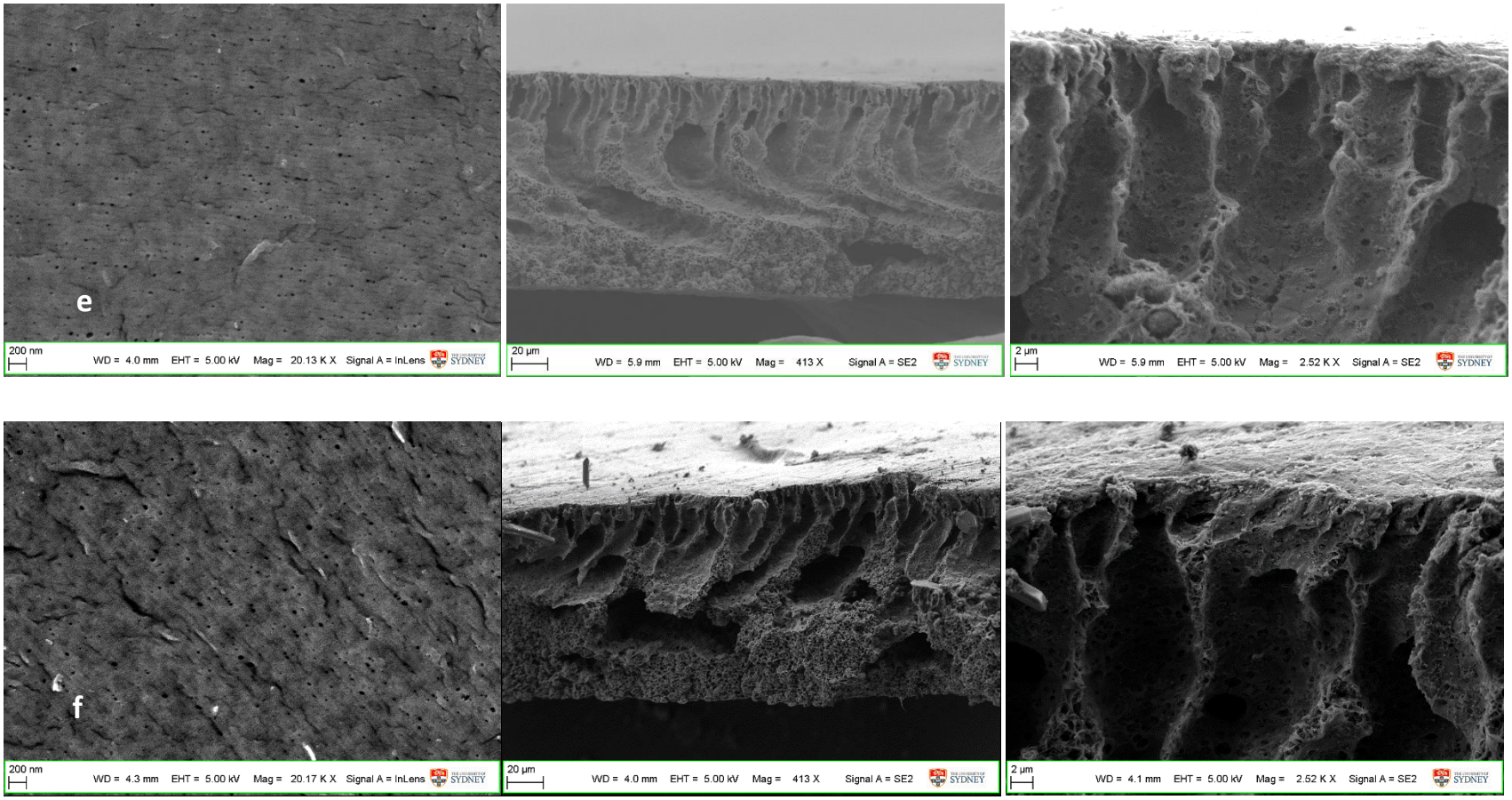

Fig. 6.6C. SEM images of the top surface and the cross-sectional views at 20 µm and 2µm respectively of the blended membranes with different compositions; (e) PIC-1.5, (f) PIC-2.

6.1.3 PVDF/MWCNT/PANI mechanical properties

Tensile strength and elongation at the point of breakage test were performed, and the results are shown in **Fig. 6.7** The modified PVDF/MWCNT/PANI nanocomposite membranes showed higher tensile strength in comparison to pristine PVDF membrane. As the concentration of MWCNT additive increased the tensile strength increased (1.1 MPa for pristine PVDF compared to a maximum of 2.1 MPa for PIC-1.5). This increase in tensile strength of modified PVDF membranes can be attributed to MWCNT's inclusion, as MWCNTs considered to be one of the stiffest and strongest materials [10]. Thus, promising in the strengthening membranes and formation of composite materials with desired mechanical properties.

On the other hand, with further MWCNT increase tensile strength slightly decreased to 1.9 for PIC-2, this may be due to aggregation occur as a result of increased MWCNT concentration and hence accelerates the break of the membrane [3]. However, elongation at break for modified PVDF membranes decreased with increasing MWCNT's concentration from 48% for pristine PVDF to 35% for PIC-2; likely due to the high rigidity of the membranes and as a result of large finger-like pores and cavities appeared [3].

In conclusion, MWCNT/PANI addition relatively enhanced the mechanical strength of the modified membranes.

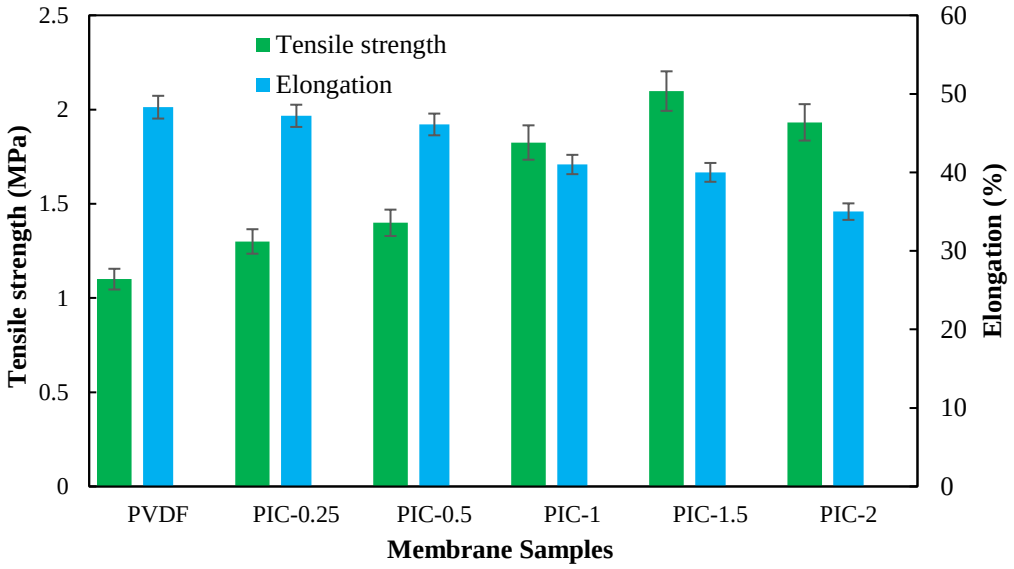

Fig.6.7 Mechanical properties: tensile strength, and elongation, of pristine PVDF and the modified membranes.

6.1.4 Membrane performance

6.1.4.1 Water permeability

The results of pure water permeability of different membranes are presented in **Fig. 6.8 and 6.9**. The inclusion of CNT as MWCNT/PANI complex in the polymer matrix highly enhanced the fabricated membrane performance for water permeability. **Fig. 6.8** showed a general comparison between pristine PVDF, 1 wt. % MWCNT/PVDF (P-CN), PANI/PVDF (PI) and 1 wt. % MWCNT/PANI/PVDF (PIC-1) membranes.

Pristine PVDF showed the lowest permeability results among membranes with 30 LMH/bar as expected because it has the smallest average pore sizes, lower porosity, and hydrophilicity relatively. For PI membrane water permeability reached 275 LMH/bar; 9 times greater compared with pristine PVDF membrane, this attributed to PANI oligomers and nanospheres migration during membrane fabrication which increases the pore sizes as explained in the previous chapter 5. It can also be noticed that simple blending method used in case of 1% MWCNT for P-CN membrane preparation affected the results and leads to low permeability

(107 LMH/bar) compared to the excellent results of 1% MWCNT in PIC-1 (1000 LMH/bar) prepared by *in situ* polymerization; this is possibly due to aggregation and low MWCNT dispersion in P-CN, which lead to less porosity and more blocked pores in the membrane compared to PIC-1. While PIC-1 succeeds in overcoming aggregation with MWCNT/PANI homogenous dispersion and presented with the highest water permeability results among the four membranes presented.

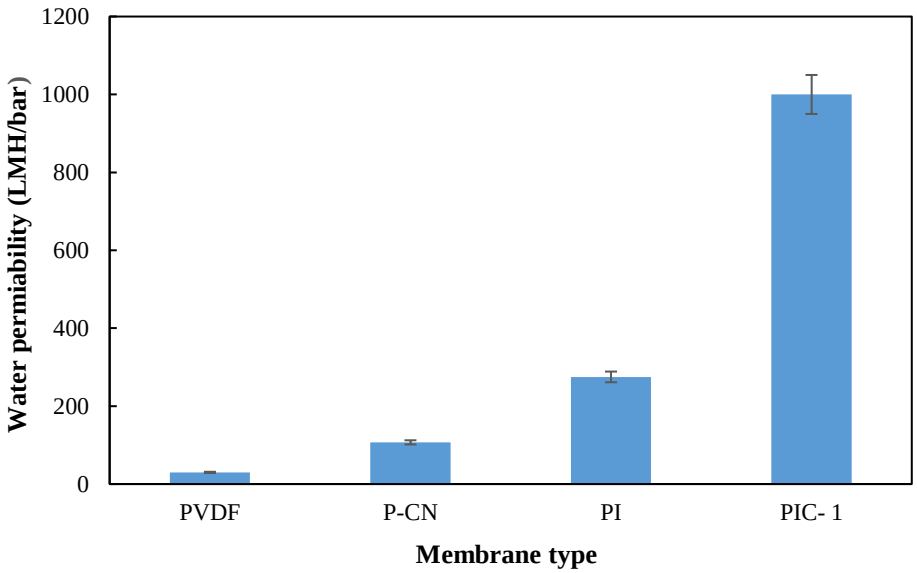

Fig. 6.8 Water permeability for pristine PVDF, P-CN simple blended 1% CNT with PVDF, PI Membrane fabricated by *in-situ* polymerization of PANI/PVDF, PIC-1 Membrane fabricated by in-situ polymerization of PANI/ 1% MWCNT/PVDF.

Fig. 6.9 showed a comparison between different MWCNT concentrations fabricated membranes permeability. As shown in **Fig. 6.9,** with the incorporation of 0.25 wt. % MWCNT for the PIC-0.25 membrane, the permeability increased to 344 LMH/bar, when MWCNT increased to 1wt. % for PIC-1, the permeability continued to rise to reach 1000LMH/bar (28 times more permeable than pristine PVDF). With the further increase to 1.5 % MWCNT for PIC-1.5, water permeability reached the maximum value of 1320 LMH/bar (35 times increase in permeability compared to pristine PVDF). This trend of

permeability results is consistent with the membrane porosity results explained in the previous section, as larger porosity decreases the hydraulic resistance and hence improves the permeate flux. Moreover, MWCNT/PANI complex addition increased the hydrophilicity of the fabricated membranes (**Fig. 6.2**) and consequently improved the water permeability.

The inclusion of MWCNT/PANI complex in the PVDF matrix formed a more porous area with well-developed finger like smaller pores on the top layer connected with larger pores in the lower structure of the membrane. The inclusion of hydrophilic MWCNT/PANI accelerates the diffusion rate between non-solvent (water) and the solvent (DMF) and so leads to the formation of the more porous layer and increase porosity [5, 11]. As shown in **Table 6.1**, by increasing MWCNT, the average pore size and porosity increased and hence water permeability also increased as (according to Hagen Poiseulle equation which stated that increased average pore size would lead to flux increase) [11].

However, with more MWCNT inclusion to 1.5 - 2 wt. % MWCNT in PIC-1.5 and PIC-2 membranes respectively, the viscosity of the casting solution increased which delay the exchange between solvent and nonsolvent with a relatively dense top layer and smaller pore size resultant membrane.

Although PIC-1.5 and PIC-2 membranes have the smallest pore size, their water permeability exceeded the other modified membranes **Fig. 6.8**, this is probably as a result of their high hydrophilicity which control water flux (**Fig. 6.2**), as mentioned before with high hydrophilicity water molecules preferentially adsorbed inside membrane pores surface with less interaction making their passage through the membrane easier and so increased water permeability [12].Within the MWCNT range used in this work 1.5 wt. % MWCNT used in PIC-1.5 membrane appears to be the optimal concentration that produces the highest membrane permeability results.

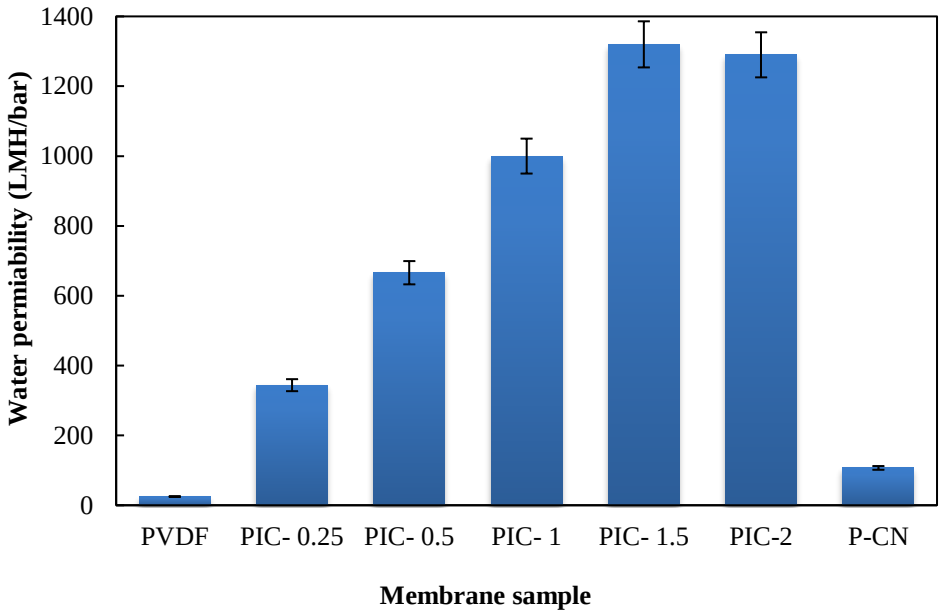

Fig. 6. 9 Effect of MWCNT concentration as MWCNT/PANI on water permeability.

6.1.4.2 HA rejection efficiency

As can be seen in **Fig. 6.10** which demonstrates a general comparison between pristine PVDF, 1% MWCNT/PVDF (P-CN), PANI/PVDF (PI) and MWCNT/PANI/PVDF (PIC-1) membranes, P-CN membrane showed the lowest HA rejection among the four membranes, which equal to 30 %. This low rejection may be due to agglomeration and low dispersion of MWCNT on the membrane surface. As the adsorption of HA governed by the high surface area of MWCNT [13], consequently, the simple blended MWCNT/PVDF membrane was less effective in increase the adsorption ability of MWCNT [14] compared to PIC-1 which shows significant improvement in HA removal reached up to 76%.

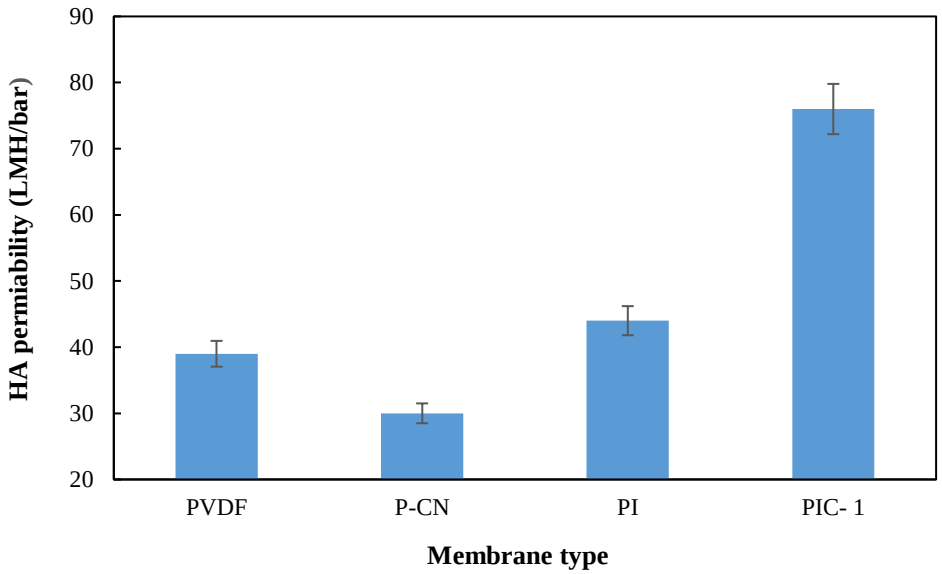

Fig. 6.10. HA permeability for pristine PVDF, P-CN simple blended 1% CNT with PVDF, PI membrane fabricated by *in-situ* polymerization of PANI/PVDF, PIC-1 membrane fabricated by in-situ polymerization of PANI/ 1% MWCNT/PVDF.

Fig. 6.11 presents HA rejection efficiency at different MWCNT concentration. It can be noticed that HA rejection increased gradually with the rise of MWCNT concentration in the modified membranes; for 0.25 wt. % MWCT in PIC-0.25 membrane HA rejection increased by 7.2 % compared to pristine PVDF membrane. Increasing the concentration of MWCNT/PANI to 1.5 wt. % in PIC-1.5 membrane showed HA rejection rise to 79 %. On the other hand, when the concentration of MWCNT reached 2 wt. % in PIC-2 membrane the rejection slightly increased to 81 %; due to the high concentration of MWCNT, the viscosity increased and this slowed down the exchange between solvent and non-solvent, resulting in a formation of the membrane with smaller pores [3].

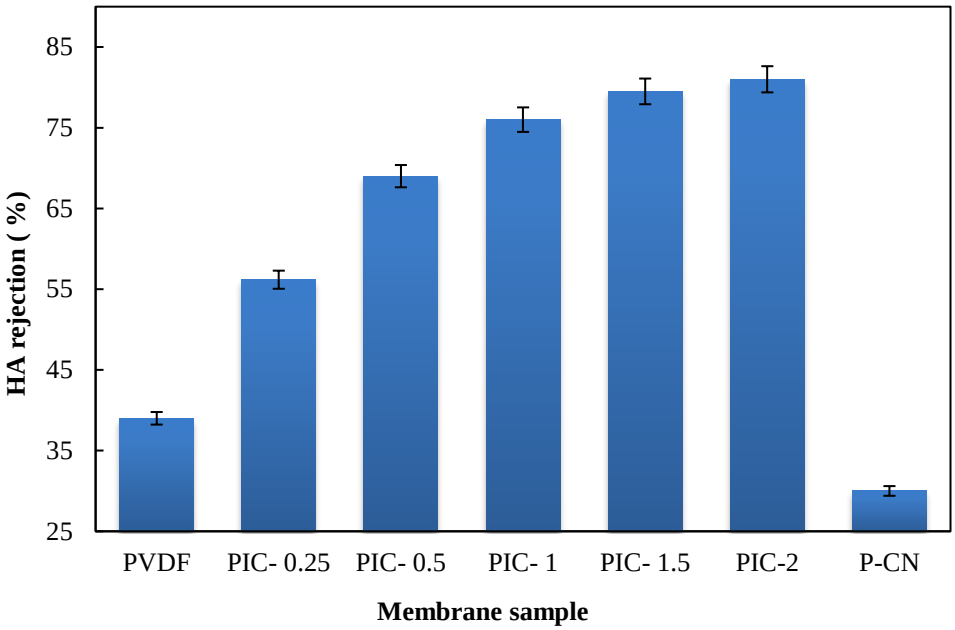

Fig. 6.11. Effect of MWCNT concentration as MWCNT/PANI on HA rejection

HA removal mechanism depends on two factors; the first is the average pore size of the membrane, the second is the adsorption of HA on the membrane surface. In our case and as a result of the fact that the HA molecule sizes are less than the modified membrane average pore size; (HA size is less than 1 nm and the modified membranes measured pore size are between (4.8-7 nm)). Thus the separation of HA is primarily dependent on the adsorption mechanisms [15]. HA rejection efficiency results for all membranes are shown in **Fig. 6.10 and 6.11**.

HA rejection is mainly governed by the interaction of membrane with feed, basically adsorption of HA on the membrane surface. HA is negatively charged molecules (contains mainly carboxylic groups and phenolic hydroxyl groups with a zeta potential of -7 mV at pH 5.5), and the membrane surface is positively charged as found by zeta potential measurements (with +12.3 mV at pH 5.5), as shown in **Fig. 6.5)**. Consequently, an electrostatic interaction occurs between HA and the membrane surface causing adsorption of HA molecules to the membrane surfaces leading to increasing in HA removal by the modified membranes in comparison to the pristine negative zeta potential of PVDF membrane (-10.3 mV at pH 5.5) [13].

In addition to the electrostatic interaction, MWCNTs considered having high adsorption capacity to organic matters which is mainly due to the π-π bonds between bulk π system on MWCNT surfaces and the HA molecules [16]. Su and Lu [17] suggested that the higher NOM adsorption on MWCNT is due to the larger surface area and volume.

According to constant pressure filtration laws [18], the adsorption of HA on the membrane surfaces depends on the pore size of the membrane, when the particle size is less than the membrane average pore size as in our study where HA particles less than membrane average pore size; thus a standard blocking model or blocking cake layer on the membrane surface [19, 20], consequently leading to flux decline.

Fig. 6.12 showed the pure water permeability of all modified membrane with time, in comparison of **Fig. 6.13** which showed the flux decline of HA rejection with time. Similar results concluded by Jucker and Clark [21] who suggested that the membrane pores are the preferable place for organic adsorption, this would demonstrate the severe flux decline of NOM fouling.

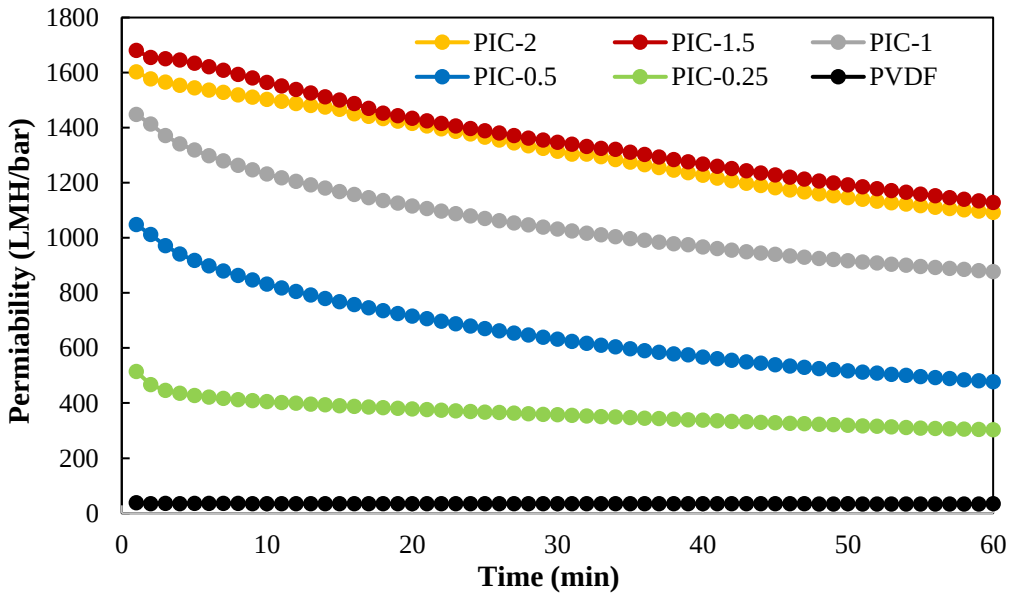

Fig. 6.12. Permeate flux for pristine and modified membranes PIC with pure water.

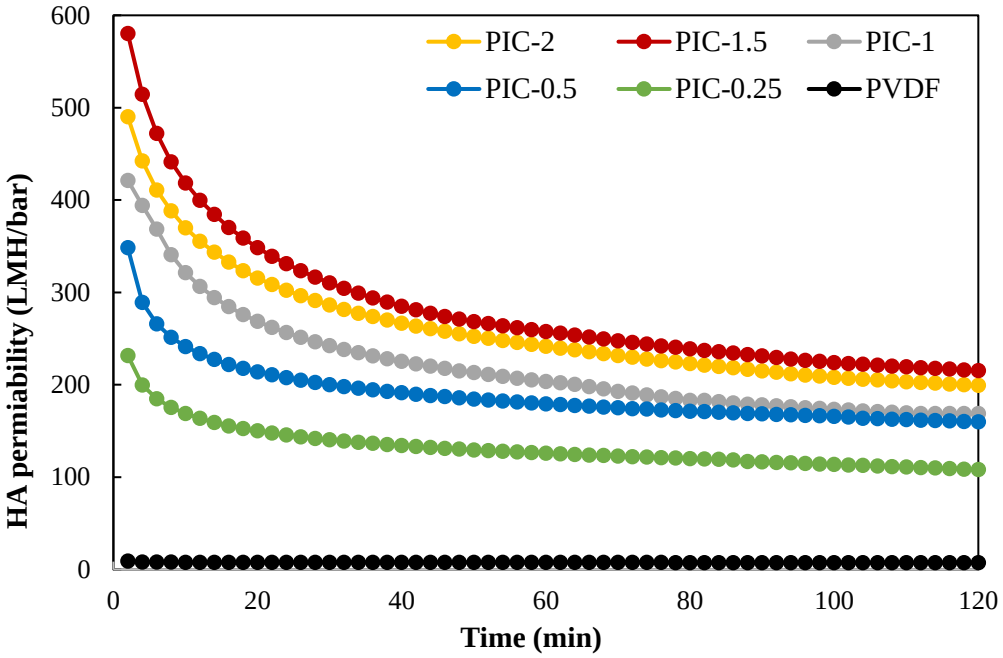

Fig. 6.13. Permeate flux for pristine and modified membranes PIC with HA solution.

Filtration test cycles were run for PIC-1.5 membrane about 350 min. The results are shown in **Fig. 6.14**, HA rejection efficiency was measured every 60 min, and the membrane was chemically washed every 120 min and then used. Results revealed that while flux declined, HA acid removal efficiency slightly decreased with cycle time, which suggests that HA adsorption on the membrane surface has not reached its capacity. Thus, the adsorptive properties of MWCNT/PANI enhanced HA removal with the high capacity membrane surface which might be due to the increased hydrophilicity of membrane surface and internal pores [22].

Flux decline is due to fouling of the membrane by shrinkage of the membrane pores and cake formation. It is noted that the increase in the membrane thickness caused by HA deposition on the membrane surface; which can be hydraulically considered to be an increase in thickness of a clean membrane with a low flux of HA [13, 23]. Therefore, even if the adsorption reached its capacity, the rejection decreased slightly with time.

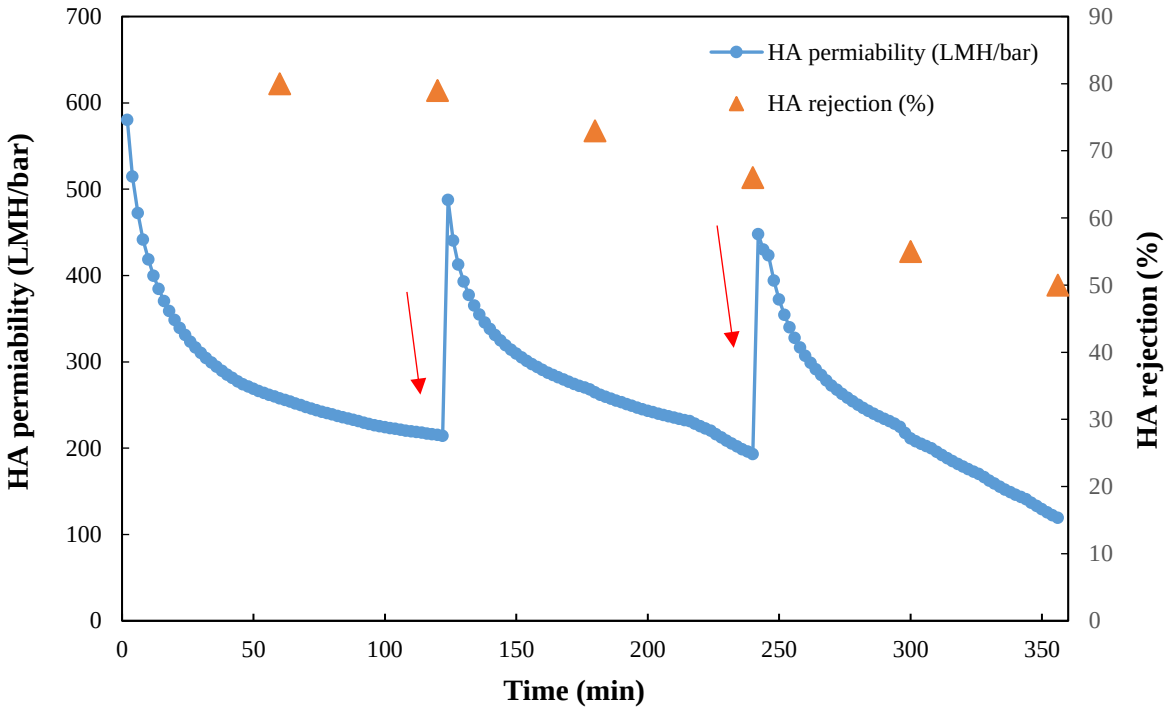

Fig. 6.14. HA Flux decline behavior of PIC-1.5 membrane versus time in three filtration cycles with chemical cleaning by acid and base (Arrows point to the time when chemical cleaning was conducted)

6.1.4.3 Membrane performance summary

MWCNT/PANI/PVDF membranes improved porosity, pore size and hydrophilicity were fabricated by increasing the amount of MWCNT/PANI complex gradually up to 2 wt. %. Results showed a good agreement between porosity and water permeability, as porosity rose to 91% for PIC-1.5 permeability increased up to 1320 LMH/bar, more additions of MWCNT/PANI to 2 wt. % slightly reduced the porosity to 88.4 %, which is still higher than with pristine PVDF.

Insertion of hydrophilic MWCNTs is advantageous to increase membrane surface hydrophilicity which increases water permeability due to the increasing affinity between water and membrane surface. In the membrane formation process through phase inversion method, MWCNT was placed on the top of the membrane for its high hydrophilicity, while in sub-layer the less hydrophilic layer was placed. Consequently, membrane surface with high

hydrophilicity and high affinity for water were fabricated and the hydrophobic pores channel below the top layer which increases the slipping effect both contribute to enhancing water permeability.

The rejection of all modified membranes was increased in comparison to pristine PVDF membrane, because of the good adsorption of NOM on the positively charged membrane surfaces due to the electrostatic interaction and the high capacity of MWCNT/PANI/PVDF membranes. The smaller pores on the top layer connected to larger finger-like pores in the lower structure are also resulting in high water permeation and HA rejection.

Within the dosage range used in this study, the optimum MWCNT/PANI dosage was 1.5 wt. %, with water permeability of 1320 LMH/bar and rejection up to 79 %.

6.1.5 Flux recovery after chemical cleaning

Flux recovery test for HA and its proper cleaning method were conducted. **Fig. 6.15** Presented flux recovery results and the total fouling ratio for all modified membranes.

Removing HA from the membrane surface was achieved by cleaning the membrane surface with both acid (HCl) and base (NaOH). HA removal occurred through hydrolysis and solubilization effect. First, NaOH hydrolysing the HA with carboxylic and phenolic functional groups, then HCl oxidizing and breaking down the functional groups of organic foulant to soluble carboxyl, ketonic and aldehyde groups, and then they detached from the membrane surface [15, 24].

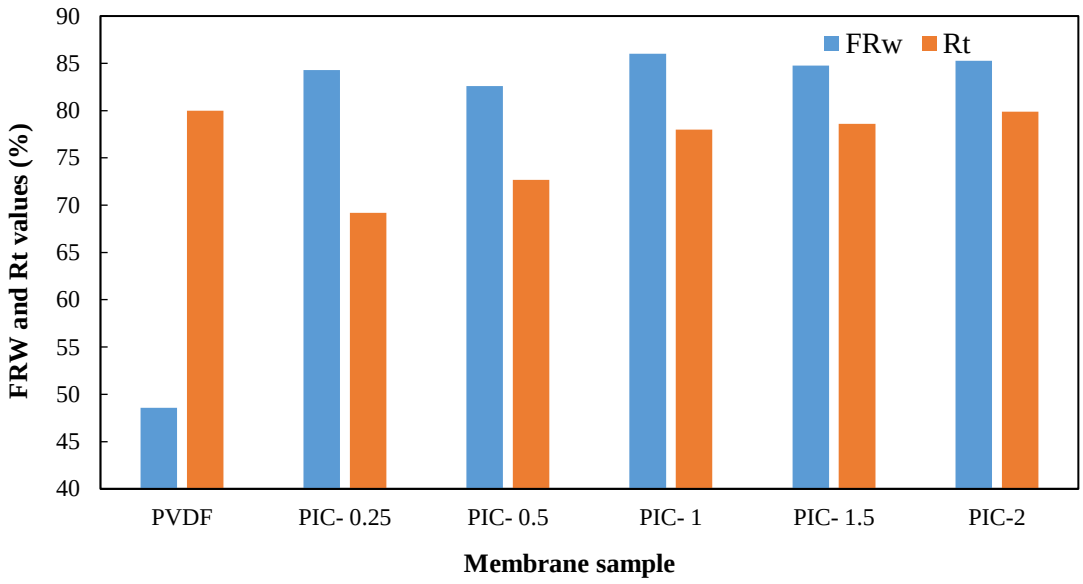

Fig. 6.15. Flux recovery and total fouling ratio for pure and PIC modified PVDF membranes.

As can be seen from **Fig. 6.15**, flux recovery F_{Rw} for all the membranes after cleaning by acid and base is between 83-85%, which is quite good as the high HA adsorption usually caused a significant fouling R_t found to be between (70-79) % as shown in **Fig. 6.15**. This good recovery suggested the easy cleanability of the modified membranes in comparison to pristine PVDF.

HA flux decline of three cycles of filtration test for PIC-1.5 shown in previous section, **Fig. 6.14,** as can be seen with cleaning with acid (HCl) and base (NaOH), most of the HA adsorbed on the membrane surface can be easily removed using both acid and base with water flux recovery up to 85 %. It can also be noticed that HA permeate flux was 85% recovered after chemical cleaning in the second and third cycles.

Although NOM usually caused significant fouling and hence flux decline [21], most of the HA adsorbed on the membrane surface can be easily removed using both acid and base.

6.2 Conclusion

MWCNT/PANI/PVDF ultrafiltration membrane was fabricated by in-situ polymerization of PANI using phase inversion method with improved water permeability and antifouling properties. The effect of MWCNT/PANI concentration on the performance of PVDF blended membrane was investigated.

MWCNT/PANI/PVDF modified membranes showed higher porosity, pore size, and hydrophilicity (CA) which decreased from 92 for pristine PVDF to 54.8 for PIC-2, the enhancement in permeability reached a maximum in PIC-1.5 up to 1320LMH/bar; (about 35 times increase compared to pristine PVDF).

Humic acid was used as a model for natural organic matter (NOM) to evaluate the rejection performance of the modified membranes. Improvement in HA rejection was shown with the inclusion of MWCNT/PANI; which is due to the electrostatic interaction and the high capacity of MWCNT/PANI/PVDF membrane. HA rejection increased with increasing MWCNT/PANI, rejection reached up to 81% in PIC-2. The flux recovery increased from 43% for pristine PVDF to 85% for PIC-1.5 modified membrane.

The MWCNT/PANI complex played a significant role in separation and water permeability enhancement in the modified membranes. The unique nature of MWCNTs and easy functionalization of well dispersed MWCNT is a promising modifier for ultrafiltration membranes for future applications.

References

[1] Huang, J.E. et al., (2003). Well-dispersed single-walled carbon nanotube/polyaniline composite films. Carbon. 41, pp.2731-2736.

[2] Raque, Sainz, et al., (2005). Soluble Self-Aligned Carbon Nanotube/polyaniline Composites. Advanced Materials 17 (3), pp. 278–81.

[3] Ma J. et al., (2013). Role of oxygen-containing groups on MWCNTs in enhanced separation and permeability performance for PVDF hybrid ultrafiltration membranes. Desalination, 320, pp. 1–9.

[4] Zhang J.G. et al., (2013). Improved hydrophilicity, permeability, antifouling and mechanical performance of PVDF composite ultrafiltration membranes tailored by oxidized low- dimensional carbon nanomaterials, Journal of Mater. Chem. A, 1 (9), pp. 3101–3111.

[5] Suhartono, Jono, and Chedly Tizaoui., (2015). "Polyvinylidene Fluoride Membranes Impregnated at Optimised Content of Pristine and Functionalised Multi-Walled Carbon Nanotubes for Improved Water Permeation, Solute Rejection and Mechanical Properties. Separation and Purification Technology 154. Elsevier B.V., pp. 290–300.

[6] J. Yin, B. Deng, (2016). Polymer-matrix nanocomposite membranes for water treatment, Journal of Mem. Sci. 479, pp. 256–275.

[7] Alam J. et al., (2013). Advances in Membrane Development Based on Electrically Conducting Polymers. Advances in Polymer Technology. 32, pp. E189-E197.

[8] Macdiarmid A.G. et al., (1987). Polyaniline: a new concept in conducting polymers. Synth. Met. 18, pp. 285-290.

[9] Kochkodan, Victor, and Nidal Hilal. (2014). A Comprehensive Review on Surface Modified Polymer Membranes for Biofouling Mitigation. Desalination 356 (October). Elsevier B.V.: 187–207. doi:10.1016/j.desal.2014.09.015.

[10] Hou, P.X., Liu, C. & Cheng, H.M., (2008). Purification of carbon nanotubes. Carbon, 46(15), pp.2003–2025.

[11] Mulder, M., (1996). Basic Principles of Membrane Technology. Dordrecht, the Netherlands: Kluwer.

[12] Liu, F. et al., (2011). Progress in the production and modification of PVDF membranes. Journal of Membrane Science, 375(1-2), pp.1–27.

[13] Hyung H., Kim J.-H., (2008). Natural organic matter (NOM) adsorption to multi-walled carbon nanotubes: effect of NOM characteristics and water quality parameters. Environ. Sci. Technol., 42 pp. 4416–4421.

[14] Lee, J. et al., (2016). High flux and high selectivity carbon nanotube composite membranes for natural organic matter removal. Separation and Purification Technology, 163, pp.109–119.

[15] Liu, Charles et al., (2001). Membrane Chemical Cleaning: From Art to Science. American Water Works Association, 25.

[16] Pan, B. & Xing, B., (2008). Adsorption mechanisms of organic chemicals on carbon nanotubes. Environmental Science and Technology, 42(24), pp.9005–9013.

[17] Su, F. S.; Lu, C. S., (2007). Adsorption kinetics, thermodynamics and desorption of natural dissolved organic matter by multiwalled carbon nanotubes. J. Environ. Sci. Health Part A, 42, pp.1543– 1552.

[18] Bowen, W. R., J. I. Calvo, and a. Hernndez. (1995). Steps of Membrane Blocking in Flux Decline during Protein Microfiltration. Journal of Membrane Science 101 (1-2), pp. 153–65.

[19] Hermia J., (1982). Constant pressure blocking filtration laws: Applications to Power-law non-Newtonian fluids, J. Trans. Inst. Chem. Eng., 60, pp. 183-187.

[20] Bowen W. R., Calvo J. I, Hernandez A., (1995). Steps of membrane blocking in flux decline during protein microfiltration, J. Membr. Sci., 101, pp. 153-165.

[21] Clark, M. M., and C. Jucker (1993): Interactions between Hydrophobic Ultrafiltration Membranes and Humic Substances, Proceedings of the Membrane Technology Conference, Baltimore, MD

[22] Liang, S. et al., (2012). A novel ZnO nanoparticle blended polyvinylidene fluoride membrane for anti-irreversible fouling. Journal of Membrane Science, 394-395, pp.184–192.

[23] Lahoussine-Turcaud, M.R., Wiesner, and J. Y. Bottero, (1990). Fouling in Tangential Flow Ultrafiltration: The Effect of Colloid Size and Coagulation Pretreatment, J. of Membrane Science, 52, pp.173-190

[24] Nguyen, Sy Thuy, and Felicity Anne Roddick. (2011). Chemical Cleaning of Ultrafiltration Membrane Fouled by an Activated Sludge Effluent. Desalination and Water Treatment 34, pp. 94–99.

CHAPTER 7. Conclusions and Recommendations

This chapter presents the summary of the findings, and the conclusions arrived at based on the findings and the scope of future work recommended.

7.1. Final Conclusions

The original contribution of this research was focused on fabrication of novel PVDF ultrafiltration membrane with enhanced water permeability and rejection efficiency for natural organic matter removal from water through modification with various additives by phase inversion method.

In the first part of this research (chapter 4), MWCNT/PDA/PVDF ultrafiltration membranes were fabricated through *in-situ* polymerization of dopamine over MWCNT to produce MWCNT/ PDA complex. This composite was added to PVDF base polymer to fabricate a blended membrane with an enhanced permeability and rejection properties using phase inversion technique. The effects of MWCNT/PDA addition on the performance of PVDF blended membrane was explored in detail, and the results showed:

- MWCNTs have exceptional water treatment capabilities and excellent adsorbent properties which are due to its large specific surface area. However, it has poor adhesion to the membrane as well as dispersion problems. Modifying MWCNTs with PDA play an important role in overcoming the dispersibility problem of MWCNT. We notice that coating MWCNTs with PDA make it more dispersible and reduce aggregation; besides CNTs retain their inherent properties. Furthermore, PDA

improves its binding to the base polymer (PVDF) which is reflected as an improvement on the performance of the blended membrane.

- Characterization and performance studies of the modified membranes revealed higher porosity, hydrophilicity and larger pore size of all modified membranes compared to pristine PVDF membrane. Modified PVDF membrane was blended with a mixture of 2% dopamine/ 1% MWCNT which showed the excellent performance enhancement results with 20 fold increase in permeability compared to pristine PVDF membrane and 12.5% increase in HA rejection. Furthermore, it demonstrated about 81% rejection of HA based on filtration test.

- HA rejection of the modified membranes reached up to 97.7% for the membrane blended with 0.25 wt. % MWCNT/PANI/PVDF, providing 28.8 % increase compared to pristine PVDF membrane.

- The modified membranes showed higher recovery flux FR_w (71-78) % and lower total flux R_t (73-81%) in comparison with pristine PVDF membrane.

These results indicate that the use of PDA/MWCNT complex as additives improved the performance of PVDF membranes, with significant enhancement in water permeability and HA removal.

In the second part of this research (chapter 5), PANI/PVDF ultrafiltration membrane was fabricated through *in-situ* polymerization of aniline over PVDF to produce a blended membrane with enhanced permeability, HA rejection, and antifouling properties.

Polyaniline (PANI) is a well-known conducting polymer. It has been used in membranes for different applications due to its stability and simple acid-base doping chemistry. PANI was prepared by the polymerization reaction.

The effects of PANI addition on the performance of PVDF blended membranes as well as the influence of the blending method on the membrane morphology, structure and performance were investigated thoroughly and the results showed that:

- A comparison between two blending methods of aniline to PVDF matrix : *in-situ* polymerization method and simple regular blending method and their effects on the morphology and structure of modified membranes was conducted, results demonstrated that the *in-situ* polymerization blending method of PVDF/PANI contributed to formation of uniform and homogeneous structure membranes with higher pore sizes and more inter-linked finger-like pores, which resulted in higher water permeability and tensile strength in comparison to the membranes fabricated using the regular blending method for membrane fabrication.

- PANI act as a pore forming agents due to PANI oligomers and PANI nanospheres migration during membrane fabrication which was advantageous to increase pore size, porosity, and the production of longer vertically-connected pores

- Characterization and performance studies of the modified PANI/PVDF membrane revealed higher porosity, hydrophilicity and larger pore size of all modified membranes compared to pristine PVDF membrane.

- Water permeability of PANI /PVDF modified membranes were 7-16 times faster than pristine PVDF and with HA rejection up to 75%.

In the third part of this research (chapter 6) and to further enhance the performance of the previously fabricated PANI/PVDF membrane, we further added MWCNT to fabricate a PVDF/MWCNT/PANI membrane with more enhanced permeability and rejection properties by *in-situ* polymerization of PANI using phase inversion method.

Depending upon the results demonstrated in part 2 of this research regarding the blending method which showed that the *in-situ* polymerization method of PANI on PVDF produced a

uniform and homogeneous structure with better performance. This approach has been used as a primary blending method to achieve *in-situ* polymerization of aniline over MWCNT.

The effect of MWCNT/PANI addition on the performance of PVDF blended membrane was investigated and the results showed:

- Characterization and performance studies of the modified membranes demonstrated that addition of MWCNT/PANI complex resulted in significant performance enhancement of the resultant modified membrane in comparison to pristine PVDF membrane. Within the MWCNT concentrations used; the membrane with (PANI/ 1.5 % MWCNT) showed the highest permeability results (1320 LMH/bar), with 40 fold permeability improvement in comparison to pristine PVDF ultrafiltration membrane. It also showed about 79% rejection for HA filtration test. This high enhancement of the fabricated membrane is attributed to the high hydrophilicity, and porosity with positive charge membrane due to the addition of MWCNT/PANI.

- PANI act as a pore forming agent and together with MWCNT which has the exceptional water treatment capabilities and excellent adsorbent properties which resulted from its large specific surface area as well as the role of PANI in improving the dispersibility and adherence of MWCNT to the base polymer. These factors contribute to the significant enhancement of the performance of the modified membranes.

- The rejection of all modified membranes was increased in comparison to pristine PVDF membrane, because of the good adsorption of negatively charged NOM on the positively charged membrane surfaces due to the electrostatic interaction and the high capacity of MWCNT/PANI/PES membrane.

- Flux recovery for the modified membranes after cleaning by acid and base was between 83-85%, which is quite good as the high HA adsorption usually caused a significant fouling found to be between (70-79) %

- The unique nature of MWCNT/PANI complex and easy functionalization of well dispersed MWCNT is a promising modifier for ultrafiltration membranes for future application.

These results indicate that the use of PANI/MWCNT complex as additives significantly improved the performance of PVDF membrane, with significant enhancement in water permeability and HA removal.

In conclusion, three novels modified PVDF-UF membranes with improved permeability, rejection efficiency, and antifouling properties were successfully fabricated and performance studies showed a great potential for their use in NOM removal from water with promising future water treatment applications.

Table 7.1 summarizes the results of modified PVDF membranes with various additives compared to the results of the modified membranes in this study.

Table 3. Comparative results of modified PVDF membranes with different additives.

References	PVDF Additives	Flux (LMH)	Rejection (%)	Porosity (%)	Contact angle (^{0})
Xiaoyu Zhao et al (2012) [1]	MWCNT/amine-ester	8	92	61	75
Chuanqi Zhao et al (2013) [2]	Graphene Oxide	27	-	76.8	64
Jin-Hong Jiang et al (2014) [3]	Dopamine	100	15	-	79.6
Hai-peng Xu (2014) [4]	Oxidized MWCNT	403	72	85	71
MA et al (2013) [5]	Oxidized MWCNT	1200	80	86	54.7
Current work	**PANI**	**400**	**35**	**89**	**73.0**
Current work	**MWCNT/dopamine**	**505**	**81**	**86**	**66.4**
Current work	**MWCNT/PANI**	**1320**	**79**	**91**	**57.1**

7.2. Recommendations for future work

- The use of more uniformed SWCNT for PVDF modification and studying its effect on the improving the PVDF membrane performance in water treatment.
- Designing a filtration process system using the modified membranes with other water pre- treatment processes to be applied on the real surface water system.
- Application of the membrane modifiers to PVDF used in other filtration processes like nanofiltration.
- Exploring another method for enhancing the performance of PVDF like using graphene and comparing the resultant membranes performance with the used method in this research
- Studying the factors affect HA membrane fouling in sea water such as pH and ionic strength.

References

[1] Zhao, X. et al., (2012). Hyperbranched-polymer functionalized multi-walled carbon nanotubes for poly (vinylidene fluoride) membranes: From dispersion to blended fouling-control membrane. Desalination, 303, pp.29–38.

[2] Zhao, C. et al., (2013). Effect of graphene oxide concentration on the morphologies and antifouling properties of PVDF ultrafiltration membranes. Journal of Environmental Chemical Engineering, 1(3), pp.349–354.

[3] Jiang, J.-H. et al., (2014). Improved hydrodynamic permeability and antifouling properties of poly(vinylidene fluoride) membranes using polydopamine nanoparticles as additives. Journal of Membrane Science, 457, pp.73–81.

[4] Xu, H.-P. et al., (2014). Preparation and characterizations of poly(vinylidene fluoride)/oxidized multi-wall carbon nanotube membranes with bi-continuous structure by thermally induced phase separation method. Journal of Membrane Science, 467, pp.142–152.

[5] Ma, J. et al., (2013). Role of oxygen-containing groups on MWCNTs in enhanced separation and permeability performance for PVDF hybrid ultrafiltration membranes. Desalination, 320, pp.1–9.

APPENDIX

Pore size distribution of pristine PVDF and modified membrans measured by BET:

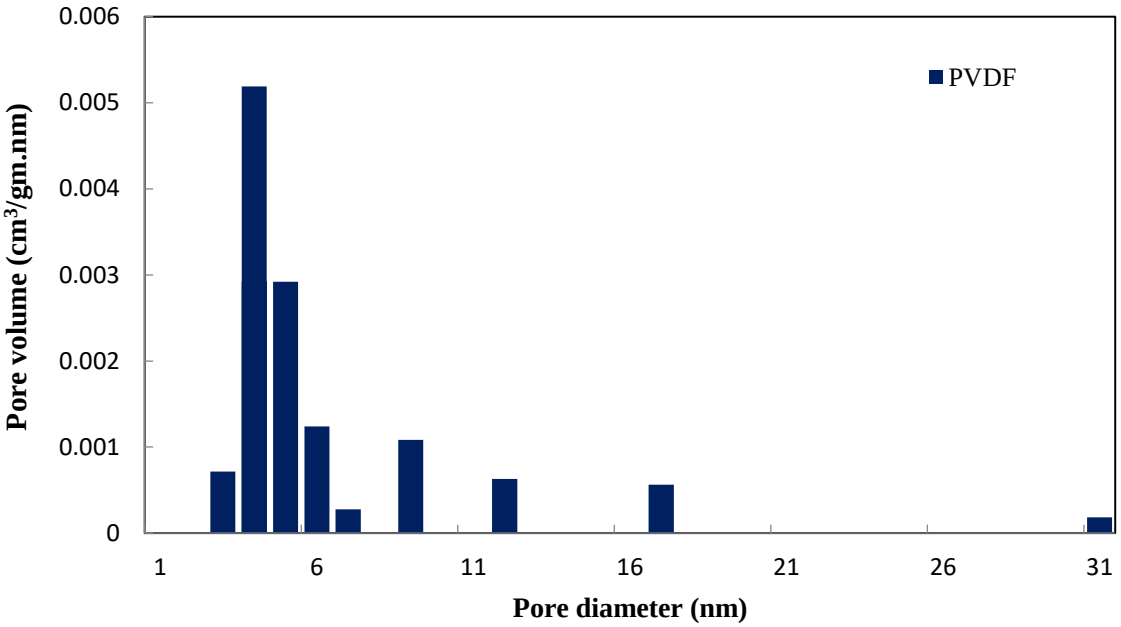

Fig. A. Pore size distribution for pristine PVDF

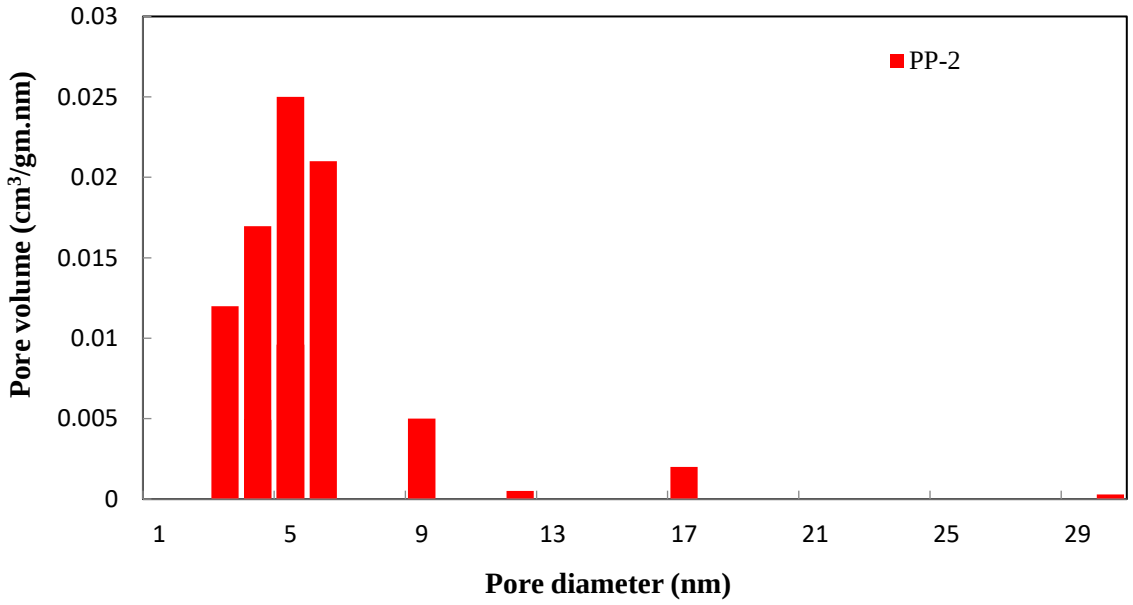

Fig. B. Pore size distribution for pristine simple blended PVDF/PANI

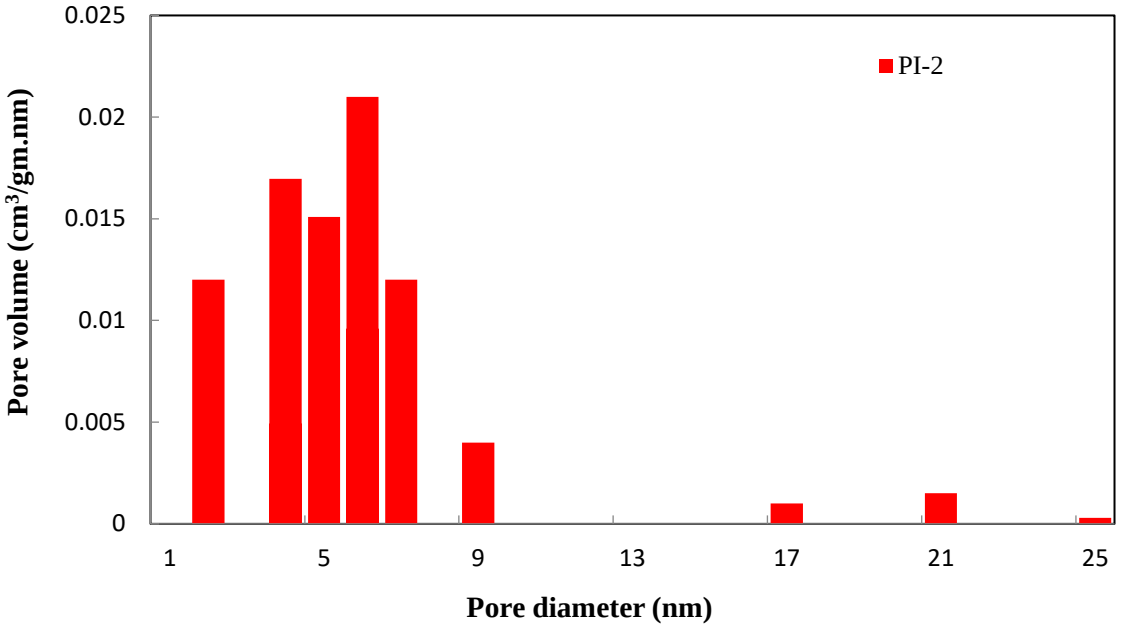

Fig. C. Pore size distribution for pristine simple blended *in-situ* PVDF/PANI

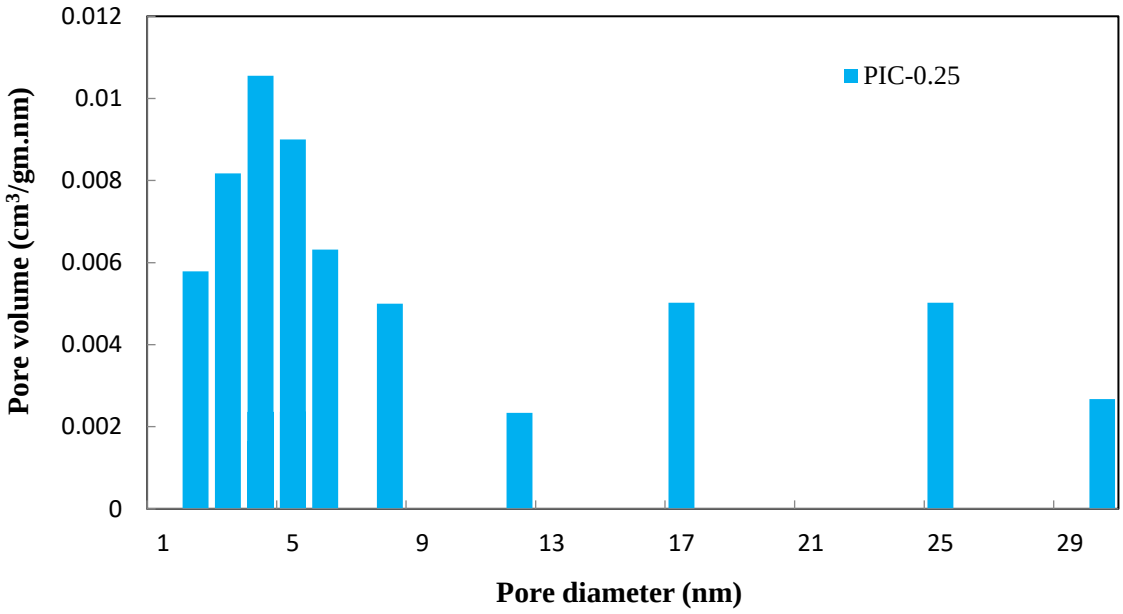

Fig. D. Pore size distribution for pristine simple blended 0.25 wt. % (PVDF/MWCNT/PANI)

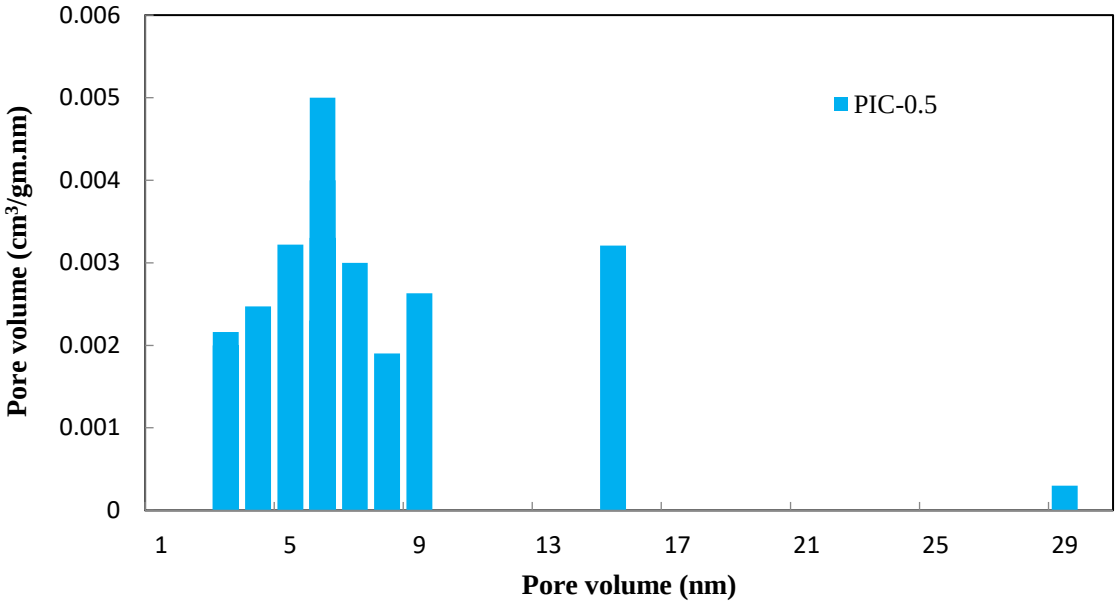

Fig. E. Pore size distribution for pristine simple blended 0.5 wt. % (PVDF/MWCNT/PANI)

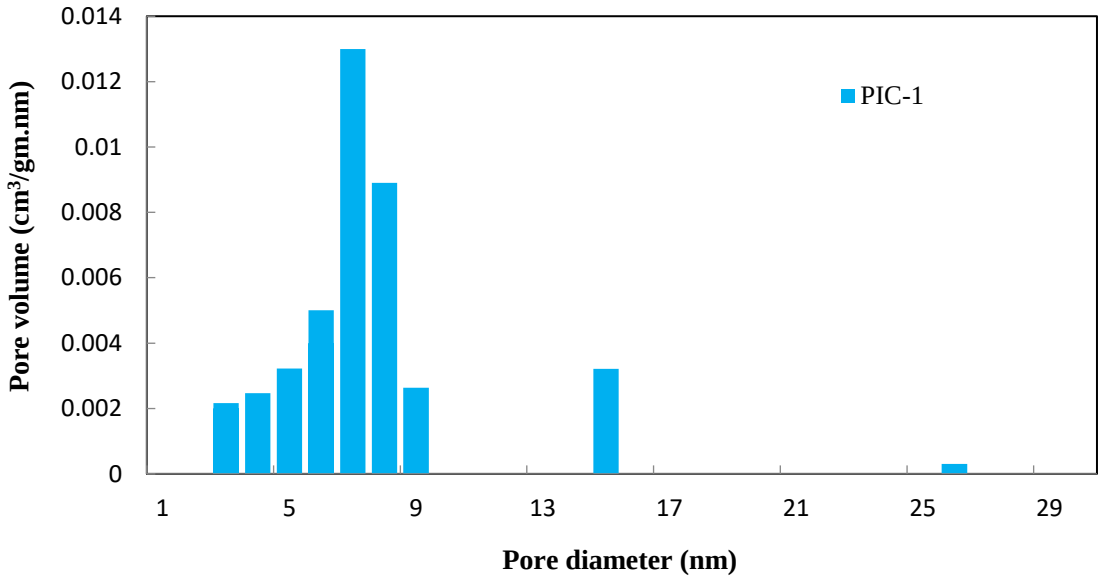

Fig. F. Pore size distribution for pristine simple blended 1 wt. % (PVDF/MWCNT/PANI) membrane

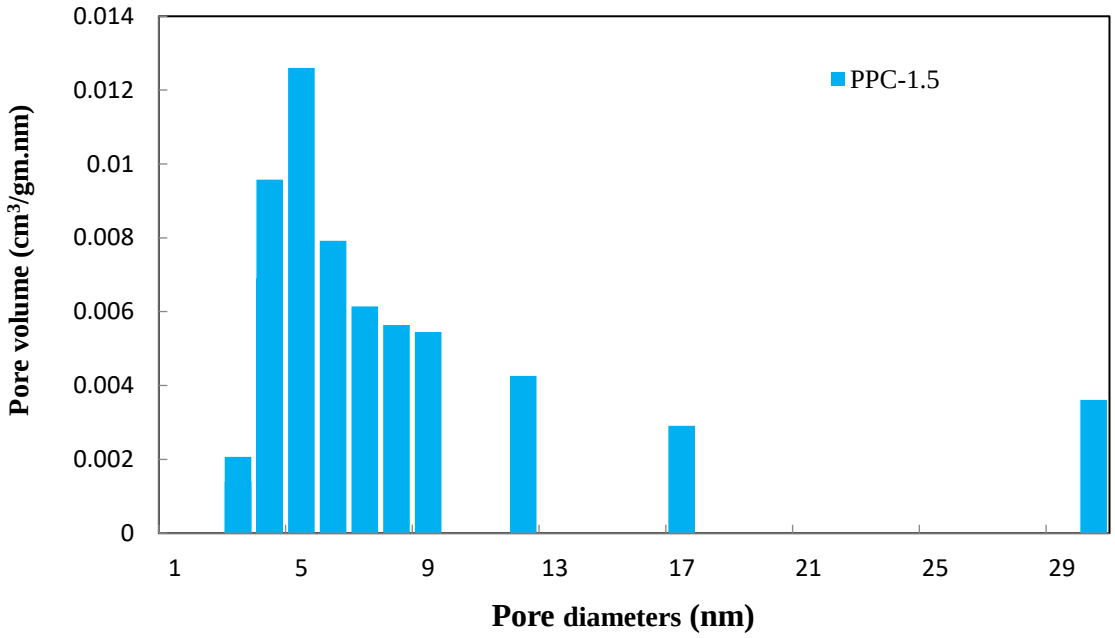

Fig. G. Pore size distribution for pristine simple blended 1.5 wt. % (PVDF/MWCNT/PANI) membrane

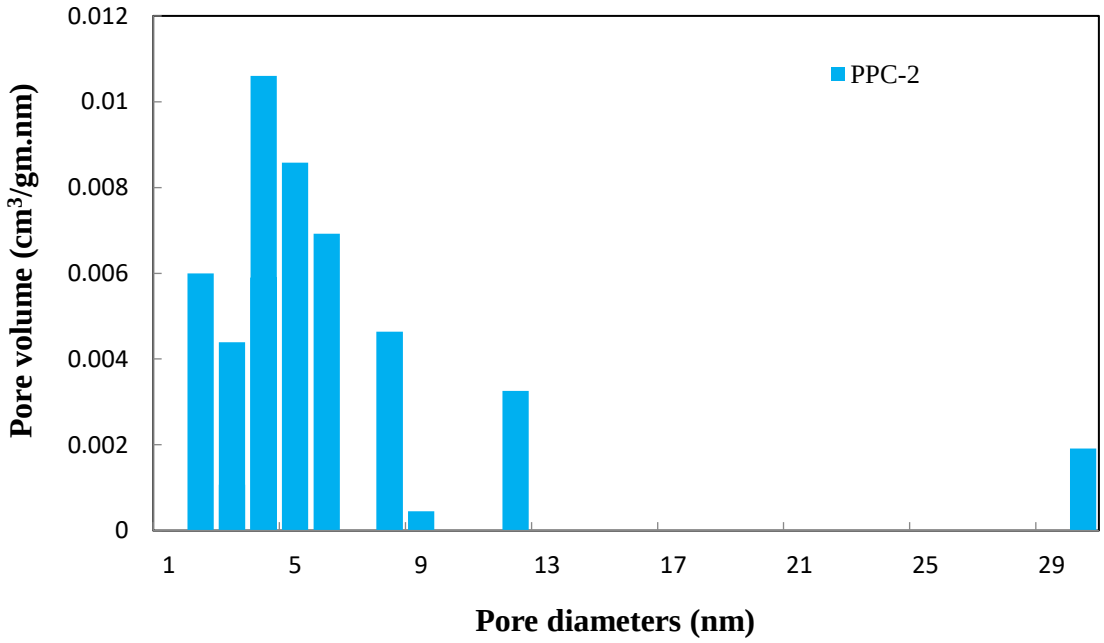

Fig. H. Pore size distribution for pristine simple blended 2 wt. % (PVDF/MWCNT/PANI) membrane